SPIRE Sensitivity Models

Matt Griffin

SPIRE-QMW-NOT-000642

Draft produced for Herschel Ground Segment Review

21 May 2007

Contents

1. Introduction

This draft revision of the SPIRE Sensitivity Models document (last issued formally in December 2004) has been produced following a review by the SPIRE consortium in late 2006/early 2007, and some iterations following discussion at the Herschel Science Team meeting in January 2007.

This document summarises the assumptions used and explains the calculations involved in the estimating the sensitivity of SPIRE for the its various observing modes as described in [1]. The models described here have been used to generate the SPIRE sensitivity figures currently implemented in HSpot.

The attached MathCad worksheets provide a full account of all the calculations:

Annex 1: Photometer sensitivity model
Annex 2: Spectrometer sensitivity model
Annex 3: Telescope obscuration factor
Annex 4: Beam FWHM and S/N enhancement from pixel co-addition

2. Assumptions and input parameters

The main assumptions made in estimating the scientific performance of the instrument are described in this section.

2.1 Telescope properties

2.1.1 Reflector temperature (T_{tel})

The nominal telescope temperature is taken as 80 K. Best and worst case values are 60 and 90 K. Note that a temperature at the lower end of the range will be achieved only if the emissivity is at the higher end of its range.

2.1.2 Effective emissivity (e_{ref})

The emissivity of the primary and secondary mirrors is assumed to be the same, with a wavelength-dependent emissivity based on the results of Fischer *et al*.2004 [2] who give the following equation for the best fit to the absorptivity of the a dusty Herschel mirror sample:

$$a = (0.0336)\,l^{-0.5} + (0.273)\,l^{-1} \qquad (1)$$

The corresponding emissivity per reflector is $e = 1 - a$, which is plotted below.

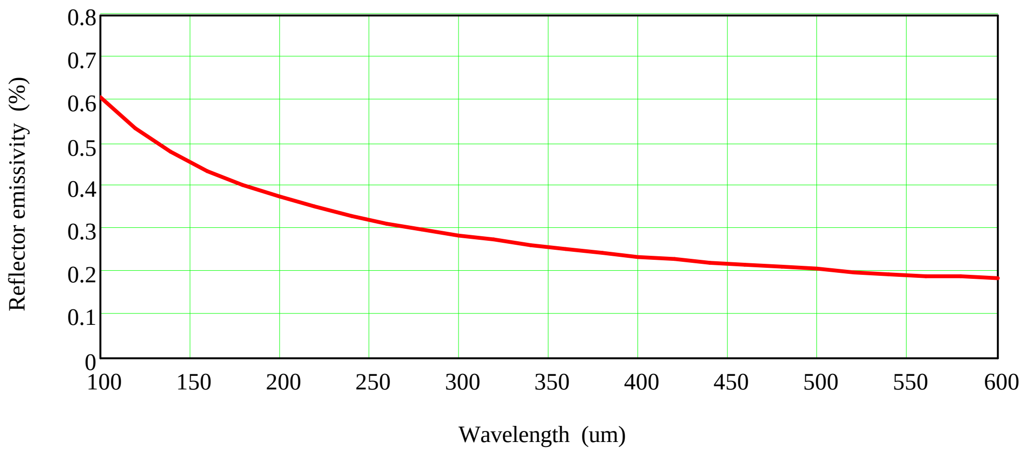

Figure 1: Herschel dusty reflector sample emissivity

In addition to the reflector emission, we also need to allow for stray light, and here the uncertainties are large. The adopted model is based on Industry's analysis as reported in Industry's stray light model report [3]. The stray light analysis is based on a nominal telescope with 70 K temperature and 3% emissivity. Two cases are presented, an optimistic case and a pessimistic one. Here we use the pessimistic case, for which the prediction is that the stray light varies between 15 and 19% of the telescope background over the 230 - 670 μm range. For simplicity, we adopt a stray light component of 20% of a 70-K, 3% emissive telescope.

That produces an overall effective emissivity as shown by the red curve in Figure 2 (where the stray light background has been characterised as the appropriate fraction of an 80-K rather than a 70-K telescope).

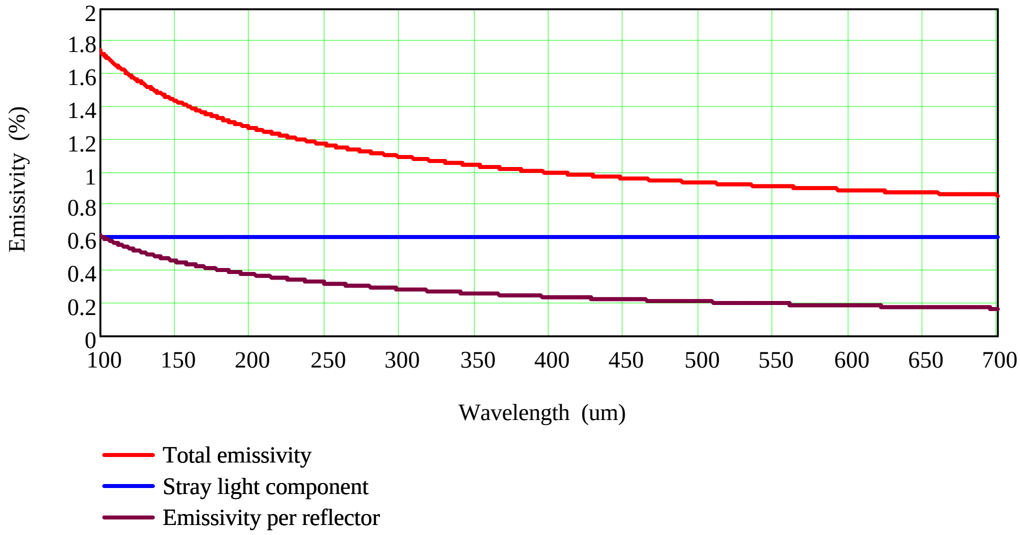

Figure 2: Overall emissivity model

Under these assumptions, the total effective emissivity varies between about 1% at 200 μm and 0.6% at 670 μm. Each reflector is assumed to have transmission (1 - e_{ref}).

2.1.3 Used diameter (D_{tel})

The physical diameter of the primary is 3.5 m but the used diameter is smaller at 3.29 m. The telescope secondary mirror is the pupil stop for the system, so that the outer edges of the primary mirror are not seen by the detectors. This is important to make sure that radiation from highly emissive elements beyond the primary reflector does not contribute stray light.

2.1.4 Obscuration factor (*Obs_factor*)

The effective collecting area of the telescope is reduced due to the hole in the primary and the secondary support structure. The overall loss of throughput is accounted for by a single obscuration factor with a value of 0.87 (corresponding to 13% loss). This has been calculated by convolving the obscuration pattern with an 8-dB Gaussian taper representing the graded illumination of the primary by the detector feedhorns (Annex 3).

2.1.5 Focal ratio (F_{tel})

The focal ratio of the Herschel telescope is 8.68.

2.2 Instrument properties

2.2.1 Instrument thermal system

There are three temperature stages in the instrument:

Level 1 (T_{L1}): This is the temperature of the main instrument box, with a nominal value of 5.5 K.

Level 0 (T_{L0}): This is the temperature of the detector box, with a nominal value of 1.8 K and best and worst case values of 1.7 and 2.2 K respectively.

^{3}He (T_o): This is the temperature of the detector arrays within the BDAs, with a nominal value of 310 mK and best and worst case values of 300 and 330 mK respectively. (The actual temperature of a bolometer at its operating point is higher than this due to heating by the bias and absorbed radiant power.)

2.2.2 Overall system transmission

For both the photometer and the FTS, the overall transmission and background power emission of all elements between the sky and the detector is represented by five elements: the two telescope mirrors, a stray light source, and two instrument elements – one at Level 1 temperature and one at Level 0. All components (filters and mirrors) at L1 (5.5 K) are lumped together and given a single total transmission and emissivity, and all L0 and 300-mK components are likewise combined. (Since the emission of components at both 0.3 K and 1.8 K is negligible, the 0.3-K components are included in the L0 element for simplicity.) Splitting the instrument into these two temperature stages allows the effects of different instrument temperatures to be estimated. The five elements and their properties are summarised in Table 1.

Index (k)	Element	Transmission	Transmission to detector feedhorn aperture	Emissivity	Temperature
1	Telescope primary	$t_1(n)$	$td_1(n) = t_2(n)t_4(n)t_5(n)$	$1 - t_1(n)$	T_{tel}
2	Telescope secondary	$t_2(n)$	$td_2(n) = t_4(n)t_5(n)$	$1 - t_1(n)$	T_{tel}
3	Stray light source	$t_2(n) = 0$	$td_3(n) = t_4(n)t_5(n)$	e_{stray}	T_{tel}
4	Level 1 (5.5 K) element	$t_4(n)$	$td_4(n) = t_5(n)$	$1 - t_1(n)$	T_{L1}
5	Level 0 (1.8 K) element	$t_5(n)$	$td_5(n) = 1$	$1 - t_1(n)$	T_{L0}

Table 1: Modelled elements of the overall optical system

The stray light component is fed into the system as an emitting element with 100% transmission, located between the secondary and the instrument. The Level 1 and Level 2 properties are different for the five bands as discussed below.

The transmission efficiency from the sky to the detector feed aperture is $t_{sky} = t_1(n)td_1(n)$

3. Photometer Model

3.1 Photometer instrument properties

3.1.1 Optical system

Final optics focal ratio (F_{fin}): The focal ratio of the photometer final optics is 5.

Mirror reflectivity and emissivity: For simplicity, all mirrors are assumed to have a reflectivity r_{mirr} = 0.995 and emissivity $e = (1 - r_{mirr})$.

3.1.2 Spectral passbands and instrument optical transmission efficiency

The overall instrument transmission will be represented by an optical efficiency function derived from component-level and ILT data. The overall transmission is based on the SVR-2 presentation by Bruce Swinyard, as shown in Figure 3.

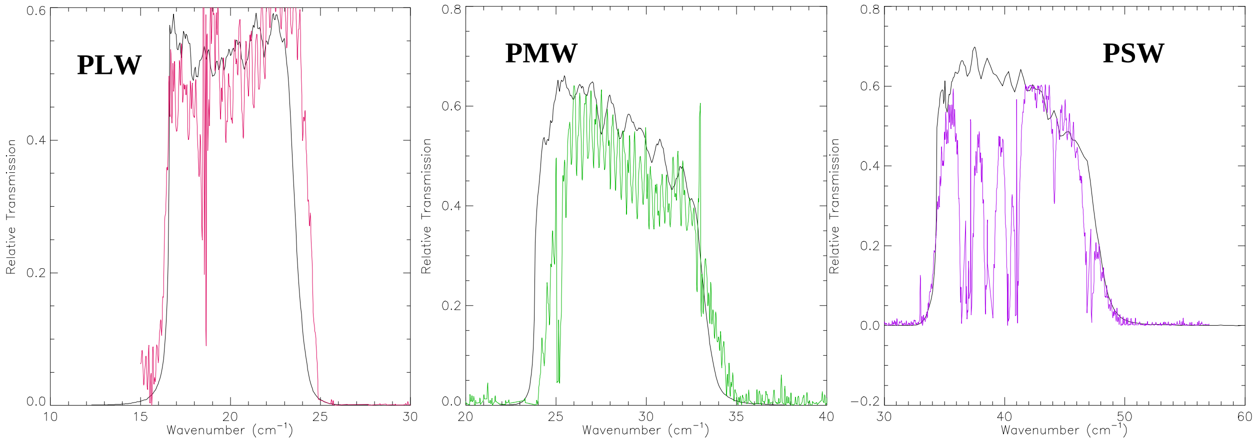

Figure 3: SPIRE filter stack transmission profiles

The overall as-measured curves are shown by the coloured lines. The transmissions are scaled to the values obtained from the stacked component transmissions (shown in black). Smoothed versions of the as-measured profiles, as shown in Figure 4 , are used for the sensitivity model. For the parts of the PSW band affected by the atmosphere in the ILT lab., a simple interpolation by eye has been done.

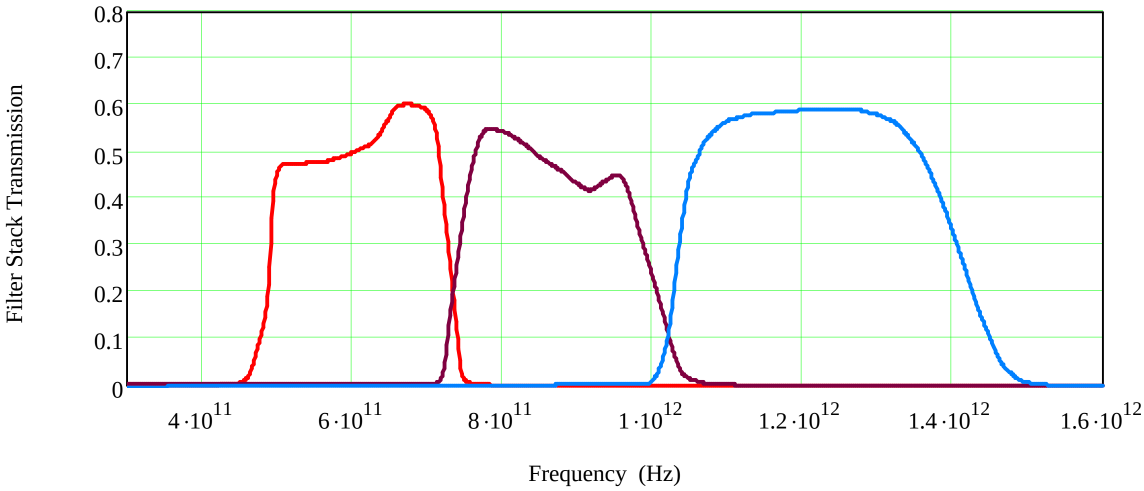

Figure 4: Modelled filter profiles

The three bands are defined by index i = (1,2, 3) for (PSW, PMW, PLW). The overall filter transmission profiles of Figure 4 are denoted $tfil_1(n)$, $tfil_2(n)$, and $tfil_3(n)$. When integrating over the bands, the following limits are adopted: PSW: 900 – 1600 GHz; PMW: 700 – 1100 GHz; PLW: 400 – 800 GHz.

The layout of the photometer optical components is shown schematically in Figure 5 and the components and their temperatures are listed in Table 2.

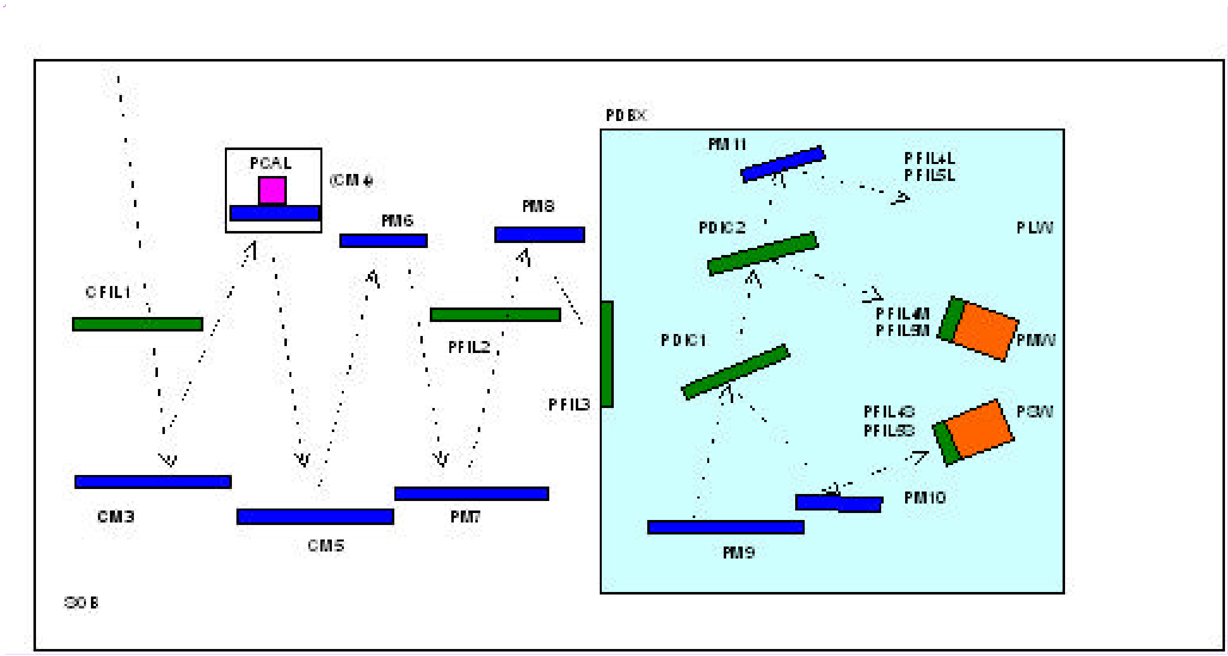

Figure 5: Layout of photometer components

No. (k)	Component			Description	Temp.
1	CM1			Primary	T_{tel}
2	CM2			Secondary	T_{tel}
3	CFIL1			Input filter	T_{L1}
4	CM3			Input mirror	T_{L1}
5	CM4			BSM	T_{L1}
6	CM5			Reimaging	T_{L1}
7	PM6			Photometer field mirror	T_{L1}
8	PM7			Offner 1	T_{L1}
9	PFIL2			Filter at baffle	T_{L1}
10	PM8			Offner 2	T_{L1}
11	PFIL3			Detector box entrance	T_{L0}
12	PM9			Offner 3	T_{L0}
	PSW	PMW	PLW		
13	PDIC1	PDIC1	PDIC1	Dichroic	T_{L0}
14	PM10	PDIC2	PDIC2	Flat (PSW) or dichroic (PMW, PLW)	T_{L0}
15	PFIL4S	PFIL4M	PM11	Blocking filter (PSW, PMW) or flat (PLW)	T_o
16	PFIL5S	-	PFIL4L	Edge defining filter (PSW, PLW), no filter (PMW)	T_o

Table 2: Photometer instrument components

Table 3 lists the numbers of mirrors and filters for the two instrument elements to be modelled.

	No. of filters	No. of mirrors
Level 1	2	6
Level 0	(3, 4, 4) for (S, M, L) bands	(2, 1, 2) for (S, M, L) bands
Total	(5, 6, 6) for (S, M, L) bands	(8, 7, 8) for (S, M, L) bands

Table 3: Numbers of mirrors and filters at Levels 1 and 2

The hole 2.8-mm hole in the BSM is taken into account by assuming it has unit emissivity and occupies a fraction of $(2.8/26)^2 = 0.012$ of the BSM area. The emissivity of, e_{BSM}, is therefore taken as 0.012. The BSM transmission is taken as 0.95 (the hole is slightly over-sized, so it's associated losses are not fully taken into account by the overall obscuration factor).

The transmission and emissivity of the Level 1 (k = 4) and Level 0 (k = 5) elements are summarised for the three bands in Table 4.

		Transmission and emissivity	
PSW	6 L1 mirrors	$(t_{mirr}{}^{5})(t_{BSM})$	Five with transmission t_{mirr}, one with t_{BSM}
	2 L1 filters	$tfil_1(n)^{2/5}$	
	L1 total	$t_4(n) = (t_{mirr}{}^{5})(t_{BSM})tfil_1(\nu)^{2/5}$	$e_4(\nu) = 1 - t_4(n)$
	2 L0 mirrors	$(t_{mirr}{}^{2})$	
	3 L0 filters	$tfil_1(n)^{3/5}$	
	L0 total	$t_5(n) = (t_{mirr}{}^{2})tfil_1(n)^{3/5}$	$e_5(\nu) = 1 - t_5(n)$
PMW	6 L1 mirrors	$(t_{mirr}{}^{5})(t_{BSM})$	Five with transmission t_{mirr}, one with t_{BSM}
	2 L1 filters	$tfil_2(\nu)^{2/6}$	
	L1 total	$t_4(n) = (t_{mirr}{}^{5})(t_{BSM})\ tfil_2(\nu)^{2/6}$	$e_4(\nu) = 1 - t_4(n)$
	1 L0 mirror	t_{mirr}	
	4 L0 filters	$tfi_2(\nu)^{4/6}$	
	L0 total	$t_5(n) = (t_{mirr})tfi_2(\nu)^{4/6}$	$e_5(\nu) = 1 - t_5(n)$
PLW	6 L1 mirrors	$(t_{mirr}{}^{5})(t_{BSM})$	
	2 L1 filters	$tfil_3(n)^{2/6}$	
	L1 total	$t_4(n) = (t_{mirr}{}^{5})(t_{BSM})tfil_3(\nu)^{2/6}$	$e_4(\nu) = 1 - t_4(n)$
	2 L0 mirrors	$t_{mirr}{}^{2}$	
	4 L0 filters	$tfi_3(\nu)^{4/6}$	
	L0 total	$t_5(n) = (t_{mirr}{}^{2})tfil_3(n)^{4/6}$	$e_5(\nu) = 1 - t_5(n)$

Table 4: Transmission and emissivity for the Level 1 and Level 0 elements.

3.1.3 Feedhorns

Feedhorn aperture diameter (D_{horn}): The feedhorn external diameters (centre-centre spacings) $Dhorn_i$ are (2.5, 3.33, 5.0) mm, sized at $2F l_i$ where F is the final optics focal ratio and l_i are the design wavelengths of (250, 333, 500) μm for (PSW, PMW, PLW). Note that these are not the same as the centre wavelengths of the filter bands. The centre-centre separations are in the ratio 1:(4/3):2, ensuring that there are several sets of detectors with coincident beam centres on the sky. The internal apertures of the horns are 0.1 mm smaller.

Feed-horn/cavity efficiency (h_{feed}): This is the overall absorption efficiency of the combination of feed-horn, cavity and bolometer element. It accounts for all losses and inefficiencies with respect to the performance of a lossless feed system. The feed efficiencies of the bolometers have been measured at unit level, and values are given in the JPL EIDPs. For each band, the median feed efficiency for that band is used, with values as follows: (0.70, 0.70, 0.77) for (PSW, PMW, PLW). This factor is taken to include the efficiency with which the background power couples to a conical feedhorn for a single-moded system (0.9).

Feedhorn throughput (AW): This is the area-solid angle product with which the detector receives incident radiation. We assume single-moded feedhorns, for which the throughput is l^2.

Spillover efficiency (h_s): This is the fraction of the detector throughput which illuminates the telescope - the remaining fraction (1 - h_s) is assumed to terminate on the cold non-emitting inside of the detector box wall, reducing the background power on the detector. A value of 0.8 is used for all bands [4].

Aperture efficiency (h_A): This is the fraction of the total power from a point source diffraction pattern that is coupled to a detector centred on the source. A value of 0.7 is used for all bands [4].

3.1.4 Bolometers

The bolometers are modelled as ideal thermal devices according to the theory of Mather [5] codified by Sudiwala *et al.* [6]. The main bolometer parameters and their nominal, best and worst case values are summarised in Table 5 below.

Data from the JPL EIDPs are used for the bolometer model. For each band, the median values of the bolometer parameters are be adopted as the nominal values. At unit-level, the bolometer and JFET yield are both high (100% for the JFETs and close to 100% for the bolometers). A yield of 95% is adopted here to allow for pixels known to be dead, excessively noisy or unusably slow at FPU level. Any additional reduction in yield will be included in the overall "pessimism factor" to be applied to the final results.

Parameter	Units	Description	PSW	PMW	PLW
R_o	Ω	Resistance parameter	92.1	69.5	104
T_g	K	Band-gap temperature	41.0	42.1	41.8
R_L	MΩ	Load resistance	16.3	16.5	16.1
G_o	pW K^{-1}	Static thermal conductance at 300 mK	65.1	65.7	67.4
C_o	pJ K^{-1}	Heat capacity at 300 mK	0.52	0.59	0.63
n		R-T index	0.5	0.5	0.5
b		Thermal conductivity power-law index	1.50	1.70	1.70
r		Heat capacity power-law index	1	1	1
yield		Fraction of working bolometer channels per array	0.95	0.95	0.95

Table 5: Bolometer parameters

3.1.5 Readout electronics

JFET and warm amplifier voltage noise: The overall noise of the combined JFET and LIA is taken to be en_A = 10 nV $Hz^{1/2}$, based on ILT measurements.

3.1.6 Observing mode parameters

The following efficiency factors are assumed:

Chopping efficiency factor (h_{ch}): The standard efficiency factor of 0.5 for square-wave chopping is applied to the demodulated signal level for all chopped observations.

Field area efficiency factor (h_{field}): To allow for some vignetting of the field at the two edges of the array, an efficiency factor h_{field} is included for scan map observations. The nominal values are (1.0, 0.95, 0.9) for (PSW, PMW, PLW).

3.2 Derived parameters

3.2.1 Telescope properties

Effective telescope area (A_{tel}): This is the geometrical area multiplied by the obscuration factor

$$A_{tel} = \frac{pD_{tel}^{2}}{4} Obs\_factor \qquad (2)$$

Plate scales (PS): The plate scale at the telescope focus is given by

$$PS_{\mathrm{tel}} = \frac{1}{D_{\mathrm{tel}} F_{\mathrm{tel}}} \quad \text{radians m}^{-1} \quad = \quad \frac{1}{D_{\mathrm{tel}} F_{\mathrm{tel}}} \frac{360}{2\pi} \frac{3600}{1000} \quad \text{arcsec mm}^{-1} \qquad (3)$$

The plate scale at the detector array is scaled with respect to this value by the ratio of the telescope *f*-number to the final optics *f*-number:

$$PS_{\mathrm{a}} = PS_{\mathrm{tel}} \frac{F_{\mathrm{tel}}}{F_{\mathrm{fin}}} . \qquad (4)$$

Beam widths: The FWHM beam widths for an 8-dB pupil edge taper have FWHM values of $1.03\lambda/D_{\mathrm{tel}}$ (see Annex 4 for derivation). This analysis takes into account the 560-mm central hole in the Herschel primary, which has the effect of making the beam slightly narrower than the diffraction limit for an unobscured mirror.

The beam widths are given by

$$FWHM_{\mathrm{i}} = \frac{1.03\lambda_{\mathrm{i}}}{D_{\mathrm{tel}}} \frac{360}{2\pi} 3600 \text{ arcsec.} \qquad (5)$$

The derived beam widths are (16, 23, 34)" for the (PSW, PMW, PLW) bands. Note that the large central obscuration causes a significant increase in the sidelobe level. Figure 6 shows the SPIRE beam profile (in units of λ/D) for the actual Herschel telescope (red curve) and, for comparison, the beam profile for an unobscured telescope. Note that large (5%) sidelobe at $1.7\lambda/D$.

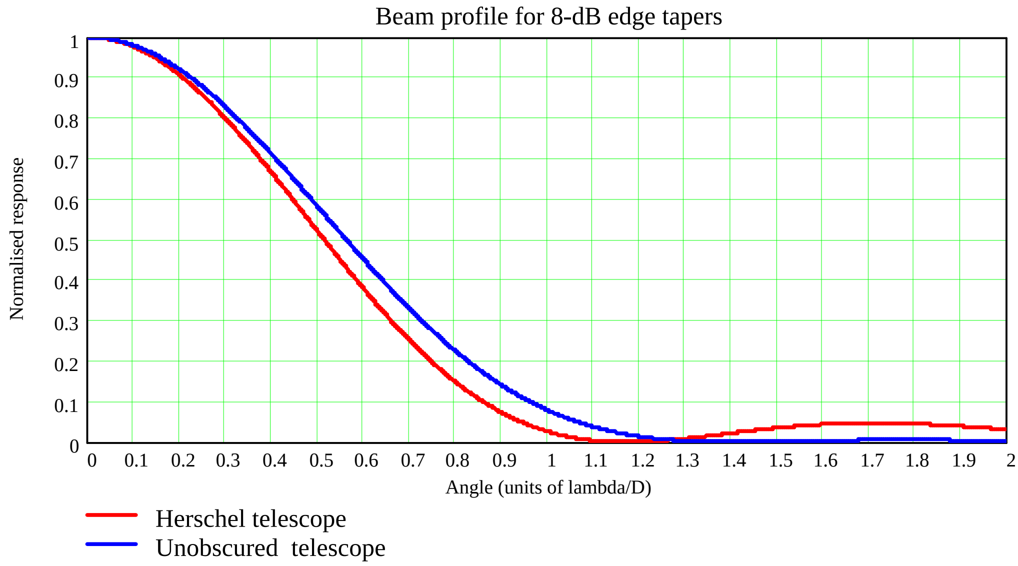

Figure 6: Normalised beam profile for 8-dB pupil edge taper. The red curve corresponds to the Herschel telescope, and the blue curve to the same telescope with zero central obscuration.

Optical modelling and ILT results, as presented by Marc Ferlet at the SVR include estimates of the FWHM beam widths based on line data, broadband measurements and modelling of the response assuming an 8-dB edge taper. The photometer results are shown in Figure 7.

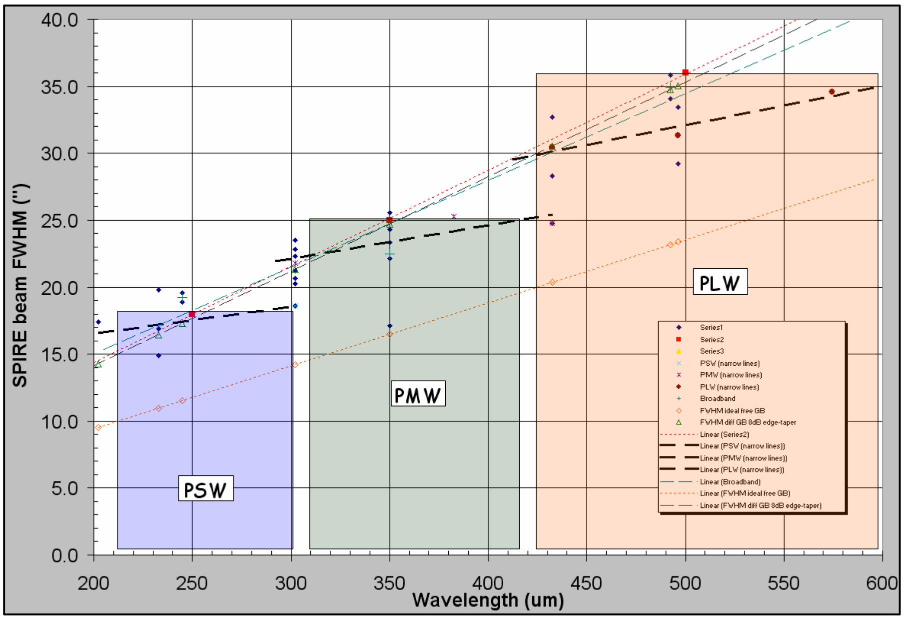

Figure 7: Beam profile measurements (from Marc Ferlet's SVR-2 presentation, slide 17)

There are various values to choose from here, but the overall results are not very different from the 8-dB edge taper model. Therefore, for each band the adopted beam FWHM will be the value at the nominal band centres: (18, 25, 36)" for (PSW, PMW, PLW).

The main beam area is approximated by

$$Abeam_i = \frac{p}{4}\left(FWHM_i\right)^2 . \qquad (6)$$

The beamwidths are be used to convert to the point source sensitivities to equivalent surface brightness sensitivities, using this simple calculation of the beam area.

3.2.2 Background power levels on the detectors

The background power absorbed by the detector from component k is given by

$$Q_{i,k} = 10^{12} h_S hfeed_i \int_{nL_i}^{nU_i} e_{i,k}(n) AW_i(n) td_{i,k}(n) B(n, T_k) dn \qquad \text{pW} \qquad (7)$$

The limits for the integrals are chosen in each case to encompass the full band in each case.

Note that, strictly speaking, the spillover efficiency factor applies only to components outside the Level-0 box. For simplicity it is applied to all components – this introduces negligible errors as the emission from inside the 2-K box is insignificant.

The total background power absorbed by the detector, Q_{det}, is the sum of all these contributions.

Photon noise limited *NEP*: The contribution to the photon noise-limited *NEP* from component k is given by

$$NEPph_{i,k}^{\ 2} \;=\; \frac{4h_S h^2}{c^2}\int_{nL_i}^{nU_i} \frac{AW_i(n)e_{i,k}(n)td_{i,k}(n)hfeed_i n^4}{exp\left(\frac{hn}{kT_k}\right)-1}\left[1 \;+\; \frac{e_{i,k}(n)td_{i,k}(n)hfeed_i}{exp\left(\frac{hn}{kT_k}\right)-1}\right]\mathrm{d}n \qquad (8)$$

The overall photon noise limited *NEP*, *NEP*ph, is the quadrature sum of the individual contributions. All contributions except those from the telescope reflectors are negligible, so only these are included in the analysis.

Note that in all cases, the result of equation (8) is closely approximated by the well-known simpler formula

$$NEPph_{i,k}^{\ 2} \;=\; \left(2Q_{det}hn_{o}\right)^{1/2} \qquad (9)$$

where n_o is the frequency at the band centre.

3.2.3 Bolometer model

Using the bolometer model of Sudiwala *et al.* [6], the following parameters of the bolometer and readout electronics are calculated as a function of the detector bias point:

- load curves;
- responsivity;
- *NEP* contributions due to phonon, Johnson, load resistor, and amplifier noise;
- overall bolometer system *NEP* at LIA output;
- time constants;
- optimum bias point (for minimum NEP);
- overall *NEP* and *DQE* (at 2-Hz chopping frequency - applicable only to the case of point source observations) at the optimum bias point due to bolometer system noise and photon noise.

The overall *NEP* is defined with respect to the power absorbed by the detector, and includes photon and detector system noise.

The bolometers have not been tested at exactly the nominal background either at unit level or during ILT. Noise performance must this be extrapolated from low-background measurements at JPL. Here we adopt the formalism used in the SVR-1 document on unit-level testing of the bolometers [7] in order to incorporate a possible degree of excess bolometer noise. The bolometer excess noise parameter, as taken as the median value for each array as extracted from the EIDPs, with the following values: (1.0, 1.1, 1.0) for (PSL, PMW, PLW). For the purpose of this model we adopt a uniform value of 1.05 for all three arrays.

The bolometer *DQE* is degraded by the factor *f* according to:

$$DQE \;=\; \frac{NEP_{ph}^{\ 2}}{\left(NEP_{ph}^{\ 2}+\left(f.NEP_{det}\right)^2\right)} \qquad (10)$$

So this is a small departure from ideal bolometer performance, and only in the case of the PMW array.

3.2.4 Per-detector Noise Equivalent Flux Densities (*NEFD*s)

The basic *NEFD* per detector is related to the overall *NEP* at the operating point, $NEPtot_{\mathrm{op}}$ by

$$NEFD\_basic \ = \ \frac{NEPtot_{\mathrm{op}}}{h_{\mathrm{A}} h_{\mathrm{feed}} A_{\mathrm{tel}} \int_{band} t_{\mathrm{sky}}(n)\,\mathrm{d}n} \ . \tag{11}$$

Point source photometry (POF 1): In this mode the source is chopped between two pixels. We assume that all six detectors used for this mode (three arrays; chopping between two detectors on each array) are performing to specification. The *NEFD* is degraded by the chopping efficiency factors h_{ch} but improved by a factor of $2^{0.5}$ due to pixel-pixel chopping. The overhead due to BSM motion is neglected, and the telescope nodding overhead is taken into account later.

$$NEFD_{\mathrm{pt}} \ = \ \frac{NEFD_{\mathrm{basic}}}{2^{0.5} h_{\mathrm{ch}}} \ , \tag{12}$$

The corresponding limiting point source flux density (5-s; 1 hr, neglecting telescope overheads) is given by

$$DS_{5s\_1\mathrm{hr\_pt}} \ = \ \frac{5.NEFD_{pt}}{\left(2^{0.5}\right)\left(3600^{0.5}\right)} \tag{13}$$

where the factor of $2^{0.5}$ in the denominator represents the relationship between post-detection bandwidth and integration time (a 1-Hz bandwidth corresponds to an integration time of 0.5 seconds).

Seven-point photometry (POF 2): In the case of seven-point photometry, the S/N loss for a given integration time is degraded with respect to the above case. The integration time is divided into eight equal portions, with the central position observed twice (at the beginning and at the end) and the six neighbour positions observed once each.

The total signal is derived by adding the signals in the eight positions: compared to the value for the central position alone, the total signal is thus increased by a factor of

$$2 \ + \ 6\exp\left[-2[\ln(2)]^{1/2} Dq_{norm}{}^{2}\right] ,$$

where Δq_{norm} is the seven-point offset normalised to the beam FWHM

The noise per position is increased by a factor of $8^{1/2}$ compared to that for a single long integration because the integration time is shared between the seven positions; and the final noise level is increased by a further $8^{1/2}$ through the co-addition of the seven signals. The final S/N is therefore reduced by a factor of

$$S\_N\_loss\_7pt(Dq_{norm}) \ = \ \frac{2 \ + \ 6\exp\left[-2[\ln(2)]^{1/2} Dq_{norm}{}^{2}\right]}{8} \ . \tag{14}$$

For a 6” offset, the S/N loss factors are (0.80, 0.90, 0.95) for the (PSW, PMW, PLW) bands, and the *NEFD* in this mode is degraded accordingly with respect to the value for POF 1.

$$NEFD_{7\mathrm{pt}} \;=\; \frac{NEFD_{\mathrm{pt}}}{S\_N\_loss\_7pt\left(Dq_{norm}\right)} \;, \tag{15}$$

and the limiting point source flux density (5-*s*; 1 hr, neglecting telescope overheads) is given by

$$DS_{5s\_1\mathrm{hr}\_7\mathrm{pt}} \;=\; \frac{5NEFD_{7\,pt}}{\left(2^{0.5}\right)\left(3600^{0.5}\right)} \tag{16}$$

Jiggle mapping (POF 3 or 4): In this mode the whole available 4 x 4 arcmin. field is chopped, so there is no improvement from pixel-pixel chopping. For mapping observations, the detector channel yield is taken into account by assuming, for simplicity, that the loss of S/N due to bad detectors is spread uniformly over the map. The required integration time to reach a given S/N scales with the number of detectors and so with (1/*yield*), so the limiting flux density scales with $(1/yield)^{0.5}$. We therefore have

$$NEFD_{\mathrm{jig}} \;=\; \frac{NEFD_{\mathrm{basic}}}{h_{\mathrm{ch}}\, yield^{\,0.5}} \;. \tag{17}$$

The need to jiggle reduces the S/N by a factor of 4. In measuring the signal from a point source, some enhancement in the S/N can be achieved by co-addition of the signals in all of the pixels in which the source is detected (see Annex 4). The improvement in point source S/N from pixel co-addition is in principle a factor of 1.52 if the signals in the pixels are weighted appropriately. For simple co-addition without weighting, the increase is a factor of 1.35. Here we adopt the lower value. So the overall degradation in point source S/N with respect to a point source observation in jiggle mode is 1.35/4 = 0.34. The 5-*s*; 1-hr point source flux density limit for a 4 x 4 arcmin map is then

$$DS_{5s\_1\mathrm{hr}\_\mathrm{jig}} \;=\; \left(\frac{5.NEFD_{\mathrm{jig}}}{(2)^{0.5}(3600)^{0.5}}\right)\left(\frac{4}{1.35}\right). \tag{18}$$

For surface brightness sensitivity,

$$DB_{5s\_1\mathrm{hr}\_\mathrm{jig}} \;=\; \left(\frac{5.NEFD_{\mathrm{jig}}}{(2)^{0.5}(3600)^{0.5}}\right)\left(\frac{1}{Abeam}\right)(4) \qquad . \tag{19}$$

Note that for the surface brightness sensitivity we do not include the point source S/N improvement factor that arises from pixel co-addition.

Scan mapping (POF 5): In this mode, used for large area maps, the telescope scans continuously, nominally without chopping or nodding. The full field 4 x 8 arcminute of view is available. The yield is taken into account in the same way as for jiggle map mode. The *NEFD* is therefore given by

$$NEFD_{\mathrm{scan}} \;=\; \frac{NEFD_{\mathrm{basic}}}{yield^{\,0.5}} \;. \tag{20}$$

The 5-*s*; 1-hr limiting flux density for point source extraction from a map is given by

$$DS_{5s\_1\mathrm{hr\_scan}} = \left(\frac{5.NEFD_{\mathrm{scan}}}{(2)^{0.5}(3600)^{0.5}h_{1/f}}\right)\left(\frac{4}{1.35}\right). \tag{21}$$

The factor $h_{1/f}$ accounts for the degradation S/N for point source extraction due to 1/*f* noise. This depends on the 1/*f* knee frequency and the beam crossing time, and has been analysed by Sibthorpe et al. [8]. For the nominal scan rate (30" s^{-1}) and 1/*f* knee frequency (100 mHz), the appropriate values for $h_{1/f}$ are (0.83, 0.80, 0.77) for (PSW, PMW, PLW).

Note that for scan mapping the factor of (4/1.35) is regarded as a bit pessimistic. But this is offset by the fact that there will be some additional noise introduced by the need to subtract a base level from the map. The latter factor may become irrelevant by the time the confusion limit is reached.

For surface brightness sensitivity,

$$DS_{5s\_1\mathrm{hr\_scan}} = \left(\frac{5.NEFD_{\mathrm{scan}}}{(2)^{0.5}(3600)^{0.5}h_{1/f}}\right)\left(\frac{1}{Abeam}\right)(4). \tag{22}$$

Again, the surface brightness sensitivity figure does not include the point source S/N improvement factor that arises from pixel co-addition.

3.2.5 Time to map a given area to a given rms sensitivity

The expected extragalactic confusion limit for SPIRE depends on the wavelength and on the adopted source count model. Here we take it to be 15 – 20 mJy 5-σ, and therefore calculate the time needed to map an area to an rms flux density limit of ΔS_{req} = 3 mJy.

The field size is (4 x 8)h_{field} arcmin. for scan mapping and 4 x 4 arcmin for jiggle mapping. An overlap efficiency of 10% is assumed (increasing the effective area that needs to be covered by 10%). The numbers of fields that need to be covered for a 1 sq. deg. map are:

$$Nfields_{\mathrm{scan}} = \left[\frac{A(60^2)}{(4)(8)h_{\mathrm{field}}h_{\mathrm{overlap}}}\right], \qquad Nfields_{\mathrm{jig}} = \left[\frac{A(60^2)}{(4)(4)h_{\mathrm{overlap}}}\right]. \tag{23}$$

The times in hours to reach an rms sensitivity of ΔS_{req} for one field for the two modes are given by

$$T\_field_{\mathrm{scan}} = \left[\frac{?\,S_{\mathrm{scan\_5}s\mathrm{\_1hr}}}{5?\,S_{\mathrm{req}}}\right]^2, \qquad T\_field_{\mathrm{jig}} = \left[\frac{?\,S_{\mathrm{jig\_5}s\mathrm{\_1hr}}}{5?\,S_{\mathrm{req}}}\right]^2 \tag{24}$$

The times in hours needed for a map of area *A* sq. deg. are then

$$T_{1\mathrm{\_map\_scan}} = (Nfields_{\mathrm{scan}})(T\_field_{\mathrm{scan}}) \qquad T_{1\mathrm{\_map\_jig}} = (Nfields_{\mathrm{jig}})(T\_field_{\mathrm{jig}}) \tag{25}$$

3.3 Results

The revised model has been computed in MathCad for the three bands, and the results are summarised in Table 6.

Band		PSW	PMW	PLW
Absorbed power (pW)		1.7	1.0	1.2
Photon noise *NEP* (W $Hz^{-1/2}$ x 10^{-17})		5.5	3.6	3.3
Overall *NEP* (W $Hz^{-1/2}$ x 10^{-17})		7.1	5.6	5.3
Basic *NEFD* (mJy $Hz^{-1/2}$)		10	14	11
$NEFD_{7pt}$ (mJy $Hz^{-1/2}$)		18	22	17
$NEFD_{scan}$ (mJy $Hz^{-1/2}$)		10	14	12
ΔS(5-σ; 1-hr) mJy	Point source (7-pt)	1.0	1.3	1.0
	4' x 4' jiggle map	3.6	4.9	4.0
	4' x 8' scan map	2.2	3.0	2.7
Time (hrs) to map 1 deg.^{2} to 3 mJy 1-*s*		2.6	5.4	4.4

Table 6: Photometer model results

4. Spectrometer Model

4.1 Spectrometer instrument properties

4.1.1 Instrument thermal system

The thermal system is the same as for the photometer (see Section 2.2.1).

4.1.2 Optical system

Mirror reflectivity and emissivity: All mirrors except for the roof-tops are assumed to have a reflectivity r_{mirr} = 0.995 and emissivity e = (1 – r_{mirr}). For the roof-tops, a value of r_{mirr} = 0.95 per surface (~ 0.90 per roof-top) will be used.

4.1.3 Spectral passbands and instrument optical transmission efficiency

Update planned: The overall transmission profiles to be used, based on stacked transmission measurements of the components and modelling of the waveguide cut-off, are as shown in Figure 8.

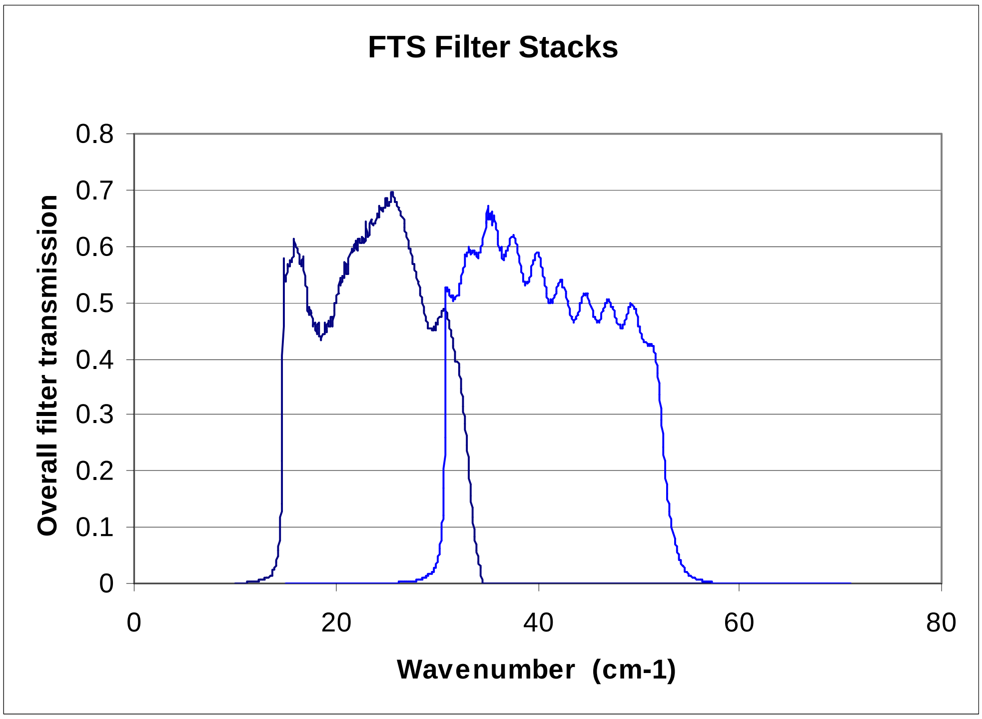

Figure 8: Spectrometer filter stack transmission profiles

For the purposes of the sensitivity model, the fringing is not a major issue (and in the actual instrument it is different in detail in any case). Smoothed versions of these plots are therefore used to characterise the overall filter transmission efficiency, as shown in Figure 9 .

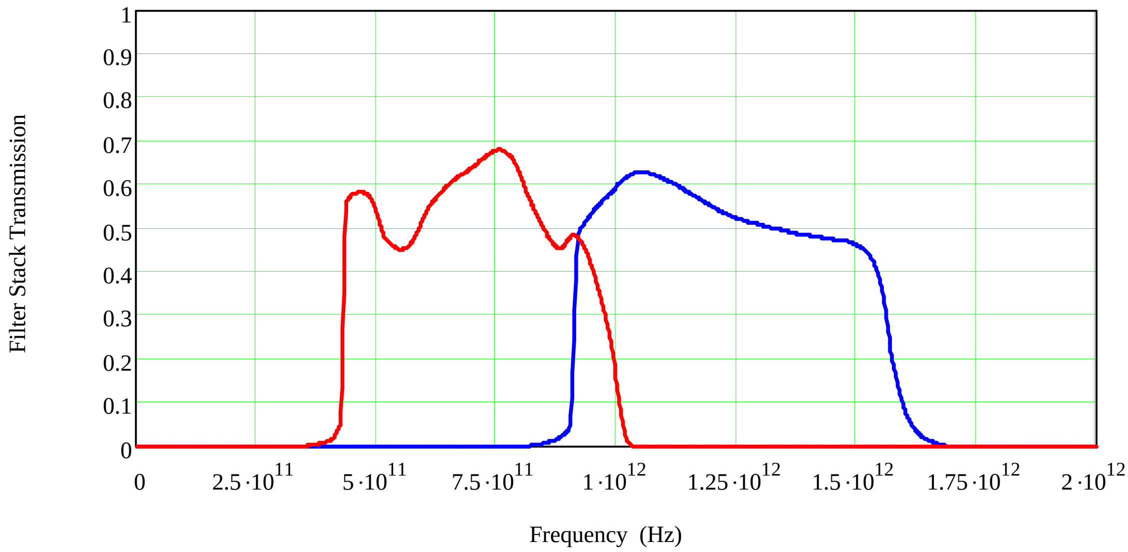

Figure 9: Modelled spectrometer filter profiles

These overall transmission profiles are denoted $tfil_1(n)$ for the SSW and $tfil_2(n)$ for the SLW. When integrating over the bands the following limits are adopted: SSW: 750 – 1700 GHz; SLW: 250 – 1050 GHz.

Operational limits for the two bands: Based on the above transmission profiles, the following limits are defined for the two bands:

SSW: 925 – 1550 GHz	≡	30.8 – 51.7 cm^{-1}	≡	193.4 – 324.2 μm
SLW: 446 – 950 GHz	≡	14.9 – 31.7 cm^{-1}	≡	315.6 – 672.3 μm

Lens transmission: The 300-mK lens over each array is assumed to have a uniform transmission of t_{lens} = 0.9.

Feedhorn external diameter (D_{horn}): The feedhorns are sized to have centre-centre spacing of $2F\lambda$ at wavelengths of (225, 390) μm for the (SSW, SLW) bands, where F is the final optics focal ratio. The internal diameter is smaller by 0.1 mm due to the wall thickness at the entrance aperture.

Beam divider properties: Each of the two beam dividers is assumed to have in-band transmission and reflection of $t_{bd} = r_{bd} = 0.487$, with an emissivity of $\varepsilon_{bd} = 1 - (t_{bd} + r_{bd}) = 0.03$. Depending on the path of a ray through the system, the attenuation due to the combination of the two beam dividers can have one of four values:

$t_{bd}r_{bd}$ $\qquad$ $r_{bd}t_{bd}$ $\qquad$ t_{bd}^2 $\qquad$ r_{bd}^2.

The average efficiency due to beam-divider loss is thus $\eta_{bd} = t_{bd}^2 + r_{bd}^2 + 2r_{bd}t_{bd} = 0.95.$ (26)

Figure 10 shows the layout of the FTS components and they are listed in Table 7.

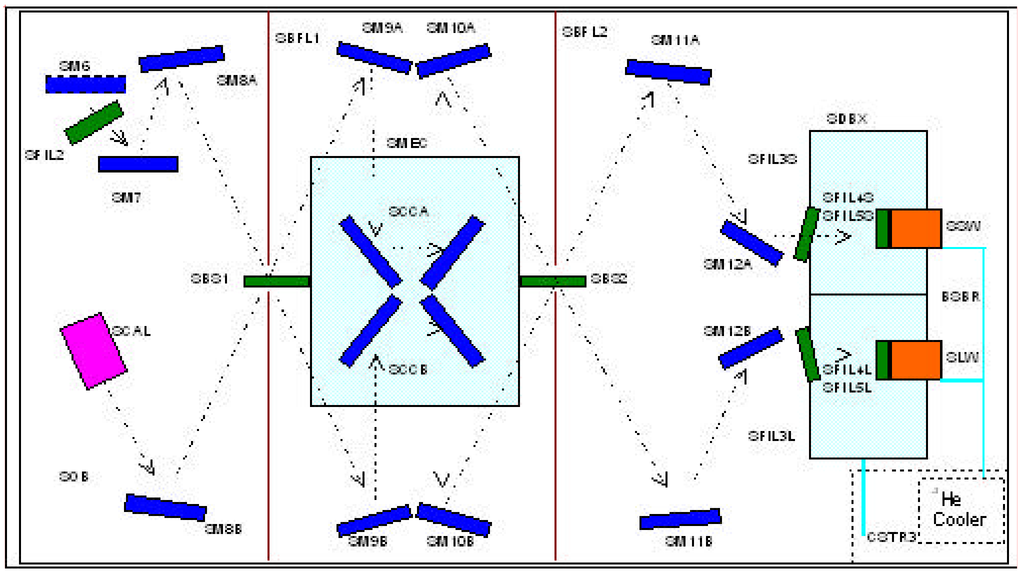

Figure 10: Spectrometer component layout

No. (k)	Component	Description	Temp.
1	CM1	Primary	T_{tel}
2	CM2	Secondary	T_{tel}
3	CFIL1	Input filter	T_{L1}
4	CM3	Input mirror	T_{L1}
5	CM4	BSM	T_{L1}
6	CM5	Reimaging	T_{L1}
7	SM6	Spectrometer field mirror	T_{L1}
8	SFIL2	Filter at baffle	T_{L1}
9	SM7	Input fold mirror	T_{L1}
10	SM8	Relay mirror	T_{L1}

11	SBS1	First beam divider	T_{L1}
12	SM9	Collimator mirror	T_{L1}
13	SRT1	Roof-top first reflector	T_{L1}
14	SRT2	Roof-top second reflector	T_{L1}
15	SM10	Camera mirror	T_{L1}
16	SBS2	Second beam divider	T_{L1}
17	SM11	Output relay mirror	T_{L1}
18	SM12	Flat mirror	T_{L1}
19	SFIL3	Detector box aperture filter	T_{L0}
20	SLENS	Correcting lens	T_o
21	SFIL4		T_o
22	SFIL5		T_o

Table 7: Spectrometer components

Table 8 lists the numbers of components for the two instrument elements to be modelled.

	No. of filters	**No. of mirrors**	**No. of beam dividers**	**No. of lenses**
Level 1	2	12 (inc. two rooftop reflectors and the BSM)	2	0
Level 0	2	0	0	1

Table 8: Numbers of spectrometer optical components at Levels 1 and 2

The transmission and emissivity of the Level 1 (k = 4) and Level 0 (k = 5) elements are summarised for the three bands in Table 9. For simplicity, half of the overall filter transmission is attributed to Level 1 and half to Level 0.

		Transmission and emissivity
SSW	12 L1 mirrors	$(t_{mirr}^{9})(t_{BSM})(t_{roof}^{2})$
	2 L1 filters	$tfil_1(n)^{1/2}$
	2 L1 beam dividers	tbd^2
	L1 total	$t_4(n) = (t_{mirr}^{9})(t_{BSM})(t_{roof}^{2})(tbd^2)\ tfil_1(n)^{1/2}$ $e_4(v) = 1 - t_4(n)$
	2 L0 filters	$tfil_1(n)^{1/2}$
	1 L0 lens	$tlens$
	L0 total	$t_5(n) = (tlens)tfil_1(n)^{1/2}$ $e_5(v) = 1 - t_5(n)$
SLW		As above except $tfil_1$ replaced by $tfil_2$

Table 9: Transmission and emissivity for the spectrometer Level 1 and Level 0 elements

4.1.4 Spectrometer throughput (*AW*)

The background power coupled to the detector is proportional to the product of the throughput (*AW*) and the feed-horn/cavity efficiency. The throughput is modelled as follows.

Each waveguide mode can propagate at frequencies higher than nc_{mode}. For circular waveguide, the cut-on wavelength is given by

$$l_c = \frac{2p\, r_o}{c_{mode}} \ . \qquad (27)$$

The parameter χ_{mode} has the values given in Table 10, which also lists the waveguide diameters and corresponding mode cut-on frequencies for the two FTS bands.

Mode	**TE11**	**TM01**	**TE21**	**TM01/ TM11**	**TE31**
c	1.841	2.405	3.054	3.832	4.201
SSW l_c (mm)	324	248	195	156	142
SSW n_c (GHz)	942.7	1208	1534	1925	2110
SLW l_c (mm)	671	513	404	322	294
SLW n_c (GHz)	447	584	742	931	1020

Table 10: Mode cut-on wavelengths and frequencies for the SSW and SLW bands

It is assumed that all waveguide modes potentially carry the same amount of power from the background. But only the fundamental mode is assumed to contribute to the signal. The throughput per mode for background power at frequency ν is taken as

$$AW(n) = l^2 = \left[\frac{c}{n}\right]^2 . \tag{28}$$

The throughput (in units of l^2) as a function of frequency increases step-wise across the band as the modes cut in, as shown by the dashed lines in Figure 11. Since in practice it is found that the variation is not so discontinuous we approximate this by a linear variation as shown by the solid lines.

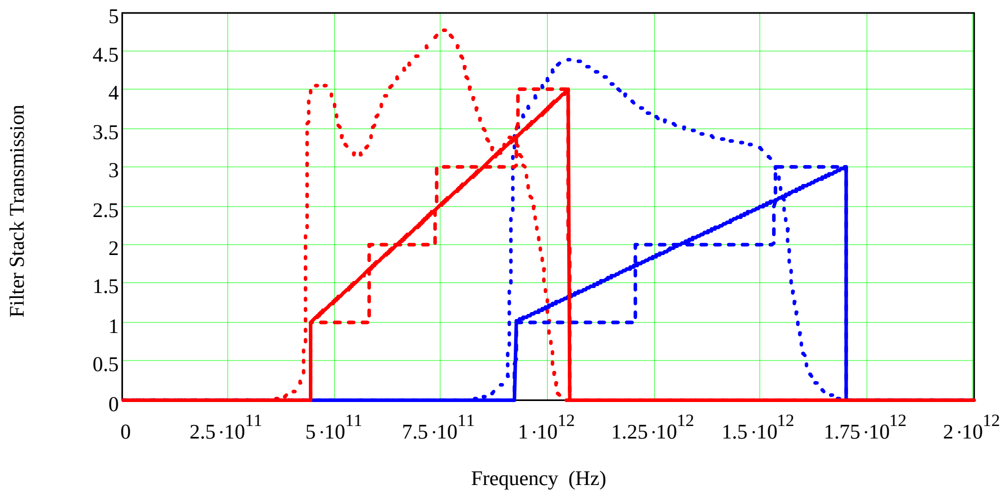

Figure 11: Step-wise throughput variation across the SSW (blue) and SLW (red) bands, and straight line approximations.

Multiplying by l^2 overall throughput is then as shown in Figure 12. Note that these numbers are similar to those quoted in Marc Ferlet's SVR-2 presentation (approx. 0.12 mm^2 sr for SSW and approx. (0.42 – 0.6) mm^2 sr for SLW).

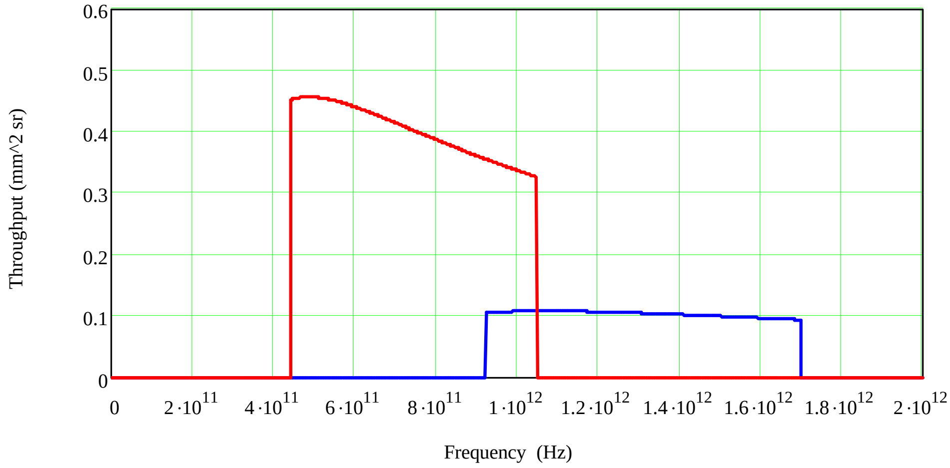

Figure 12: Modelled throughput variation across the two spectrometer bands

4.1.5 Spectrometer efficiency factors

Feed efficiency: The various modes are likely to couple to the detector with different efficiency factors. The mode-coupling efficiency factor is the overall absorption efficiency of the combination of feed-horn, cavity and bolometer element, defined in the same way as for the photometer.

SSW: Te following efficiencies are quoted in Chattopadhyay *et al*. [9] for the three SSW modes:

$$\eta SW_{\mathrm{TE11}} = 0.84 \qquad \eta SW_{\mathrm{TM01}} = 0.57 \qquad \eta SW_{\mathrm{TE21}} = 0.78\,.$$

For simplicity, we assume a constant efficiency across the band given by the average of these: $\eta_{\mathrm{feed}} = 0.73$.

SLW: Chattopadhyay *et al*. [9] quote a value of $\eta LW_{\mathrm{TE11}} = 0.7$ for the overall efficiency at 350 µm and 0.6 at 450 µm. The lower 450-µm value is attributed to the TM01 mode having reduced coupling efficiency to the detector cavity. Here we assume the same efficiency as of 0.7 as for the fundamental mode (TE11), across the whole band.

Aperture efficiency (η_A): This has the same definition as for the photometer. For the SW band, an aperture efficiency of $\eta A_{\mathrm{nom}} = 0.7$ is assumed across the band. For the LW band, we take into account the loss in efficiency at longer wavelengths due to the horn aperture size getting smaller in relation to the optimal value of $2F\lambda$. The LW horn is $2F\lambda$ at 390 µm but only $1.2F\lambda$ at 670 µm, for which the corresponding aperture efficiency is 0.5 [4]. We assume a value of $\eta A_{\mathrm{nom}} = 0.7$ up to 400 µm, and a linear drop to 0.5 over the range 400 to 670 µm, as shown in Figure 13.

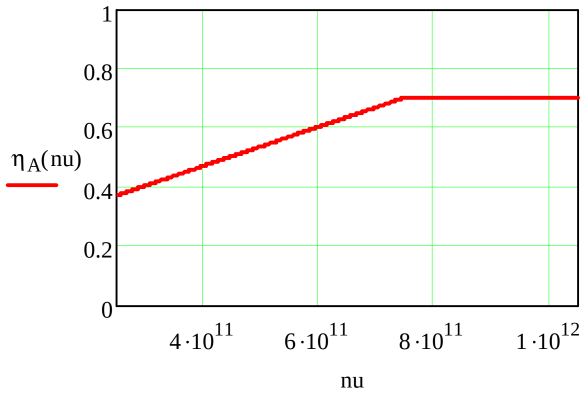

Figure 13: Assumed variation of aperture efficiency with frequency for the FTS

Spillover efficiency (h_S): As for the photometer, this is the fraction of the detector throughput which illuminates the telescope with a fraction ($1 - h_s$) assumed to terminate on the inside of the 2-K detector box. A uniform spillover efficiency of 0.75 is assumed across both bands.

FTS modulation efficiency: A factor of 2 is adopted for the $\cos^2$ modulation efficiency of the FTS. (Note: the efficiency is conventionally quoted as $8^{0.5}$ [10]. The additional $2^{0.5}$ here corresponds to the conversion from post-detection bandwidth to integration time. This is accounted for separately in this model.)

Mirror scan speed (v_{mirr}): The nominal scan speed of the FTS moving mirror is 0.5 mm s^{-1}. The optical path difference is scanned at a rate $v_{scan} = 4(v_{mirr})$ - four times the mirror scan rate due to the folding of the FTS optics.

Audio frequency ranges for the two arrays (f_{elec}): The incident radiation frequencies are converted to audio frequencies in the electrical output of the detector by the motion of the scan mirror. The electrical frequency, f_{elec}, corresponding to OPD scan speed v_{scan} and wavenumber s is given by

$$f_{elec} = v_{scan} s . \qquad (29)$$

For the nominal scan rate, the electrical frequency range is 3.0 – 6.7 Hz for the SLW band and 6.2 – 10.5 Hz for the SSW band.

4.1.6 Background power levels on the detectors

If the power incident on the array is the same from each port (perfect nulling) then the intensity on the array is always the same at all positions of the scan mirror. The background power absorbed (in-band) power is thus equal to 100% of the telescope power that is propagated through the system.

$$Q_{i,k} = \left(10^{12}\right) h_S hfeed_i \int_{Band} e_{i,k}(n)\, td_{i,k}(n)\, AW_i(n)\, B(n, T_{tel})\, dn \qquad \text{pW.} \qquad (30)$$

The limits for the integrals are chosen to encompass the full band in each case. The total background power absorbed by the detector, Q_{det}, is the sum of all these contributions.

Photon noise *NEP*: The contribution of each element to the overall photon noise *NEP* is given by

$$NEPph_{\mathrm{i,k}}^{\;2} = \frac{4h_{\mathrm{S}}h^2}{c^2}\int_{nL_{\mathrm{i}}}^{nU_{\mathrm{i}}} \frac{AW_{\mathrm{i}}(n)e_{\mathrm{i,k}}(n)td_{\mathrm{i,k}}(n)hfeed_{\mathrm{i}}n^4}{exp\left(\frac{hn}{kT_{\mathrm{k}}}\right)-1}\left[1 + \frac{e_{\mathrm{i,k}}(n)td_{\mathrm{i,k}}(n)hfeed_{\mathrm{i}}}{exp\left(\frac{hn}{kT_{\mathrm{k}}}\right)-1}\right]\mathrm{d}n\ . \qquad (31)$$

As for the photometer, this is closely approximated by the familiar simple expression.

4.1.7 Bolometers

As for the photometer, the bolometer parameters are extracted from the EIDP spreadsheets referred to in [7] and are summarised in Table 11.

Parameter	Units	Description	SSW	SLW
R_o	Ω	Resistance parameter	79.3	92.2
T_g	K	Band-gap temperature	42.1	41.0
R_L	MΩ	Load resistance	19.2	23.2
G_o	pW K^{-1}	Static thermal conductance at 300 mK	194	163
C_o	pJ K^{-1}	Heat capacity at 300 mK	1.02	1.0
n		*R-T* index	0.5	0.5
b		Thermal conductivity power-law index	1.30	1.23
r		Heat capacity power-law index	1	1
yield		Fraction of working bolometer channels per array	0.9	0.9

Table 11: Bolometer parameters for the spectrometer

As for the photometer, an excess noise factor shall be included. The values derived from the SVR EIDPs are (1.0, 1.1) for (SSW, SLW). These factors are small – effectively we are assuming that the bolometer performance is close to ideal. For the purpose of the model we adopt a single value of 1.05 for both arrays.

The overall NEP and DQE are calculated pessimistically for each band by adopting the *highest* audio frequency corresponding to that band: $f_{\mathrm{elec}}(sU)$.

4.1.8 Readout electronics

The parameters and their assumed values are the same as for the photometer.

4.2 Derived parameters

4.2.1 Telescope properties

Effective telescope area (A_{tel}): as for photometer model.

Plate scales (*PS*): as for photometer model.

Centre-centre beam spacing on the sky: The spacings between the beams on the sky for the two arrays are given by the plate scales multiplied by the horn external diameters: 49” for the SLW array and 28.3” for the SSW array.

Beam widths: Marc Ferlet's optical modelling now predicts the beam width as a function of wavelength as shown below (from his SVR presentation, slide 18). These numbers will be used and applied to convert to the equivalent surface brightness sensitivities. For SSW, the FWHM varies between 15.5" and 17" from the centre to the band edges. A value of 16" is adopted for the whole band. For SLW, the FWHM varies between 32" and 40" from the centre to the band edges. A value of 35" is adopted for the whole band..

4.2.2 FTS resolving power

We assume that the FTS will operate in one of three modes:

High resolution:	$\Delta s_H = 0.04$ cm^{-1}	$\Delta n_H = 100c\Delta s_H = 1.2$ GHz
Medium resolution	$\Delta\sigma_M = 0.25$ cm^{-1}	$\Delta n_M = 100c\Delta s_H = 7.5$ GHz
Low resolution:	$\Delta s_L = 1$ cm^{-1}	$\Delta n_L = 100c\Delta s_L = 30$ GHz

The resolving power ($l/\Delta l = n/\Delta n$) is given by

$$Res(l) = \frac{10000}{l(?\, s)} , \tag{32}$$

where l is in μm

An alternative version of the resolving power, more familiar to astronomers, involves taking Δs to be the FWHM of the instrument spectral response function. For high resolution mode, this would result in $\Delta s = 0.048$ cm^{-1} instead of 1/(2xOPD) = 0.04 cm^{-1}.

4.2.3 Per-detector NEFDs

Assuming that the S/N in the spectrum is the same as that in the interferogram, and that there are negligible degradations in performance due to non-ideal effects, the basic *NEFD* per detector is related to the overall *NEP* by

$$NEFD\_basic(n, ?\, n) = \frac{\left(2^{1/2}\right)NEP_{\mathrm{tot}}}{h_{\mathrm{A}}(n)hfeed_{\mathrm{ch}}h_{\mathrm{cosq}}A_{\mathrm{tel}}t_{\mathrm{sky}}?\, n} . \tag{33}$$

The same equation applied to both single and double-sided scans for a given integration time .

4.2.4 5-s; 1-hr sensitivities for point source observation (SOF 1)

Point source (SOF 1): The 5-s limiting flux density for a 1-hr observation is

$$DS_{5s\_\mathrm{1hr\_pt}}(n) = \frac{5NEFD\_basic(n, ?\, n)}{2^{0.5}}\frac{1000}{(3600)^{0.5}} \quad \text{mJy.} \tag{34}$$

For the same integration time, the 5-s limiting line strength in is

$$DF_{5s\_\mathrm{1hr\_pt}}(n) = \left[DS_{5s\_\mathrm{1hr\_pt}}(n)\right]Dn\left[\frac{10^{-26}}{1000}\right] \quad \text{W m}^{-2} , \tag{35}$$

where the factor in brackets takes into account the fact that ΔS is in mJy Hz$^{-1/2}$.

Spectral mapping (SOF 2): The field size for jiggle mapping is roughly circular with diameter 2.6 arcmin. The need to jiggle reduces the S/N by a factor of 4 in the same way as for the photometer. We adopt the same factor of 0.34 as for the photometer, although this may be pessimistic since the beam widths are larger than the diffraction limit over significant portions of the spectral bands, resulting in some degree of oversampling.

$$\Delta S_{5\sigma\_1\mathrm{hr\_map}}(\nu) = \frac{\Delta S_{5\sigma\_1\mathrm{hr\_pt}}(\nu)}{0.34} \qquad \Delta F_{5\sigma\_1\mathrm{hr\_map}}(\nu) = \frac{\Delta F_{5\sigma\_1\mathrm{hr\_pt}}(\nu)}{0.34}. \tag{36}$$

4.3 Results

The revised model has been computed in MathCad, and Table 12 summarises the results.

		SSW New telescope	**SLW New telescope**
Absorbed power (pW)		4.1	4.9
Photon noise NEP (W Hz$^{-1/2}$ x 10^{-17})		8.8	7.2
Overall NEP (W Hz$^{-1/2}$ x 10^{-17})		12	10
Basic NEFD (mJy Hz$^{-1/2}$)		20	17
ΔF (5-σ; 1-hr) (W m^{-2} x 10^{-17}) $\Delta\sigma$ = 0.04 cm^{-1}	Point source Fully-sampled map	1.5 5.0	1.2 4.0
ΔS (5-σ; 1-hr) (mJy) $\Delta\sigma$ = 1 cm^{-1}	Point source Fully-sampled map	48 160	39 130

Table 12: FTS sensitivity (at band centres) brought about by adoption of the new model and new telescope

5. Figures to be adopted for HSPOT

For both models, the new figures are based on the best current knowledge of nearly all parameters. There are no margin factors or other allowances for unforeseen problems, whereas the previous models implicitly or explicitly included margin in various parts of the calculation. As discussed at the SPIRE SVR-2, an overall "pessimism factor" will be applied to take into account any unmodelled effects that could degrade the sensitivity. Following discussion within the consortium and at the Herschel Science Team in January 2006, it was decided to adopt the following approach:

The as-calculated sensitivities are degraded by the following "pessimistic factors": sqrt(3) for the photometer and 2 for the FTS. The larger value for the FTS takes into account the uncertainties which remain and the need for further analysis and comparison with ILT results.

In both cases the Observers Manual contains strong statements warning users to be aware of the fact that the calculations are based on best available information and models, and that the in-flight performance of SPIRE could be worse or better by a factor of two or more due to uncertainties in the model.

The nominal case photometer sensitivities are then as in Table 13. The new nominal case is typically better a factor of about 2 in sensitivity (four in speed). Note that the time to map 1 sq. deg. are not directly comparable as the new values do not include any overheads.

		PSW	PMW	PLW
Δ*S*(5-σ; 1-hr) mJy	Point source (7-pt)	1.8	2.2	1.7
	4’ x 4’ jiggle map	6.2	8.4	7.1
	4’ x 8’ scan map	3.7	5.3	4.6
Time (hrs) to map 1 deg.^{2} to 3 mJy 1-*s*		7.8	16	13

Table 13: Nominal photometer sensitivities

For the FTS, the nominal case variation of point source sensitivity limit across the two bands is as shown in Figure 14 (line flux) and Figure 15 (continuum flux density in low-res mode).

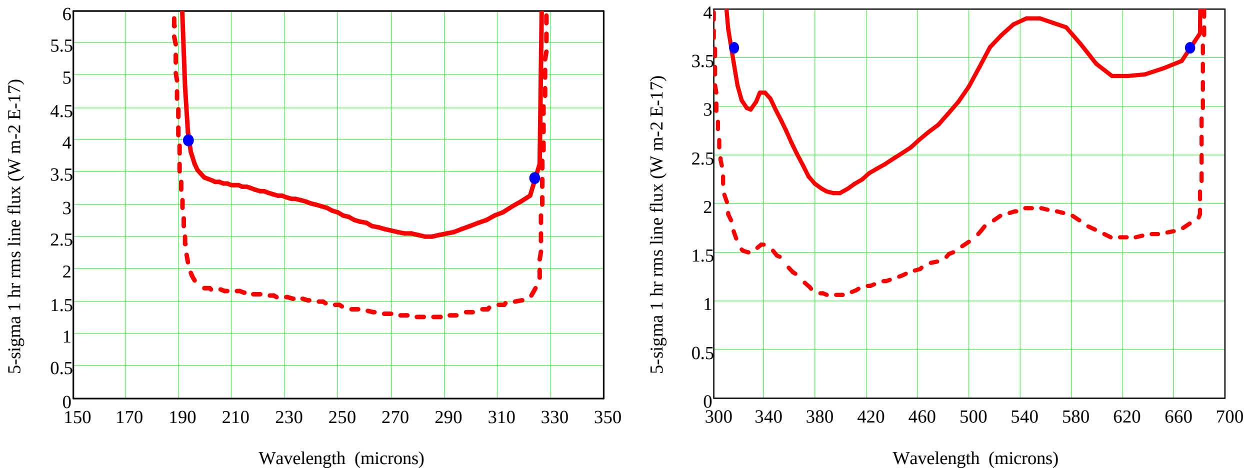

Figure 14: 5 *s* ; 1 hr line flux limit vs. wavelength for SSW (left) and SLW (right). Dotted lines: limits as computed. Solid lines: nominal case (as computed x 2). The operational limits of the bands are indicated by the blue dots.

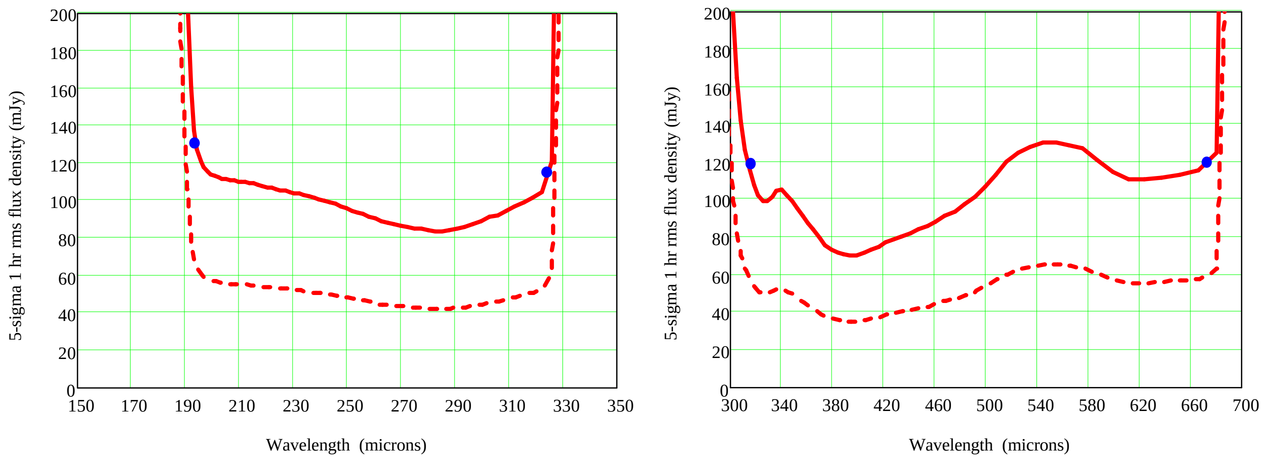

Figure 15: Low resolution mode 5 *s* ; 1 hr flux density limit vs. wavelength for SSW (left) and SLW (right). Dotted lines: limits as computed. Solid lines: nominal case (as computed x 2) The operational limits of the bands are indicated by the blue dots.

6. List of annexes

Annex 1: Photometer MathCAD Model (SPIRE_Phot_9.mcd)

Annex 2: Spectrometer MathCAD Model (SPIRE_FTS_8.mcd)

Annex 3: Calculation of telescope obscuration factor

Annex 4: SPIRE beams and S/N enhancement from pixel co-addition

7. References

1 Griffin, M, Swinyard, B, and King, K. Operating Modes for the SPIRE Instrument. SPIRE-RAL-DOC-000320, Version 3.3, 2 June 2005.

2 Fischer, J, T Klassen, N Hovenier, G Jacob, A Poglitsch, and O Sternberg. Cryogenic far-infrared laser absorptivity measurements of the Herschel Space Observatory telescope mirror coatings. *Applied Optics*, 43, 3765, 2004.

3 Frey, H. and Hartmann, H, Herschel Straylight Calculation Results, *HP-2-ASED-TN-0023*, 29 Sept. 2004.

4 Griffin, M, J J Bock, and W K Gear. The Relative Performance of Filled and Feedhorn-Coupled Focal Plane Architecture. *Applied Optics*, 31, 6543, 2003.

5 Mather J C. Bolometer noise: nonequilibrium theory. *Applied Optics* 21, 1125, 1982.

6 Sudiwala R V, M J Griffin, and A L Woodcraft. Thermal modelling and characterisation of semiconductor bolometers. *Int. J. Infrared. Mm. Waves,* 23, 575, 2002.

7 Griffin, M.. Bolometer Array Performance Estimation from JPL EIDP Spreadsheets. *SPIRE-UCF-REP-002569*, 16 Jan. 2006.

8 Sibthorpe, B., Waskett, T., and Griffin, M. The impact of 1/*f* noise on extraction of extended structure from scanning photometric observations. *MNRAS* (submitted).

9 Chattopadhyay, G., J Glenn, J J Bock, B K Rownd, M Caldwell, and M J Griffin. Feedhorn Coupled Bolometer Arrays for SPIRE: design, simulations and measurement. *IEEE Transactions on Microwave Theory and Techniques*. 51, 10, 2139, 2003.

10 Treffers, R Signal-to-noise ratio in Fourier spectroscopy. *Applied Optics*, 16, 3103, 1977.

Annex 1: Revised Photometer sensitivity model — SPIRE_Phot_9.mcd

Updated after January 2007 HST — January 16 2007

Constants $h \equiv 6.626\cdot 10^{-3\cdot}$ $c \equiv 3\cdot 10^{8}$ $kb \equiv 1.38\cdot 10^{-23}$

$origin \equiv 1$

Planck function $$B(nu,T) := \frac{2\cdot h\cdot nu^{3}}{c^{2}\cdot\left(e^{\frac{h\cdot nu}{kb\cdot T}}-1\right)}$$

Key Input parameters

Index for the three bands $i \equiv 1,2..3$ **1 = PSW** **PM = PMW** **3 = PLW**

Reflector temp. (K) $Ttel := 80$ **Used diameter (m)** $Dtel \equiv 3.285$

Obscuration factor $Obs\_factor \equiv 0.872$ **Telescope focal ratio** $Ftel \equiv 8.68$

Telescope emissivity

Formula from Fischer et al. $$\varepsilon_{ref}(nu) := 0.0336\cdot\left(\frac{c\cdot 10^{6}}{nu}\right)^{-0.5} + 0.273\cdot\left(\frac{c\cdot 10^{6}}{nu}\right)^{-1}$$

Total telescope emissivity $$\varepsilon_{tel}(nu) := 2\cdot\varepsilon_{ref}(nu)$$

Stray light model

Based on pessimistic industry model:
20% of a 70-K telescope with 3% emissivity

$T_{stray} := 70$ $\varepsilon_{stray} := 0.2\cdot 0.03$

Overall total emissivity including stray light (referred to 80 K) $$\varepsilon_{tot}(nu) := \varepsilon_{tel}(nu) + \varepsilon_{stray}\cdot\frac{70}{80}$$

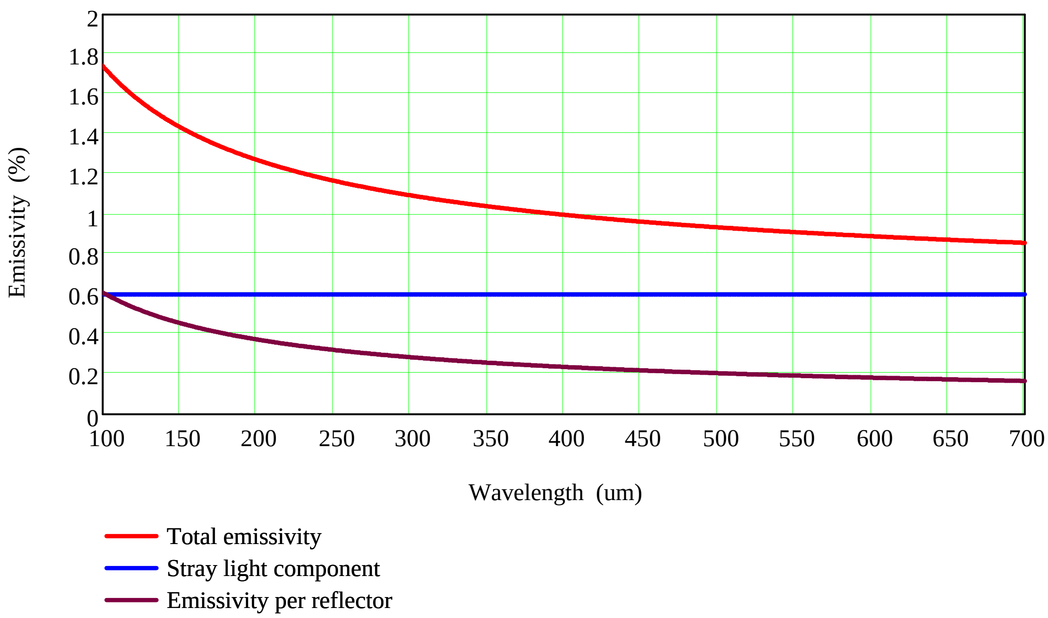

Spillover efficiency (signal) $\eta_S \equiv 0.8$

Background coupling efficiency $\eta_B := 0.9$

Aperture efficiency $\eta_A := 0.7$

Final optics focal ratio $Ffin \equiv 5$

Instrument mirror reflectivity $t_{mirr} := 0.995$

Mirror emissivity $\varepsilon_{mirr} := 1 - t_{mirr}$

BSM transmission $t_{BSM} := 0.95$

BSM emissivity $\varepsilon_{BSM} := 0.012$

Feedhorn throughput (m² sr) $A\Omega(\nu) := \left(\frac{c}{\nu}\right)^2$

Chopping efficiency $\eta ch := 0.5$

He-3 temp. (K) $To \equiv 0.310$

Level-1 temp. (K) $TL1 := 5.5$

Level-0 temp. (K) $TL0 := 1.8$

JFET plus amplifier noise (V Hz^-1/2) $enA := 10 \cdot 10^{-9}$

Field area efficiency factor $\eta field_i := \begin{bmatrix} 1.0 \\ 0.95 \\ 0.90 \end{bmatrix}$

Bolometer yield $yield_i \equiv \begin{bmatrix} 0.95 \\ 0.95 \\ 0.95 \end{bmatrix}$

Feed efficiency $\eta feed_i := \begin{bmatrix} 0.7 \\ 0.7 \\ 0.77 \end{bmatrix}$

Bolometer parameters

Material band-gap temperature (K) $T_{G_i} := \begin{bmatrix} 41.0 \\ 42.1 \\ 41.8 \end{bmatrix}$

Resistance parameter (W) $R_{S_i} := \begin{bmatrix} 92.1 \\ 69.5 \\ 104 \end{bmatrix}$

Load resistance (MW) $R_{L_i} \equiv \begin{bmatrix} 16.3 \\ 16.5 \\ 16.1 \end{bmatrix}$

Heat capacity at 300 mK (pJ K-1) $Co_i \equiv \begin{bmatrix} 0.52 \\ 0.59 \\ 0.63 \end{bmatrix}$

Thermal conductivity index $\beta_i \equiv \begin{bmatrix} 1.5 \\ 1.7 \\ 1.7 \end{bmatrix}$

Thermal conductance at 300 mK (pW K-1) $G_i := \begin{bmatrix} 65.1 \\ 65.7 \\ 67.4 \end{bmatrix}$

Material parameter $\delta_i := \frac{T_{G_i}}{To}$

Static thermal conductance at bath temp. (pW K⁻¹) $GS0_i := G_i \cdot 10^{-12} \cdot \left(\frac{To}{0.300}\right)^{\beta_i}$

R-T power law index $n \equiv 0.5$

Heat capacity index $\rho_i \equiv 1$

Noise degradation factor $f_i := \begin{bmatrix} 1.05 \\ 1.05 \\ 1.05 \end{bmatrix}$

Bands

$$\begin{pmatrix} PLW \\ PMW \\ PSW \\ SLW \\ SSW \end{pmatrix} :=$$

Worksheet

$Freq_{PL} := PLW^{\langle 0 \rangle} \cdot 100 \cdot c \quad tfil_3(nu) := linterp\left(Freq_{PL}, PLW^{\langle 1 \rangle}, nu\right)$

$Freq_{PM} := PMW^{\langle 0 \rangle} \cdot 100 \cdot c \quad tfil_2(nu) := linterp\left(Freq_{PM}, PMW^{\langle 1 \rangle}, nu\right)$

$Freq_{PS} := PSW^{\langle 0 \rangle} \cdot 100 \cdot c \quad tfil_1(nu) := linterp\left(Freq_{PS}, PSW^{\langle 1 \rangle}, nu\right)$

Plot bads with old nominal edges for comparison

$\lambda Lold_i \equiv$

208.3
303.0
431.0

$\lambda Uold_i \equiv$

291.7
420.0
603.2

$TopU_i := \dfrac{c \cdot 10^6}{\lambda Lold_i} \qquad TopL_i := \dfrac{c \cdot 10^6}{\lambda Uold_i}$

$TopU_i =$

$1.440 \cdot 10^{12}$
$9.901 \cdot 10^{11}$
$6.961 \cdot 10^{11}$

$TopL_i =$

$1.028 \cdot 10^{12}$
$7.143 \cdot 10^{11}$
$4.973 \cdot 10^{11}$

$s := 0..1$

$TopSWL_s := TopU_1 \quad TopSWU_s := TopL_1 \quad TopMWL_s := TopU_2 \quad TopMWU_s := TopL_2$

$TopLWL_s := TopU_3 \quad TopLWU_s := TopL_3$

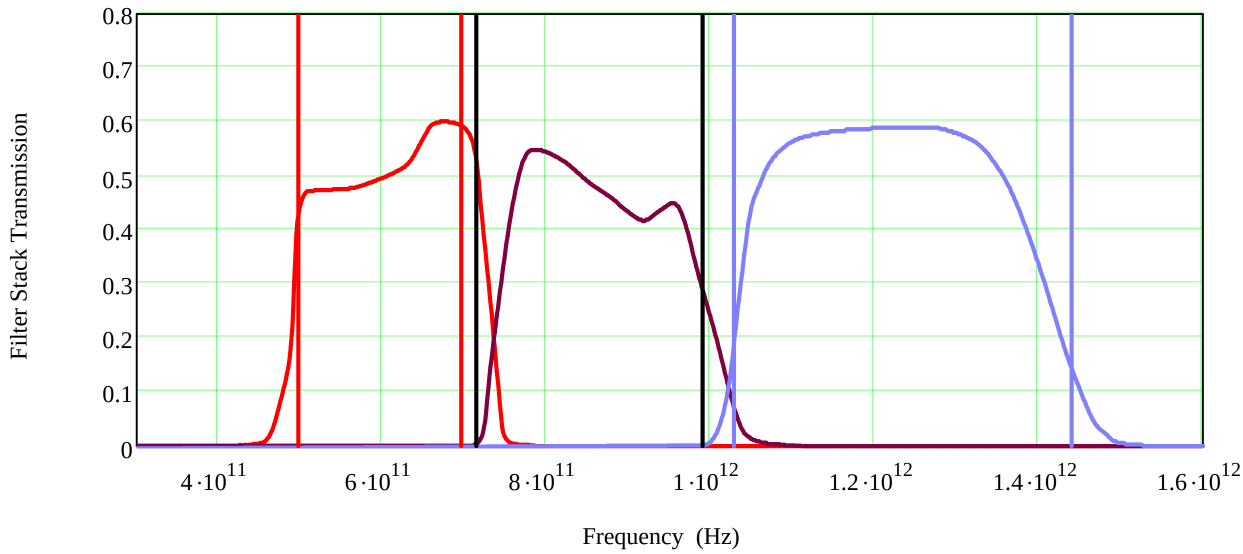

Limits for integration over the filter passbands

$\nu limL_i :=$

$9 \cdot 10^{11}$
$7 \cdot 10^{11}$
$4 \cdot 10^{11}$

$\nu limU_i :=$

$1.6 \cdot 10^{12}$
$1.1 \cdot 10^{12}$
$8 \cdot 10^{11}$

Top-hat approximations **PLW**

Specify two frequencies between which to derive the mean level

$\nu_{3\_L} := 5.0 \cdot 10^{11}$ $\nu_{3\_U} := 7.195 \cdot 10^{11}$

Calculate mean value in that interval

$$tfil_{pk_3} := \frac{\int_{\nu_{3\_L}}^{\nu_{3\_U}} tfil_3(nu)\, dnu}{\nu_{3\_U} - \nu_{3\_L}} \qquad tfil_{pk_3} = 0.521$$

Calculate points at which mean value is 50% of this level

$$\frac{tfil_{pk_3}}{2} = 0.260$$

Specify 50% points and central freq. (Hz) and wavelength (mm)

$\nu L_3 := 4.906 \cdot 10^{11}$ $\nu U_3 := 7.323 \cdot 10^{11}$

$\nu o_3 := 0.5 \cdot (\nu L_3 + \nu U_3)$ $\nu o_3 = 6.114 \times 10^{11}$

$\lambda o_3 := \frac{c}{\nu o_3}$ $\lambda o_3 \cdot 10^6 = 491$

Bandwidth and resolution

$\Delta\nu_3 := \nu U_3 - \nu L_3$ $Res_3 := \frac{\nu o_3}{\Delta\nu_3}$ $Res_3 = 2.53$

Define top-hat approximation

$$TH_3(\nu) := \text{if}\left(\left|\nu - \nu o_3\right| < \frac{\Delta\nu_3}{2}, 1, 0\right) \qquad tfil_{pk_3} = 0.521$$

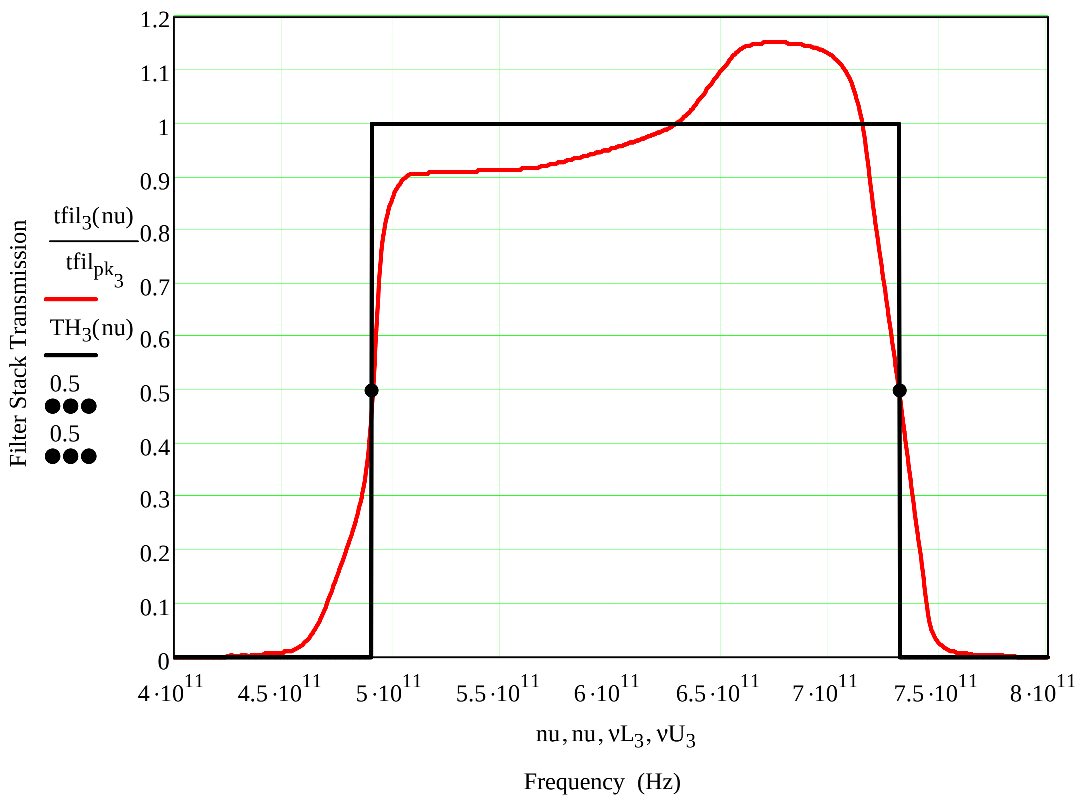

PMW

Specify two frequencies between which to derive the mean level

$\nu_{2\_L} := 7.6 \cdot 10^{11}$ $\qquad$ $\nu_{2\_U} := 9.5 \cdot 10^{11}$

Calculate mean value in that interval

$$tfil_{pk_2} := \frac{\int_{\nu_{2\_L}}^{\nu_{2\_U}} tfil_2(nu)\, dnu}{\nu_{2\_U} - \nu_{2\_L}} \qquad tfil_{pk_2} = 0.483$$

Calculate points at which mean value is 50% of this level

$$\frac{tfil_{pk_2}}{2} = 0.242$$

Specify 50% points and central freq. (Hz) and wavelength (mm)

$\nu L_2 := 7.40 \cdot 10^{11}$ $\qquad$ $\nu U_2 := 9.98 \cdot 10^{11}$

$\nu o_2 := 0.5 \cdot (\nu L_2 + \nu U_2)$ $\qquad$ $\nu o_2 = 8.690 \times 10^{11}$

$\lambda o_2 := \frac{c}{\nu o_2}$ $\qquad$ $\lambda o_2 \cdot 10^6 = 345$

Bandwidth and resolution

$\Delta\nu_2 := \nu U_2 - \nu L_2$ $\qquad$ $Res_2 := \frac{\nu o_2}{\Delta\nu_2}$ $\qquad$ $Res_2 = 3.37$

Define top-hat approximation

$$TH_2(\nu) := \text{if}\left(\left|\nu - \nu o_2\right| < \frac{\Delta\nu_2}{2}, 1, 0\right)$$

$tfil_{pk_2} = 0.483$

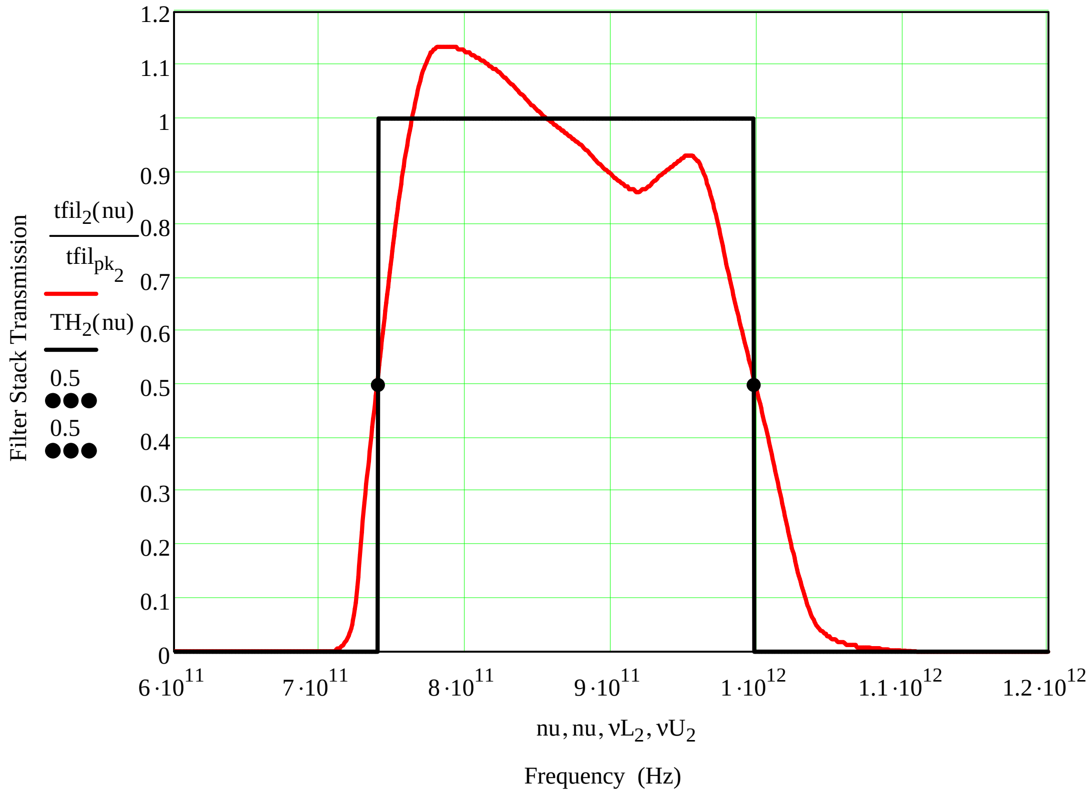

PSW

Specify two frequencies between which to derive the mean level

$\nu_{1\_L} := 1.08 \cdot 10^{12}$ $\nu_{1\_U} := 1.34 \cdot 10^{12}$

Calculate mean value in that interval

$$tfil_{pk_1} := \frac{\int_{\nu_{1\_L}}^{\nu_{1\_U}} tfil_1(nu)\, dnu}{\nu_{1\_U} - \nu_{1\_L}}$$

$tfil_{pk_1} = 0.579$

Calculate points at which mean value is 50% of this level

$\frac{tfil_{pk_1}}{2} = 0.289$

Specify 50% points and central freq. (Hz) and wavelength (mm)

$\nu L_1 := 1.036 \cdot 10^{12}$ $\nu U_1 := 1.411 \cdot 10^{12}$

$\nu o_1 := 0.5 \cdot (\nu L_1 + \nu U_1)$ $\nu o_1 = 1.224 \times 10^{12}$

$\lambda o_1 := \frac{c}{\nu o_1}$ $\lambda o_1 \cdot 10^6 = 245$

Bandwidth and resolution

$\Delta\nu_1 := \nu U_1 - \nu L_1$ $Res_1 := \frac{\nu o_1}{\Delta\nu_1}$ $Res_1 = 3.26$

Define top-hat approximation

$TH_1(\nu) := if\left(|\nu - \nu o_1| < \frac{\Delta\nu_1}{2}, 1, 0\right)$ $tfil_{pk_1} = 0.579$

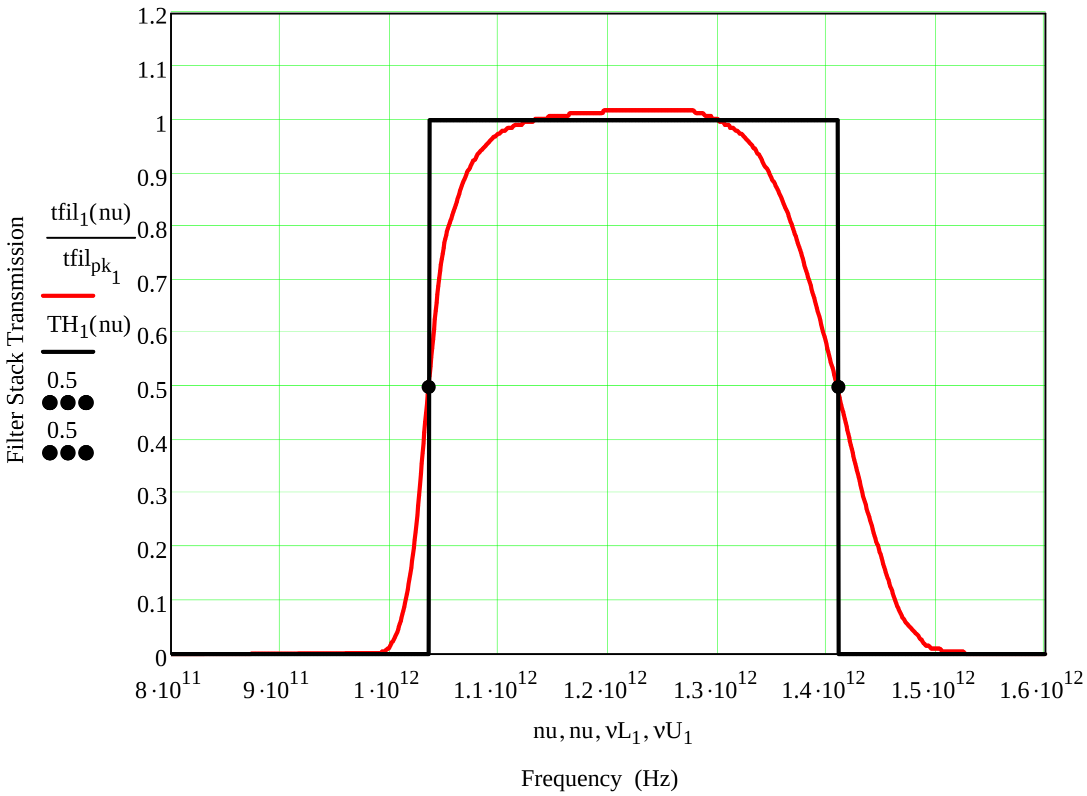

Summary of filter top-hat approximations

Lowe Edge (GHz)	Upper Edge (GHz)	Lower Edge (mm)	Upper Edge (mm)	Centre (mm)	l/Dl

$$\nu L_i \cdot 10^{-9} = \begin{pmatrix} 1036 \\ 740 \\ 491 \end{pmatrix} \quad \nu U_i \cdot 10^{-9} = \begin{pmatrix} 1411 \\ 998 \\ 732 \end{pmatrix} \quad \frac{c \cdot 10^6}{\nu U_i} = \begin{pmatrix} 213 \\ 301 \\ 410 \end{pmatrix} \quad \frac{c \cdot 10^6}{\nu L_i} = \begin{pmatrix} 290 \\ 405 \\ 611 \end{pmatrix} \quad \lambda o_i \cdot 10^6 = \begin{pmatrix} 245 \\ 345 \\ 491 \end{pmatrix} \quad Res_i = \begin{pmatrix} 3.26 \\ 3.37 \\ 2.53 \end{pmatrix}$$

Select channel and filter band for computation

$ch := 1 \qquad t_{fil}(\nu) := tfil_1(\nu)$

1 for PSW
2 for PMW
3 for PLW

$k := 1, 2..5$

Transmissions of individual elements

Telescope primary $\quad t_1(\nu) := 1 - \varepsilon_{ref}(\nu) \qquad \varepsilon_1(\nu) := \varepsilon_{ref}(\nu)$

Telescope secondary $\quad t_2(\nu) := 1 - \varepsilon_{ref}(\nu) \qquad \varepsilon_2(\nu) := \varepsilon_{ref}(\nu)$

Stray light source $\quad t_3(\nu) := 1 \qquad \varepsilon_3(\nu) := \varepsilon_{stray}$

Level 1 $\quad t_4(\nu) := t_{mirr}{}^5 \cdot t_{BSM} \cdot t_{fil}(\nu)^{\frac{2}{6}} \qquad \varepsilon_4(\nu) := 1 - t_4(\nu)$

Level 0 $\quad t_5(\nu) := t_{mirr}{}^2 \cdot t_{fil}(\nu)^{\frac{4}{6}} \qquad \varepsilon_5(\nu) := 1 - t_5(\nu)$

Transmissions to detector

Telescope primary $\quad td_1(\nu) := t_2(\nu) \cdot t_4(\nu)\, t_5(\nu)$

Sky $\quad t_{sky}(\nu) := t_1(\nu) \cdot td_1(\nu)$

Telescope secondary $\quad td_2(\nu) := t_4(\nu) \cdot t_5(\nu)$

Stray light source $\quad td_3(\nu) := t_4(\nu) \cdot t_5(\nu)$

Level 1 $\quad td_4(\nu) := t_5(\nu)$

Level 0 $\quad td_5(\nu) := 1$

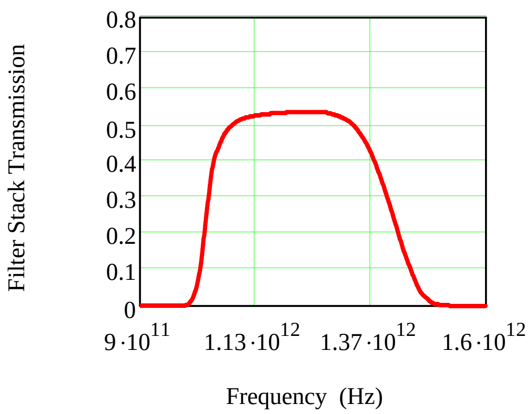

Beamwidths

Effective telescope area (m²)

$$Atel := \frac{\pi \cdot Dtel^2}{4} \cdot Obs\_factor \qquad Atel = 7.39$$

Plate scale at telescope focus (arcsec/mm):

$$PStel := \frac{1}{Dtel \cdot Ftel} \cdot \frac{360}{2 \cdot \pi} \cdot 3.6 \qquad PStel = 7.23$$

Plate scale at arrays (arcsec/mm):

$$PSa := PStel \cdot \frac{Ftel}{Ffin} \qquad PSa = 12.6$$

Beamwidths (arcsec.) and areas (sr):

$$FWHM_i := \frac{1.03 \cdot \lambda o_i}{Dtel} \cdot \frac{360}{2 \cdot \pi} \cdot 3600$$

$$FWHM_i = \begin{pmatrix} 15.9 \\ 22.3 \\ 31.7 \end{pmatrix}$$

$$\pi \left(1.03 \cdot \lambda o_i \right)^2$$

$$Abeam_i = \begin{pmatrix} 4.64 \times 10^{-9} \\ 9.20 \times 10^{-9} \\ 1.86 \times 10^{-8} \end{pmatrix}$$

Over-ride with nominal values (arcsec.)

$FWHM_i :=$

18
25
36

$$Abeam_i := \left(\frac{FWHM_i}{3600} \cdot \frac{2 \cdot \pi}{360} \right)^2 \cdot \frac{\pi}{4}$$

$Abeam_i =$

5.981·10-9
1.154·10-8
2.392·10-8

$\left(Abeam_i\right)^{-1} \cdot 10^{-6} =$

167.2
86.7
41.8

Background power levels on the detectors (pW)

Primary

$$Q_1 := 10^{12} \cdot \eta_S \cdot \eta_B \cdot \eta feed_{ch} \cdot \int_{\nu limL_{ch}}^{\nu limU_{ch}} \varepsilon_1(\nu) \cdot td_1(\nu) \cdot A\Omega(\nu) \cdot B(\nu, Ttel)\, d\nu \qquad Q_1 = 0.48$$

Secondary

$$Q_2 := 10^{12} \cdot \eta_S \cdot \eta_B \cdot \eta feed_{ch} \cdot \int_{\nu limL_{ch}}^{\nu limU_{ch}} \varepsilon_2(\nu) \cdot td_2(\nu) \cdot A\Omega(\nu) \cdot B(\nu, Ttel)\, d\nu \qquad Q_2 = 0.48$$

Stray light

$$Q_3 := 10^{12} \cdot \eta_S \cdot \eta_B \cdot \eta feed_{ch} \cdot \int_{\nu limL_{ch}}^{\nu limU_{ch}} \varepsilon_3(\nu) \cdot td_3(\nu) \cdot A\Omega(\nu) \cdot B(\nu, T_{stray})\, d\nu \qquad Q_3 = 0.73$$

Level 1

$$Q_4 := 10^{12} \cdot \eta_S \cdot \eta_B \cdot \eta feed_{ch} \cdot \int_{\nu limL_{ch}}^{\nu limU_{ch}} \varepsilon_4(\nu) \cdot td_4(\nu) \cdot A\Omega(\nu) \cdot B(\nu, TL1)\, d\nu \qquad Q_4 = 2.07 \times 10^{-3}$$

Level 0

$$\int_{\nu limL_{ch}}^{\nu limU_{ch}} \varepsilon_5(\nu) \cdot td_5(\nu) \cdot A\Omega(\nu) \cdot B(\nu, TL0)\, d\nu \qquad Q_5 = 1.06 \times 10^{-9}$$

Summary

$$Q_k = \begin{pmatrix} 0.48 \\ 0.48 \\ 0.73 \\ 2.07 \times 10^{-3} \\ 1.06 \times 10^{-9} \end{pmatrix}$$

Total background power (pW)

$$Q_{tot} := Q_1 + Q_2 + Q_3 + Q_4 + Q_5 \qquad Q_{tot} = 1.70$$

Photon noise limited NEP (W Hz$^{-1/2}$ E-17)

$$NEPph_1 := \left[\frac{4\cdot\eta_S\cdot\eta_B\cdot h^2}{c^2}\cdot\left[\int_{\nu limL_{ch}}^{\nu limU_{ch}} \frac{A\Omega(\nu)\cdot\varepsilon_1(\nu)\cdot td_1(\nu)\cdot\eta feed_{ch}\cdot\nu^4}{e^{\frac{h\cdot\nu}{kb\cdot Ttel}}-1}\cdot\left(1+\frac{\varepsilon_1(\nu)\cdot td_1(\nu)\cdot\eta feed_{ch}}{e^{\frac{h\cdot\nu}{kb\cdot Ttel}}-1}\right)d\nu\right]\right]^{0.5}\cdot 10^{17}$$

$$NEPph_2 := \left[\frac{4\cdot\eta_S\cdot\eta_B\cdot h^2}{c^2}\cdot\left[\int_{\nu limL_{ch}}^{\nu limU_{ch}} \frac{A\Omega(\nu)\cdot\varepsilon_2(\nu)\cdot td_2(\nu)\cdot\eta feed_{ch}\cdot\nu^4}{e^{\frac{h\cdot\nu}{kb\cdot Ttel}}-1}\cdot\left(1+\frac{\varepsilon_2(\nu)\cdot td_2(\nu)\cdot\eta feed_{ch}}{e^{\frac{h\cdot\nu}{kb\cdot Ttel}}-1}\right)d\nu\right]\right]^{0.5}\cdot 10^{17}$$

$$NEPph_3 := \left[\frac{4\cdot\eta_S\cdot\eta_B\cdot h^2}{c^2}\cdot\left[\int_{\nu limL_{ch}}^{\nu limU_{ch}} \frac{A\Omega(\nu)\cdot\varepsilon_3(\nu)\cdot td_3(\nu)\cdot\eta feed_{ch}\cdot\nu^4}{e^{\frac{h\cdot\nu}{kb\cdot Ttel}}-1}\cdot\left(1+\frac{\varepsilon_3(\nu)\cdot td_3(\nu)\cdot\eta feed_{ch}}{e^{\frac{h\cdot\nu}{kb\cdot Ttel}}-1}\right)d\nu\right]\right]^{0.5}\cdot 10^{17}$$

$$NEPph_4 := \left[\frac{4\cdot\eta_S\cdot\eta_B\cdot h^2}{c^2}\cdot\left[\int_{\nu limL_{ch}}^{\nu limU_{ch}} \frac{A\Omega(\nu)\cdot\varepsilon_4(\nu)\cdot td_4(\nu)\cdot\eta feed_{ch}\cdot\nu^4}{e^{\frac{h\cdot\nu}{kb\cdot TL1}}-1}\cdot\left(1+\frac{\varepsilon_4(\nu)\cdot td_4(\nu)\cdot\eta feed_{ch}}{e^{\frac{h\cdot\nu}{kb\cdot TL1}}-1}\right)d\nu\right]\right]^{0.5}\cdot 10^{17}$$

$$NEPph_5 := \left[\frac{4\cdot\eta_B\cdot h^2}{c^2}\cdot\left[\int_{\nu limL_{ch}}^{\nu limU_{ch}} \frac{A\Omega(\nu)\cdot\varepsilon_5(\nu)\cdot td_5(\nu)\cdot\eta feed_{ch}\cdot\nu^4}{e^{\frac{h\cdot\nu}{kb\cdot TL0}}-1}\cdot\left(1+\frac{\varepsilon_5(\nu)\cdot td_5(\nu)\cdot\eta feed_{ch}}{e^{\frac{h\cdot\nu}{kb\cdot TL0}}-1}\right)d\nu\right]\right]^{0.5}\cdot 10^{17}$$

Summary

$$NEPph_k = \begin{pmatrix} 2.80 \\ 2.80 \\ \\ 0.18 \\ 1.15\times 10^{-4} \end{pmatrix}$$

$$NEPph_{tot} := \left[\left(NEPph_1\right)^2+\left(NEPph_2\right)^2+\left(NEPph_3\right)^2+\left(NEPph_4\right)^2+\left(NEPph_5\right)^2\right]^{0.5}$$

$$NEPph_{tot} = 5.49$$

Bolometer model

Material band-gap temperature (K)	Resistance parameter (Ω)	Load resistance (MΩ)	Static thermal conductance at 300 mK (pW K-1)	Heat capacity at 300 mK (pJ K-1)
$T_{G_{ch}} = 41.0$	$R_{S_{ch}} = 92$	$R_{L_{ch}} = 16.3$	$G_{ch} = 65.100$	$Co_{ch} = 0.52$

Heat capacity index	Thermal conductivity index	R-T power law index	Loading parameter	Resistance parameter (W)
$\rho_{ch} = 1.0$	$\beta_{ch} = 1.5$	$n = 0.500$	$\gamma_{ch} := \dfrac{Q_{tot}\cdot 10^{-12}}{To\cdot GS0_{ch}}$	$R_{S_{ch}} = 92.1$

Bias parameter

$$b := 0, 1 .. 200$$

$$\phi_b := 1 + \frac{b}{200}$$

Resistance (MΩ)

$$R_b := R_{S_{ch}}\cdot \exp\left[\left[\left(\frac{\delta_{ch}}{\phi_b}\right)^n\right]\right]\cdot 10^{-6}$$

Electrical power (if P < 0, set P = 0)

$$PP_b := To\cdot GS0_{ch}\cdot\left[\frac{(\phi_b)^{\beta_{ch}+1} - 1}{\beta_{ch}+1} - \gamma_{ch}\right]$$

$$P_b := \mathrm{if}\left(PP_b < 0, 0, PP_b\right)$$

Temp. coeff of resistance

$$\alpha_b := \frac{-n\cdot(\delta_{ch})^n}{(\phi_b)^{n+1}\cdot To}$$

Load curves: V (mV) and I (nA)

$$V_b := \left(P_b\cdot R_b\right)^{0.5}\cdot 10^6 \qquad I_b := \left(\frac{P_b}{R_b\cdot 10^6}\right)^{0.5}\cdot 10^9$$

Select bias voltage to correspond to the optimum bias point calculated below (based on best NEP)

$$Vo := 0.0159$$

Load line equation

$$Vload_b := \left(Vo - I_b\cdot 10^{-9}\cdot R_{L_{ch}}\cdot 10^6\right)\cdot 1000$$

Check: determine the point on the calculated VI nearest to the optimum operating point

$$Diff_b := \left|V_b - Vload_b\right|$$

$$Op\_pt\_S_b := \mathrm{if}\left(Diff_b = \min(Diff), b, 0\right) \qquad Op\_S := \max(Op\_pt\_S) \qquad Op\_S = 34$$

This is the same as the value calculated below for optimum NEP

Gd and Ge (pW K-1)

$$Gd_b := GS0_{ch} \cdot \left[(\phi_b)^{\beta_{ch}} \right]$$

$$Ge_b := Gd_b - \alpha_b \cdot P_b \cdot \left(\frac{R_{L_{ch}} - R_b}{R_{L_{ch}} + R_b} \right)$$

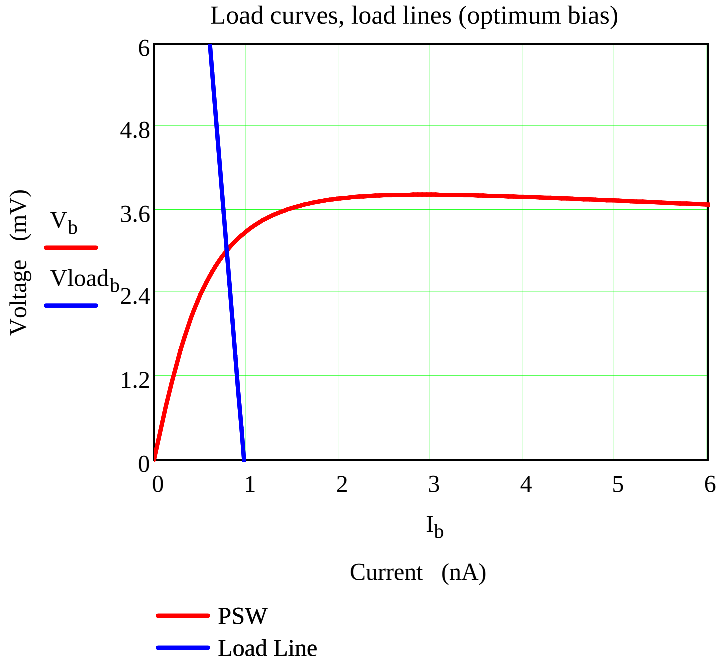

Dynamic impedance (MW)

$$Z_b := \frac{Gd_b + \alpha_b \cdot P_b}{Gd_b - \alpha_b \cdot P_b} \cdot R_b$$

Heat capacity (J K-1)

$$C_b := Co \cdot 10^{-12} \cdot \left(\frac{To \cdot \phi_b}{0.300} \right)^{\rho}$$

DC Responsivity (V W-1):

$$S_b := \mathrm{if}\left[I_b = 0, 1, \frac{(R_b - Z_b) \cdot 10^6}{2 \cdot V_b \cdot 10^{-3}} \cdot \frac{R_{L_{ch}}}{Z_b + R_{L_{ch}}} \right]$$

Normalised responsivity

$$Snorm := \frac{S}{\max(S)}$$

Operating point for maximum responsivity

$$Sopt_b := \mathrm{if}\left(Snorm_b = \max(Snorm), b, 0 \right) \qquad \max(Sopt) = 32$$

Bolometer voltage (mV) and current (nA) at optimum operating point for peak responsivity

$$I_{\max(Sopt)} = 0.73 \qquad V_{\max(Sopt)} = 2.90$$

Optimum bias voltages (mV) for peak responsivity

$$Vo\_opt := V_{\max(Sopt)} + I_{\max(Sopt)} \cdot R_{L_{ch}} \qquad Vo\_opt = 14.8$$

Note that this is slightly lower bias point than for optimum NEP

Phonon NEP
(W Hz$^{-1/2}$ E-17):

$$NEPp_b := \text{if}\left[I_b = 0, 1, \left[4\cdot kb\cdot To^2\cdot GS0_{ch}\cdot\frac{\beta_{ch}+1}{2\cdot\beta_{ch}+3}\cdot\frac{(\phi_b)^{2\cdot\beta_{ch}+3}-1}{(\phi_b)^{\beta_{ch}+1}-1}\right]^{0.5}\right]\cdot 10^{17}$$

Johnson NEP
(W Hz$^{-1/2}$2 E-17):

$$NEPj_b := \left[4\cdot kb\cdot To^2\cdot GS0_{ch}\cdot\frac{(\phi_b)^{2\cdot\beta_{ch}+2\cdot n+3}}{n^2\cdot(\delta_{ch})^{2\cdot n}\cdot\left[\frac{(\phi_b)^{\beta_{ch}+1}-1}{\beta_{ch}+1}-\gamma_{ch}\right]}\right]^{0.5}\cdot 10^{17}$$

Load resistor NEP
(W Hz-1/2W Hz$^{-1/2}$

$$NEPload_b := \left(\frac{4\cdot kb\cdot To}{R_{L_{ch}}\cdot 10^6}\right)^{0.5}\cdot\left|\frac{Z_b\cdot R_{L_{ch}}\cdot 10^6}{Z_b+R_{L_{ch}}}\right|\cdot\frac{1}{S_b}\cdot 10^{17}$$

Amplifier NEP
(W Hz$^{-1/2}$ E-17):

$$NEPamp_b := \frac{enA}{S_b}\cdot 10^{17}$$

Total DC detector NEP at
LIA output (W Hz$^{-1/2}$ E-17):

$$NEPlia_b := \left[\left(NEPp_b\right)^2+\left(NEPj_b\right)^2+\left(NEPamp_b\right)^2+\left(NEPload_b\right)^2\right]^{0.5}$$

Optimum NEP values
(W Hz$^{-1/2}$ E-17)

$NEPop := \min(NEPlia)$ $\quad$ $NEPop = 4.15$

Optimum bias points
for best NEP

$index_b := \text{if}\left(NEPlia_b = \min(NEPlia), b, 0\right)$ $\quad$ $p := \max(index)$ $\quad$ $p = 34$

Optimum bias
voltages for
best NEP

Bolometer voltage
(mV) and current (nA)

$I_p = 0.79$ $\quad$ $V_p = 3.01$

Optimum bias
voltages (mV)

$Vo\_opt := V_p + I_p\cdot R_{L_{ch}}$ $\quad$ $Vo\_opt = 15.9$

Responsivity (V W-1), time constants (ms), and 3-dB freq. at optimum bias

DC responsivity	**Effective time constant (ms)**	**Physical time constant (ms)**	**3-dB freq. (Hz)**	**DC detector NEPop ($W\ Hz^{-1/2}$ E-17)**
$Sop := S_p$	$\tau e := \frac{C_p}{Ge_p}$	$\tau phys := \frac{Ge_p}{Gd_p} \cdot \tau e$	$fo := \frac{1}{2 \cdot \pi \cdot \tau e}$	$NEPop = 4.15$
$Sop = 3.31 \times 10^8$	$\tau e \cdot 1000 = 19.45$	$\tau phys \cdot 1000 = 24.3$	$fo = 8.2$	

NEP degradation at 2-Hz as a function of 3-dB freq.

$$Deg := \left[\frac{1}{1 + \left(\frac{2}{fo}\right)^2}\right]^{-0.5} \qquad Deg = 1.029$$

Overall DC NEP (det. + photon noise) (W Hz-1/PM E-17)

$$NEPtot_b := \left[NEPph_{tot}{}^2 + \left(f_{ch} \cdot NEPlia_b\right)^2\right]^{0.5}$$

Overall DC NEP (det. + photon noise) ($W\ Hz^{-1/2}$ E-17) and DQE at op. point (referred to the power absorbed by the detector)

$$NEPtotop\_DC := \left[NEPph_{tot}{}^2 + \left(f_{ch} \cdot NEPop\right)^2\right]^{0.5} \qquad DQEop\_DC := \left(\frac{NEPph_{tot}}{NEPtotop\_DC}\right)^2$$

$$NEPtotop\_DC = 7.01 \qquad DQEop\_DC = 0.614$$

2-Hz overall NEP

$$NEPtotop := \left[NEPph_{tot}{}^2 + \left(f_{ch} \cdot NEPop \cdot Deg\right)^2\right]^{0.5} \qquad NEPtotop = 7.09$$

Overall NEP degradation factor for 2-Hz operation

$$Deg\_op := \frac{NEPtotop}{NEPtotop\_DC} \qquad Deg\_op = 1.011$$

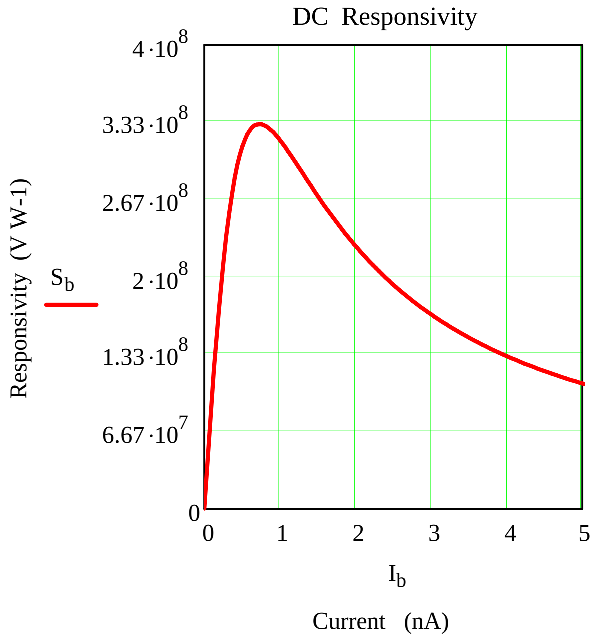

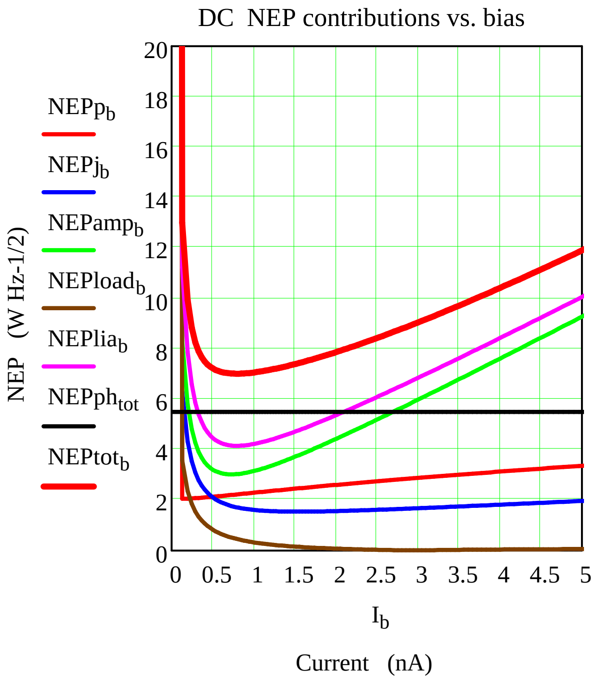

Total noise at LIA output (nV Hz$^{-1/2}$)

$$entot_b := NEPtot_b \cdot 10^{-17} \cdot S_b \cdot 10^9$$

DC DQE:

$$DQE_b := \left(\frac{NEPph_{tot}}{NEPtot_b}\right)^2$$

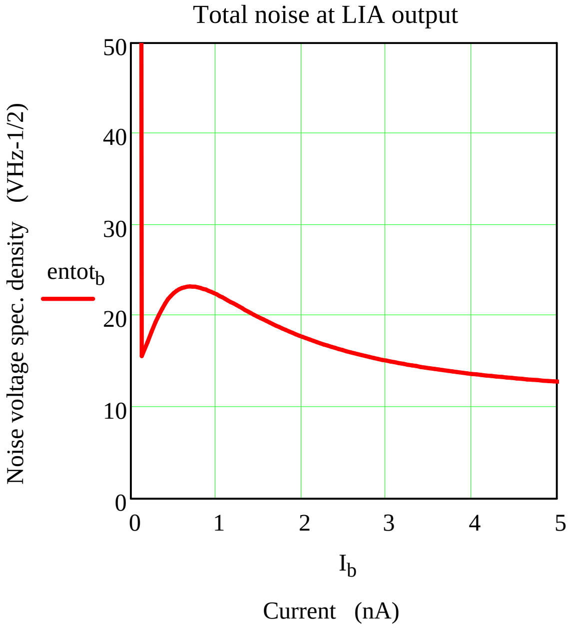

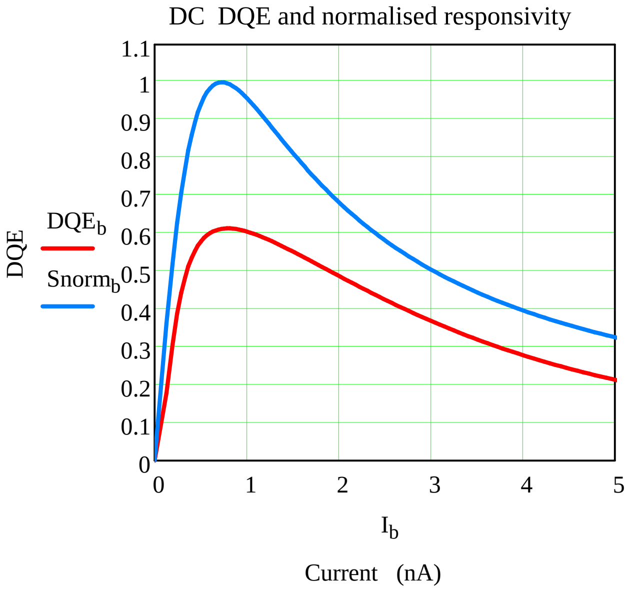

Total noise at LIA output at operating point(nV Hz$^{-1/2}$)

$$entot\_op := Sop \cdot NEPtotop \cdot 10^{-17} \qquad entot\_op \cdot 10^9 = 23.4$$

Per-detector Noise Equivalent Flux Densities (NEFDs) and limiting sensitivities for the various observing modes

Basic NEFD (mJy Hz$^{-1/2}$)

$$NEFD\_basic := \frac{NEPtotop \cdot 10^{-17} \cdot 10^{26} \cdot 1000}{\eta_A \cdot \eta feed_{ch} \cdot Atel \cdot \int_{\nu limL_{ch}}^{\nu limU_{ch}} t_{sky}(\nu)\, d\nu} \qquad NEFD\_basic = 10.0$$

Signal power in pW per Jy

$$Q_{source} := 10^{12} \cdot 10^{-26} \cdot \eta_A \cdot \eta feed_{ch} \cdot Atel \cdot \int_{\nu limL_{ch}}^{\nu limU_{ch}} t_{sky}(\nu)\, d\nu \qquad Q_{source} = 7.075 \times 10^{-3}$$

Total background power expressed in Jy

$$\frac{Q_{tot}}{Q_{source}} = 240 \qquad Sop = 3.307 \times 10^8 \qquad ch = 1.000$$

POF1: Chopped point source photometry

NEFD (mJy Hz$^{-1/2}$) for point source chopped observations (POF 1)

$$NEFDpt := \frac{NEFD\_basic}{\eta ch \cdot 2^{0.5}}$$

Chopping factor degrades basic NEFD but factor of SQRT(2) improvement from pixel-pixel chopping. 100% yield of key pixels is assumed.

5-s; 1-hr limiting sensitivity (mJy)

$$NEFDpt = 14.2$$

$$\Delta S\_5\sigma\_1hr\_pt := \frac{NEFDpt}{2^{0.5}} \cdot \frac{5}{3600^{0.5}} \qquad \Delta S\_5\sigma\_1hr\_pt = 0.83$$

$$\Delta S\_1\sigma\_1s\_pt := \frac{NEFDpt}{2^{0.5}} \qquad \Delta S\_1\sigma\_1s\_pt = 10.02$$

POF 2: Seven-point photometry

Nominal 7-point offset (arcsec) and as fraction of FWHM

$\Delta\theta := 6 \qquad \Delta\theta := \dfrac{\Delta\theta}{FWHM_{ch}} \qquad \Delta\theta = 0.33$

Relative signal in offset positions

$Offset\_Sig(\Delta\theta norm) := \exp\left[-\left(\Delta\theta norm \cdot 2 \cdot \ln(2)^{0.5}\right)^2\right] \qquad Offset\_Sig(\Delta\theta) = 0.73$

S/N loss in doing seven-point

$S\_N\_loss\_7pt(\Delta\theta norm) := \dfrac{1}{8} \cdot (2 + 6 \cdot Offset\_Sig(\Delta\theta norm))$

S/N loss factor vs. offset as a fraction of FWHM

$S\_N\_loss\_7pt(\Delta\theta) = 0.80$

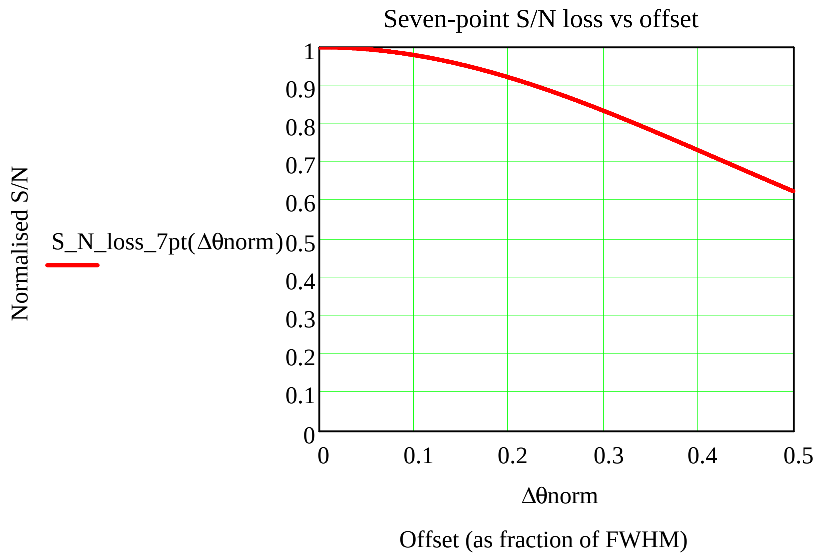

NEFD (mJy Hz$^{-1/2}$) for seven-point chopped observations (POF 2)

$NEFD\_7pt := \dfrac{NEFDpt}{S\_N\_loss\_7pt(\Delta\theta)} \qquad NEFD\_7pt = 17.7$

1-s; 1-s limiting sensitivity (mJy)

$\Delta S\_1\sigma\_1s\_7pt := \dfrac{NEFD\_7pt}{2^{0.5}} \qquad \Delta S\_1\sigma\_1s\_7pt = 12.51$

5-s; 1-hr limiting sensitivity (mJy)

$\Delta S\_5\sigma\_1hr\_7pt := \dfrac{NEFD\_7pt}{2^{0.5}} \cdot \dfrac{5}{3600^{0.5}} \qquad \Delta S\_5\sigma\_1hr\_7pt = 1.04$

POF 3 or 4: Field (jiggle) mapping with 4 x 4 arcmin fov (POF 4 is with rastering)

NEFD (mJy $Hz^{-1/2}$) for field mapping (jiggle mode (POF 3 or 4)

$$NEFDjig := \frac{NEFD\_basic}{\eta ch \cdot \left(yield_{ch}\right)^{0.5}}$$

No factor of SQRT(2) in the denominator as we are not pixel-pixel chopping.

Loss in S/N for point source due to need to make a map:

S/N improvement through pixel co-addition $SN\_imp := 1.35$

S/N reduction through decrease in integration time/point by factor of 16 $SN\_red := 4$

Overall reduction in S/N $SN\_factor := \frac{SN\_imp}{SN\_red}$ $SN\_factor = 0.338$

5-s; 1-hr limiting sensitivity (mJy) for extracted point sources

$$\Delta S\_5\sigma\_1hr\_jig := \frac{5 \cdot NEFDjig}{2^{0.5} \cdot 3600^{0.5}} \cdot \frac{SN\_red}{SN\_imp}$$ **mJy**

1-s; 1-s limiting sensitivity (mJy) for extracted point sources

$$\Delta S\_1\sigma\_1s\_jig := \frac{NEFDjig}{2^{0.5}} \cdot \frac{SN\_red}{SN\_imp}$$ **mJy**

1-s; 1-s limiting sensitivity for surface brightness (MJy sr^{-1})

$$\Delta B\_1\sigma\_1s\_jig := \frac{\Delta S\_1\sigma\_1s\_jig \cdot 10^{-3}}{Abeam_{ch} \cdot 10^{6}} \cdot SN\_imp$$ **MJy sr-1**

Note: Point source S/N improvement factor taken out for surface brightess observations

POF 5: Scan mapping

Degradation in point source S/N in extraction of a point source from a scan map due to 1/f noise

$\eta_{1\_f_i} :=$

0.83
0.80
0.77

NEFD (mJy $Hz^{-1/2}$) for scan map

$$NEFDscan := \frac{NEFD\_basic}{\left(yield_{ch}\right)^{0.5}}$$ $NEFDscan = 10.28$

5-s; 1-hr limiting sensitivity (mJy) for extracted point source

$$\Delta S\_5\sigma\_1hr\_scan := \frac{5 \cdot NEFDscan}{2^{0.5} \cdot 3600^{0.5} \cdot SN\_factor \cdot \eta_{1\_f_{ch}}}$$ $\Delta S\_5\sigma\_1hr\_scan = 2.16$

1-s; 1-s limiting sensitivity (mJy) for extracted point sources

$$\Delta S\_1\sigma\_1s\_scan := \frac{NEFDscan}{2^{0.5} \cdot \eta_{1\_f_{ch}}} \cdot \frac{SN\_red}{SN\_imp}$$ $\Delta S\_1\sigma\_1s\_scan = 25.95$

1-s; 1-s limiting sensitivity for surface brightness (MJy sr^{-1})

$$\Delta B\_1\sigma\_1s\_scan := \frac{\Delta S\_1\sigma\_1s\_scan \cdot 10^{-3}}{Abeam_{ch} \cdot 10^{6}} \cdot SN\_imp$$

Note: Again, point source S/N improvement factor taken out for surface brightess observations

Integration time to map 1 sq.deg. to the 3 mJy rms in scan-map and jiggle map-modes

Note: This analysis does not include telescope or instrument overheads

Required rms (mJy) $\Delta Sreq := 3$

Area to be mapped (sq. deg.) $Area := 1$

Effective field size $Field\_scan := 4 \cdot 8 \cdot \eta field_{ch}$ $\quad Field\_jig := 4 \cdot 4$

Overlap factor $\eta_{overlap} := 0.9$ **Note: It is assumed (pessimistically) that the overlap between fields does not lead to any S/N enhancement**

Number of fields to be mapped

$$Nfields\_scan := \frac{(Area \cdot 60)^2}{Field\_scan \cdot \eta_{overlap}} \qquad Nfields\_jig := \frac{(Area \cdot 60)^2}{Field\_jig \cdot \eta_{overlap}}$$

$Nfields\_scan = 125$ $\quad Nfields\_jig = 250$

Time needed to reach required rms over one field (hours)

$$T\_field\_scan := \left(\frac{\Delta S\_5\sigma\_1hr\_scan}{\Delta Sreq \cdot 5}\right)^2 \qquad T\_field\_jig := \left(\frac{\Delta S\_5\sigma\_1hr\_jig}{\Delta Sreq \cdot 5}\right)^2$$

$T\_field\_scan \cdot 3600 = 74.815$ $\quad T\_field\_jig = 0.057$

Time needed for 1 sq. deg. map (hours)

$T\_1\_sq\_deg\_scan := Nfields\_scan \cdot T\_field\_scan$

$T\_1\_sq\_deg\_jig := Nfields\_jig \cdot T\_field\_jig$

$T\_1\_sq\_deg\_scan = 2.6$ $\quad T\_1\_sq\_deg\_jig = 14.3$

Annex 2: FTS sensitivity model

Updated after January HST

SPIRE_FTS_8_Working.mcd

January 16 2007

Constants: $h \equiv 6.626\cdot 10^{-3\cdot}$ $kb \equiv 1.3806\cdot 10^{-23}$

$origin := 1$ $c \equiv 2.998\cdot 10^{8}$

$i \equiv (1, 2 .. 2)$

Planck function:

$$B(\nu, T) := \frac{2\cdot h\cdot \nu^{3}}{c^{2}\cdot\left[\exp\left(\left(\frac{h\cdot\nu}{kb\cdot T}\right)\right) - 1\right]}$$

Key Input parameters

Index for the three bands $i \equiv 1, 2 .. 2$ **1 = SSW** **2 = SLW**

Reflector temp. (K) $Ttel := 80$ **Used diameter (m)** $Dtel \equiv 3.285$

Obscuration factor $Obs\_factor \equiv 0.872$ **Telescope focal ratio** $Ftel \equiv 8.68$

Telescope emissivity

Formula from Fischer et al.

$$\varepsilon_{ref}(nu) := 0.0336 \cdot \left(\frac{c \cdot 10^6}{nu}\right)^{-0.5} + 0.273 \cdot \left(\frac{c \cdot 10^6}{nu}\right)^{-1}$$

Total telescope emissivity

$$\varepsilon_{tel}(nu) := 2 \cdot \varepsilon_{ref}(nu)$$

Stray light model

Based on pessimistic industry model:
20% of a 70-K telescope with 3% emissivity

$T_{stray} := 70$ $\varepsilon_{stray} := 0.2 \cdot 0.03$

Overall total emissivity including stray light (referred to 80 K)

$$\varepsilon_{tot}(nu) := \varepsilon_{tel}(nu) + \varepsilon_{stray} \cdot \frac{70}{80}$$

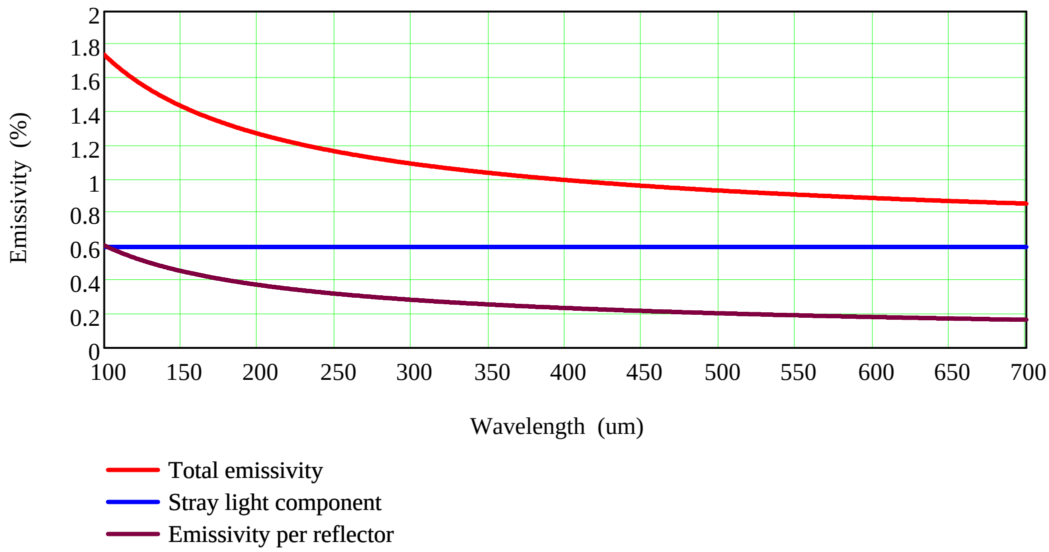

Spillover efficiency (signal) $\eta_S \equiv 0.8$ **Aperture efficiency (signal)** $\eta_A := 0.7$

Final optics focal ratio $Ffin \equiv 5$

Instrument mirror reflectivity $t_{mirr} := 0.995$ **Mirror emissivity** $\varepsilon_{mirr} := 1 - t_{mirr}$

Roof-top mirror reflectivity per surface $t_{roof} := 0.95$ **Roof-top emissivity** $\varepsilon_{roof} := 1 - t_{roof}$

BSM transmission $t_{BSM} := 0.95$ **BSM emissivity** $\varepsilon_{BSM} := 0.88$

Beam divider efficiency $t_{bd} := 0.95$

Lens transmission $t_{lens} := 0.9$ **Feedhorn throughput (m² sr)** $A\Omega(\nu) := \left(\frac{c}{\nu}\right)^2$

Scan speed (mm s-1) $vmirr \equiv 0.5$ **Cos² modulation efficiency** $\eta cosq \equiv 0.5$

He-3 temp. (K) $To := 0.310$

Level-1 temp. (K) $TL1 := 5.5$

Bolometer yield $yield_i \equiv$

0.9
0.9

Level-0 temp. (K) $TL0 := 1.8$

Filter transmission factor $trans\_fac := 1.0$

JFET plus amplifier noise (V Hz$^{-1/2}$) $enA := 10 \cdot 10^{-9}$

Bolometer parameters

Material band-gap temperature (K) $T_{G_i} :=$	Resistance parameter (W) $R_{S_i} :=$	Load resistance (MW) $R_{L_i} \equiv$	Heat capacity at 300 mK (pJ K-1) $Co_i \equiv$	Thermal conductivity index $\beta_i \equiv$	Thermal conductance at 300 mK (pW K-1) $G_i :=$
42.1	79.3	19.2	1.02	1.30	194
41.0	92.2	23.2	1.00	1.23	163

Material parameter

$$\delta_i := \frac{T_{G_i}}{To}$$

Static thermal conductance at bath temp. (pW K^{-1})

$$GS0_i := G_i \cdot 10^{-12} \cdot \left(\frac{To}{0.300}\right)^{\beta_i}$$

R-T power law index $n \equiv 0.5$

Heat capacity index $\rho_i \equiv 1$

Noise degradation factor $f_i :=$

1.05
1.05

Feed efficiency

SSW $\eta\_SW\_TE11 := 0.84$ $\eta\_SW\_TM01 := 0.57$ $\eta\_SW\_TE21 := 0.78$

For simplicity, we adopt the average value across the bands

$$\eta_{feed_1} := \frac{\eta\_SW\_TE11 + \eta\_SW\_TM01 + \eta\_SW\_TE21}{3} \qquad \eta_{feed_1} = 0.73$$

SLW $\eta_{feed_2} := 0.70$

Aperture efficiencies

SSW **A constant value of 0.7 is assumed.**

SLW **SLW horn is 2Fl at 390 mm but only 1.2Fl at 670 mm, for which the aperture efficiency is 0.5. We assume a linear drop to 0.5 from 400 mm to 670 mm.**

$a := 0, 1 .. 2$

$\nu\_a_a :=$

$c \cdot \frac{10^6}{670}$
$c \cdot \frac{10^6}{400}$
$c \cdot \frac{10^6}{315}$

$\eta_{Ap_a} :=$

0.5
0.7
0.7

$\eta_A(nu) := linterp(\nu\_a, \eta_{Ap}, nu)$

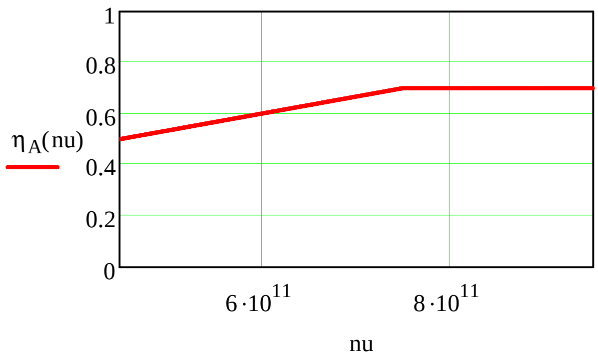

Bands

$$\begin{pmatrix} PLW \\ PMW \\ PSW \\ SLW \\ SSW \end{pmatrix} :=$$

Worksheet

$$Freq_{SS} := SSW^{\langle 0 \rangle} \cdot 100 \cdot c \qquad tfil_1(nu) := linterp\left(Freq_{SS}, SSW^{\langle 1 \rangle}, nu\right) \cdot trans\_fac$$

$$Freq_{SL} := SLW^{\langle 0 \rangle} \cdot 100 \cdot c \qquad tfil_2(nu) := linterp\left(Freq_{SL}, SLW^{\langle 1 \rangle}, nu\right) \cdot trans\_fac$$

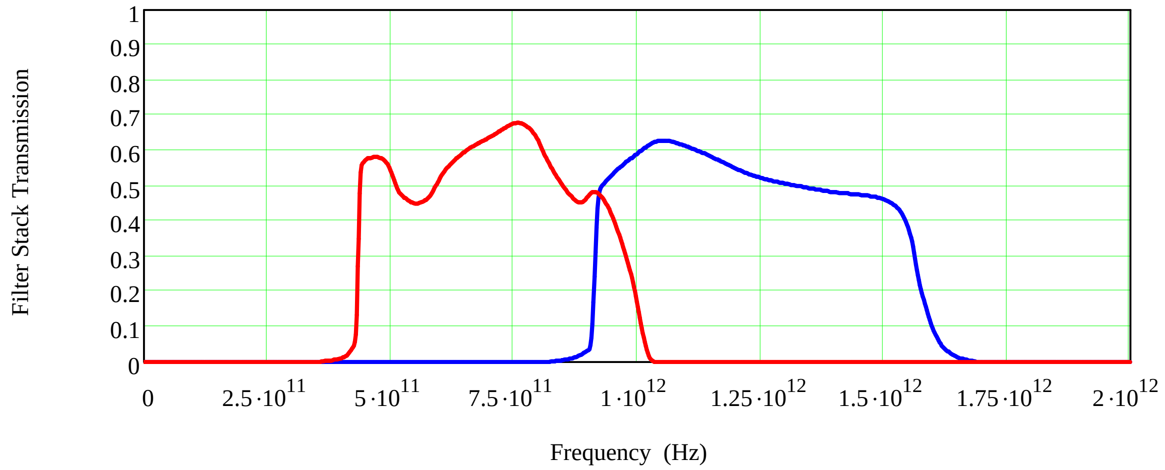

Limits for integration over the filter passbands

$\nu limL_i :=$ $\nu limU_i :=$

$\nu limL_i$	$\nu limU_i$
$7.5 \cdot 10^{11}$	$1.70 \cdot 10^{12}$
$2.5 \cdot 10^{11}$	$1.05 \cdot 10^{12}$

Select channel and filter band for computation

$ch := 1$ $\quad t_{fil}(\nu) := tfil_1(\nu)$

1 for SSW
2 for SLW

Transmissions of individual elements

$k := 1, 2 .. 5$

Telescope primary	$t_1(\nu) := 1 - \varepsilon_{ref}(\nu)$	$\varepsilon_1(\nu) := \varepsilon_{ref}(\nu)$
Telescope secondary	$t_2(\nu) := 1 - \varepsilon_{ref}(\nu)$	$\varepsilon_2(\nu) := \varepsilon_{ref}(\nu)$
Stray light source	$t_3(\nu) := 1$	$\varepsilon_3(\nu) := \varepsilon_{stray}$
Level 1	$t_4(\nu) := t_{mirr}{}^9 \cdot t_{BSM} \cdot t_{roof}{}^2 \cdot t_{bd}{}^2 \cdot t_{fil}(\nu)^{0.5}$	$\varepsilon_4(\nu) := 1 - t_4(\nu)$
Level 0	$t_5(\nu) := t_{lens} \cdot t_{fil}(\nu)^{0.5}$	$\varepsilon_5(\nu) := 1 - t_5(\nu)$

Transmissions to detector

Telescope primary	$td_1(\nu) := t_2(\nu) \cdot t_4(\nu)\, t_5(\nu)$
Telescope secondary	$td_2(\nu) := t_4(\nu) \cdot t_5(\nu)$
Stray light source	$td_3(\nu) := t_4(\nu) \cdot t_5(\nu)$
Level 1	$td_4(\nu) := t_5(\nu)$
Level 0	$td_5(\nu) := 1$

Transmission from sky to detector for selected channel

$t_{sky}(\nu) := t_1(\nu) \cdot td_1(\nu)$

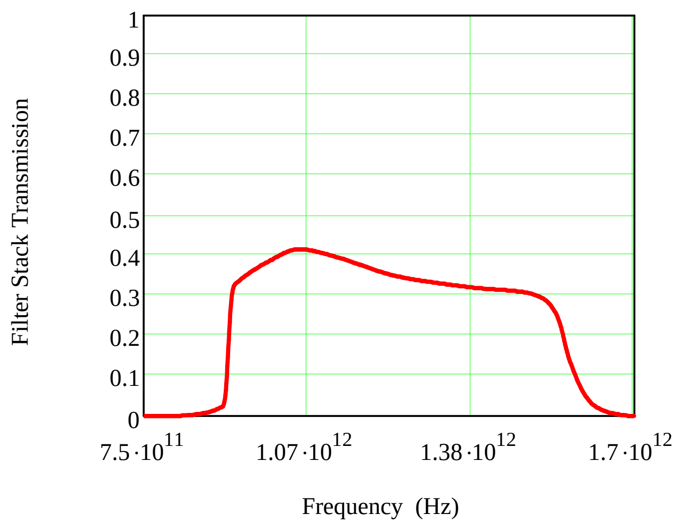

Mode propagation

SSW propagates three modes: TE11, TM01, TE21
SLW propagates four modes: TE11, TM01, TE21, TM11

Waveguide radii (mm)

$$rw_i := \begin{bmatrix} 95 \\ 197 \end{bmatrix}$$

Mode cut-on frequencies

TE11

$$\lambda_{cTE11_i} := \frac{2\cdot\pi\cdot rw_i}{1.841} \qquad \nu_{cTE11_i} := \frac{c\cdot 10^6}{\lambda_{cTE11_i}} \qquad \lambda_{cTE11_i} = \begin{bmatrix} 324 \\ 672 \end{bmatrix} \qquad \nu_{cTE11_i}\cdot 10^{-9} = \begin{bmatrix} 925 \\ 446 \end{bmatrix}$$

TM01

$$\lambda_{cTM01_i} := \frac{2\cdot\pi\cdot rw_i}{2.405} \qquad \nu_{cTM01_i} := \frac{c\cdot 10^6}{\lambda_{cTM01_i}} \qquad \lambda_{cTM01_i} = \begin{bmatrix} 248 \\ 515 \end{bmatrix} \qquad \nu_{cTM01_i}\cdot 10^{-9} = \begin{bmatrix} 1208 \\ 583 \end{bmatrix}$$

TE21

$$\lambda_{cTE21_i} := \frac{2\cdot\pi\cdot rw_i}{3.054} \qquad \nu_{cTE21_i} := \frac{c\cdot 10^6}{\lambda_{cTE21_i}} \qquad \lambda_{cTE21_i} = \begin{bmatrix} 195 \\ 405 \end{bmatrix} \qquad \nu_{cTE21_i}\cdot 10^{-9} = \begin{bmatrix} 1534 \\ 740 \end{bmatrix}$$

TM11

$$\lambda_{cTM11_i} := \frac{2\cdot\pi\cdot rw_i}{3.832} \qquad \nu_{cTM11_i} := \frac{c\cdot 10^6}{\lambda_{cTM11_i}} \qquad \lambda_{cTM11_i} = \begin{bmatrix} 156 \\ 323 \end{bmatrix} \qquad \nu_{cTM11_i}\cdot 10^{-9} = \begin{bmatrix} 1925 \\ 928 \end{bmatrix}$$

TE31

$$\lambda_{cTE31_i} := \frac{2\cdot\pi\cdot rw_i}{4.201} \qquad \nu_{cTE31_i} := \frac{c\cdot 10^6}{\lambda_{cTE31_i}} \qquad \lambda_{cTE31_i} = \begin{bmatrix} 142 \\ 295 \end{bmatrix} \qquad \nu_{cTE31_i}\cdot 10^{-9} = \begin{bmatrix} 2110 \\ 1018 \end{bmatrix}$$

Throughput as a function of frequency

$$T1(\nu) := \mathrm{if}\left(\nu > \nu_{cTE11_1}, 1, 0\right) \qquad T2(\nu) := \mathrm{if}\left(\nu > \nu_{cTE11_2}, 1, 0\right)$$

$$T1(\nu) := \mathrm{if}\left(\nu < \nu_{cTM01_1}, T1(\nu), 0\right) \qquad T2(\nu) := \mathrm{if}\left(\nu < \nu_{cTM01_2}, T2(\nu), 0\right)$$

$$T1(\nu) := \mathrm{if}\left(\nu > \nu_{cTM01_1}, 2, T1(\nu)\right) \qquad T2(\nu) := \mathrm{if}\left(\nu > \nu_{cTM01_2}, 2, T2(\nu)\right)$$

$$T1(\nu) := \mathrm{if}\left(\nu > \nu_{cTE21_1}, 3, T1(\nu)\right) \qquad T2(\nu) := \mathrm{if}\left(\nu > \nu_{cTE21_2}, 3, T2(\nu)\right)$$

$$T1(\nu) := \mathrm{if}\left(\nu > \nu_{cTM11_1}, 4, T1(\nu)\right) \qquad T2(\nu) := \mathrm{if}\left(\nu > \nu_{cTM11_2}, 4, T2(\nu)\right)$$

$$T1(\nu) := \mathrm{if}\left(\nu > \nu limU_1, 0, T1(\nu)\right) \qquad T2(\nu) := \mathrm{if}\left(\nu > \nu limU_2, 0, T2(\nu)\right)$$

Approximate throughput (in units of 1^2) variation with frequency by a straight line

$$A\Omega 1(\nu) := \left[1 + \left(\nu - \nu_{cTE11_1}\right)\cdot\left(\frac{3-1}{\nu limU_1 - \nu_{cTE11_1}}\right)\right] \qquad A\Omega 2(\nu) := \left[1 + \left(\nu - \nu_{cTE11_2}\right)\cdot\left(\frac{4-1}{\nu limU_2 - \nu_{cTE11_2}}\right)\right]$$

$$A\Omega 1(\nu) := \mathrm{if}\left(\nu < \nu_{cTE11_1}, 0, A\Omega 1(\nu)\right) \qquad A\Omega 2(\nu) := \mathrm{if}\left(\nu < \nu_{cTE11_2}, 0, A\Omega 2(\nu)\right)$$

$$A\Omega 1(\nu) := \mathrm{if}\left(\nu > \nu limU_1, 0, A\Omega 1(\nu)\right) \qquad A\Omega 2(\nu) := \mathrm{if}\left(\nu > \nu limU_2, 0, A\Omega 2(\nu)\right)$$

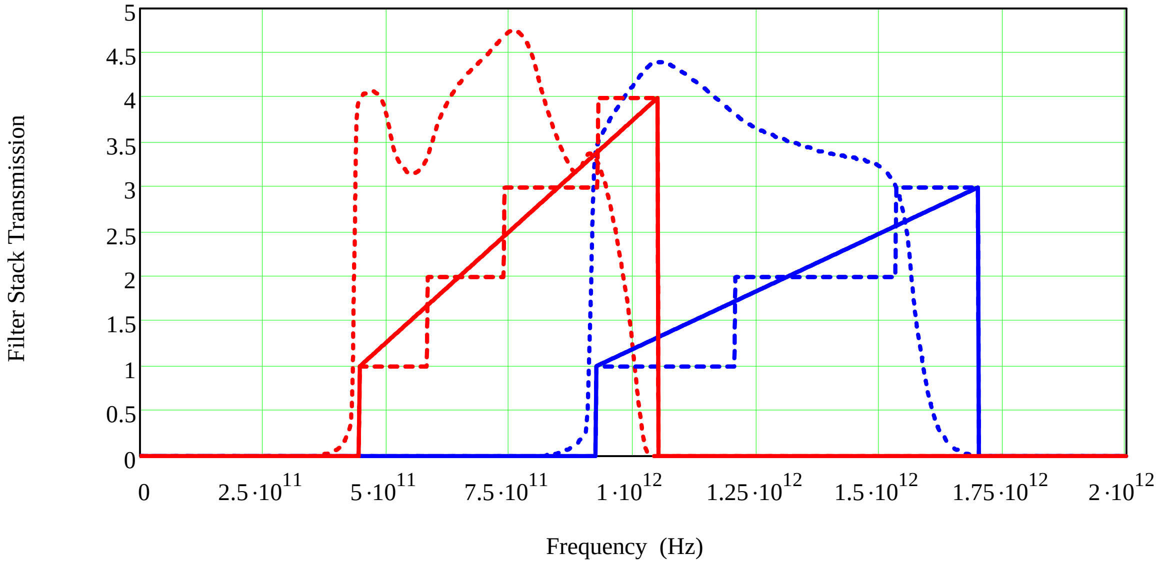

Dotted	**=**	**Filter profiles (arb. units)**
Dashed	**=**	**Throughputs assuming 12 per mode**
Solid	**=**	**Straight line approximations**

Throughput in m^2 sr vs. frequency

$$A\Omega_1(\nu) := A\Omega1(\nu)\cdot\left(\frac{c}{\nu}\right)^2 \qquad A\Omega_2(\nu) := A\Omega2(\nu)\cdot\left(\frac{c}{\nu}\right)^2$$

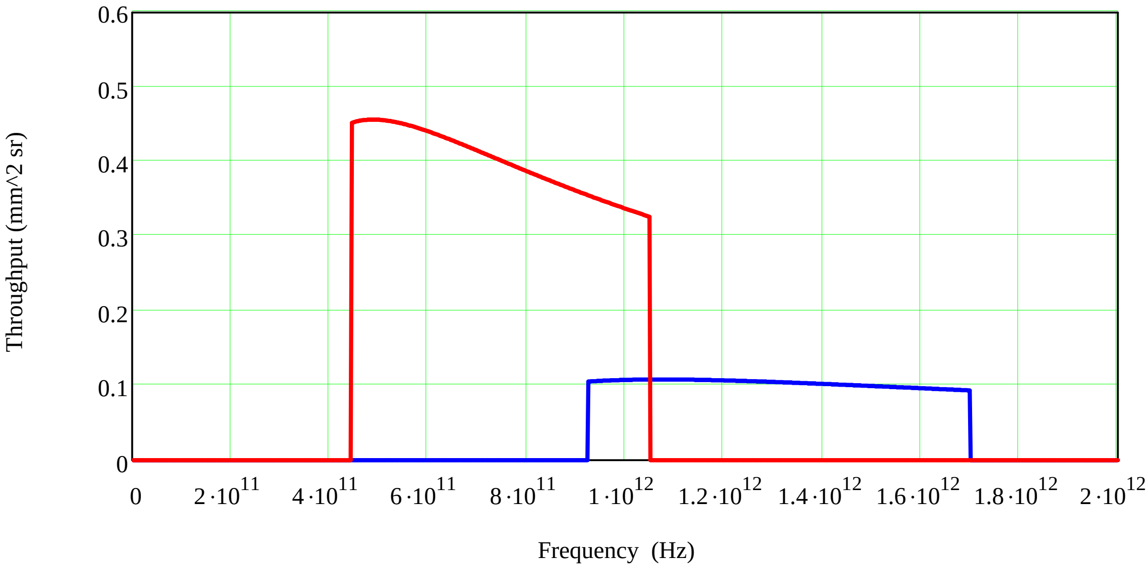

Note: These values are of the same order as thevalues calculated by Marc Ferlet for SVR-2

Throughput for selected channel

$$A\Omega(\nu) := \text{if}\left[ch = 1, A\Omega1(\nu)\cdot\left(\frac{c}{\nu}\right)^2, A\Omega2(\nu)\cdot\left(\frac{c}{\nu}\right)^2\right]$$

Operational frequency limits for the two bands

$\nu min_1 := \nu_{cTE11_1}$ $\qquad \lambda max_1 := \dfrac{c \cdot 10^6}{\nu min_1}$ $\qquad \sigma min_1 := \dfrac{10000}{\lambda max_1}$

$\nu max_1 := 1.55 \cdot 10^{12}$ $\qquad \lambda min_1 := \dfrac{c \cdot 10^6}{\nu max_1}$ $\qquad \sigma max_1 := \dfrac{10000}{\lambda min_1}$

$\nu min_2 := \nu_{cTE11_2}$ $\qquad \lambda max_2 := \dfrac{c \cdot 10^6}{\nu min_2}$ $\qquad \sigma min_2 := \dfrac{10000}{\lambda max_2}$

$\nu max_2 := 9.5 \cdot 10^{11}$ $\qquad \lambda min_2 := \dfrac{c \cdot 10^6}{\nu max_2}$ $\qquad \sigma max_2 := \dfrac{10000}{\lambda min_2}$

$\lambda min_1 = 193.4$ $\qquad \lambda max_1 = 324.2$ $\qquad \sigma min_1 = 30.8$ $\qquad \sigma max_1 = 51.7$

$\lambda min_2 = 315.6$ $\qquad \lambda max_2 = 672.3$ $\qquad \sigma min_2 = 14.9$ $\qquad \sigma max_2 = 31.7$

Nominal band centres

$\nu o_1 := 0.5\left(\nu min_1 + \nu max_1\right)$ $\qquad \nu o_2 := 0.5\left(\nu min_2 + \nu max_2\right)$

$\nu o_1 = 1.24 \times 10^{12}$ $\qquad \nu o_2 = 6.98 \times 10^{11}$

OPD scan rate (mm s-1)

$vscan := vmirr \cdot 4$

Audio frequency ranges (Hz) for the two bands

$felec(\sigma) := \left(vscan \cdot 10^{-3}\right) \cdot (\sigma \cdot 100)$

	$felec(\sigma min_i)$	$felec(\sigma max_i) =$
SW	6.2	10.3
LW	3.0	6.3

Derived parameters

Telescope

Effective telescope area (m^2)

$$Atel := \frac{\pi \cdot Dtel^2}{4} \cdot Obs\_factor \qquad Atel = 7.39$$

Plate scale at telescope focus (arcsec/mm):

$$PS := \frac{1}{Dtel \cdot Ftel} \cdot \frac{360}{2 \cdot \pi} \cdot 3.6 \qquad PS = 7.23$$

Background power levels on the detectors (pW)

Primary

$$Q_1 := 10^{12} \cdot \eta_S \cdot \eta_{feed_{ch}} \cdot \int_{\nu limL_{ch}}^{\nu limU_{ch}} \varepsilon_1(\nu) \cdot td_1(\nu) \cdot A\Omega(\nu) \cdot B(\nu, Ttel)\, d\nu \qquad Q_1 = 1.18$$

Secondary

$$Q_2 := 10^{12} \cdot \eta_S \cdot \eta_{feed_{ch}} \cdot \int_{\nu limL_{ch}}^{\nu limU_{ch}} \varepsilon_2(\nu) \cdot td_2(\nu) \cdot A\Omega(\nu) \cdot B(\nu, Ttel)\, d\nu \qquad Q_2 = 1.18$$

Stray light

$$Q_3 := 10^{12} \cdot \eta_S \cdot \eta_{feed_{ch}} \cdot \int_{\nu limL_{ch}}^{\nu limU_{ch}} \varepsilon_3(\nu) \cdot td_3(\nu) \cdot A\Omega(\nu) \cdot B(\nu, T_{stray})\, d\nu \qquad Q_3 = 1.74$$

Level 1

$$Q_4 := 10^{12} \cdot \eta_S \cdot \eta_{feed_{ch}} \cdot \int_{\nu limL_{ch}}^{\nu limU_{ch}} \varepsilon_4(\nu) \cdot td_4(\nu) \cdot A\Omega(\nu) \cdot B(\nu, TL1)\, d\nu \qquad Q_4 = 0.01$$

Level 0

$$Q_5 := 10^{12} \cdot \eta_{feed_{ch}} \cdot \int_{\nu limL_{ch}}^{\nu limU_{ch}} \varepsilon_5(\nu) \cdot td_5(\nu) \cdot A\Omega(\nu) \cdot B(\nu, TL0)\, d\nu \qquad Q_5 = 1.90 \times 10^{-10}$$

Summary

$Q_k =$

1.18
1.18
1.74
0.01
1.90·10-10

Total background power (pW)

$$Q_{tot} := Q_1 + Q_2 + Q_3 + Q_4 + Q_5 \qquad Q_{tot} = 4.10$$

Photon noise limited NEP (W Hz$^{-1/2}$ E-17)

$$NEPph_1 := \left[\frac{4\cdot\eta_S\cdot h^2}{c^2}\cdot\left[\int_{\nu limL_{ch}}^{\nu limU_{ch}}\frac{A\Omega(\nu)\cdot\varepsilon_1(\nu)\cdot td_1(\nu)\cdot\eta_{feed_{ch}}\cdot\nu^4}{e^{\frac{h\cdot\nu}{kb\cdot Ttel}}-1}\cdot\left(1+\frac{\varepsilon_1(\nu)\cdot td_1(\nu)\cdot\eta_{feed_{ch}}}{e^{\frac{h\cdot\nu}{kb\cdot Ttel}}-1}\right)d\nu\right]\right]^{0.5}\cdot 10^{17}$$

$$NEPph_2 := \left[\frac{4\cdot\eta_S\cdot h^2}{c^2}\cdot\left[\int_{\nu limL_{ch}}^{\nu limU_{ch}}\frac{A\Omega(\nu)\cdot\varepsilon_2(\nu)\cdot td_2(\nu)\cdot\eta_{feed_{ch}}\cdot\nu^4}{e^{\frac{h\cdot\nu}{kb\cdot Ttel}}-1}\cdot\left(1+\frac{\varepsilon_2(\nu)\cdot td_2(\nu)\cdot\eta_{feed_{ch}}}{e^{\frac{h\cdot\nu}{kb\cdot Ttel}}-1}\right)d\nu\right]\right]^{0.5}\cdot 10^{17}$$

$$NEPph_3 := \left[\frac{4\cdot\eta_S\cdot h^2}{c^2}\cdot\left[\int_{\nu limL_{ch}}^{\nu limU_{ch}}\frac{A\Omega(\nu)\cdot\varepsilon_3(\nu)\cdot td_3(\nu)\cdot\eta_{feed_{ch}}\cdot\nu^4}{e^{\frac{h\cdot\nu}{kb\cdot Ttel}}-1}\cdot\left(1+\frac{\varepsilon_3(\nu)\cdot td_3(\nu)\cdot\eta_{feed_{ch}}}{e^{\frac{h\cdot\nu}{kb\cdot Ttel}}-1}\right)d\nu\right]\right]^{0.5}\cdot 10^{17}$$

$$NEPph_4 := \left[\frac{4\cdot\eta_S\cdot h^2}{c^2}\cdot\left[\int_{\nu limL_{ch}}^{\nu limU_{ch}}\frac{A\Omega(\nu)\cdot\varepsilon_4(\nu)\cdot td_4(\nu)\cdot\eta_{feed_{ch}}\cdot\nu^4}{e^{\frac{h\cdot\nu}{kb\cdot TL1}}-1}\cdot\left(1+\frac{\varepsilon_4(\nu)\cdot td_4(\nu)\cdot\eta_{feed_{ch}}}{e^{\frac{h\cdot\nu}{kb\cdot TL1}}-1}\right)d\nu\right]\right]^{0.5}\cdot 10^{17}$$

$$NEPph_5 := \left[\frac{4\cdot\eta_S\cdot h^2}{c^2}\cdot\left[\int_{\nu limL_{ch}}^{\nu limU_{ch}}\frac{A\Omega(\nu)\cdot\varepsilon_5(\nu)\cdot td_5(\nu)\cdot\eta_{feed_{ch}}\cdot\nu^4}{e^{\frac{h\cdot\nu}{kb\cdot TL0}}-1}\cdot\left(1+\frac{\varepsilon_5(\nu)\cdot td_5(\nu)\cdot\eta_{feed_{ch}}}{e^{\frac{h\cdot\nu}{kb\cdot TL0}}-1}\right)d\nu\right]\right]^{0.5}\cdot 10^{17}$$

$$NEPph_{tot} := \left[\left(NEPph_1\right)^2+\left(NEPph_2\right)^2+\left(NEPph_3\right)^2+\left(NEPph_4\right)^2+\left(NEPph_5\right)^2\right]^{0.5}$$

$NEPph_k =$

4.51
4.51
6.00
0.40
5.09·10-5

$NEPph_{tot} = 8.77$

$$\left(2\cdot Q_{tot}\cdot 10^{-12}\cdot h\cdot \nu o_{ch}\right)^{0.5}\cdot 10^{17} = 8.2$$

Bolometer model

Material band-gap temperature (K)	Resistance parameter (Ω)	Load resistance (MΩ)	Static thermal conductance at 300 mK (pW K-1)	Heat capacity at 300 mK (pJ K-1)
$T_{G_{ch}} = 42.1$	$R_{S_{ch}} = 79$	$R_{L_{ch}} = 19.2$	$G_{ch} = 194.0$	$Co_{ch} = 1.02$

Heat capacity index	Thermal conductivity index	R-T power law index	Loading parameter	Resistance parameter (W)
$\rho_{ch} = 1.0$	$\beta_{ch} = 1.3$	$n = 0.5$	$\gamma_{ch} := \dfrac{Q_{tot} \cdot 10^{-12}}{To \cdot GS0_{ch}}$	$R_{S_{ch}} = 79.3$

OPD scan rate (mm s-1) $vscan := vmirr \cdot 4$

Bias parameter

$$b := 0, 1 .. 200$$
$$\phi_b := 1 + \frac{b}{200}$$

Resistance (MΩ)

$$R_b := R_{S_{ch}} \cdot \exp\left[\left[\left(\frac{\delta_{ch}}{\phi_b}\right)^n\right]\right] \cdot 10^{-6}$$

Electrical power (if P < 0, set P = 0)

$$PP_b := To \cdot GS0_{ch} \cdot \left[\frac{(\phi_b)^{\beta_{ch}+1} - 1}{\beta_{ch} + 1} - \gamma_{ch}\right]$$

$$P_b := \mathrm{if}\left(PP_b < 0, 0, PP_b\right)$$

Temp. coeff of resistance

$$\alpha_b := \frac{-n \cdot (\delta_{ch})^n}{(\phi_b)^{n+1} \cdot To}$$

Load curves: V (mV) and I (nA)

$$V_b := \left(P_b \cdot R_b\right)^{0.5} \cdot 10^6 \qquad I_b := \left(\frac{P_b}{R_b \cdot 10^6}\right)^{0.5} \cdot 10^9$$

Select bias voltage to correspond to the optimum bias point calculated below (based on best NEP)

$$Vo := 0.0297$$

Load line equation

$$Vload_b := \left(Vo - I_b \cdot 10^{-9} \cdot R_{L_{ch}} \cdot 10^6\right) \cdot 1000$$

Check: determine the point on the calculated VI nearest to the optimum operating point

$$Diff_b := \left|V_b - Vload_b\right|$$

$$Op\_pt\_S_b := \mathrm{if}\left(Diff_b = \min(Diff), b, 0\right) \qquad Op\_S := \max(Op\_pt\_S) \qquad Op\_S = 31$$

This is the same as the value calculated below for optimum NEP

Gd and Ge (pW K-1)

$$Gd_b := GS0_{ch} \cdot \left[(\phi_b)^{\beta_{ch}} \right]$$

$$Ge_b := Gd_b - \alpha_b \cdot P_b \cdot \left(\frac{R_{L_{ch}} - R_b}{R_{L_{ch}} + R_b} \right)$$

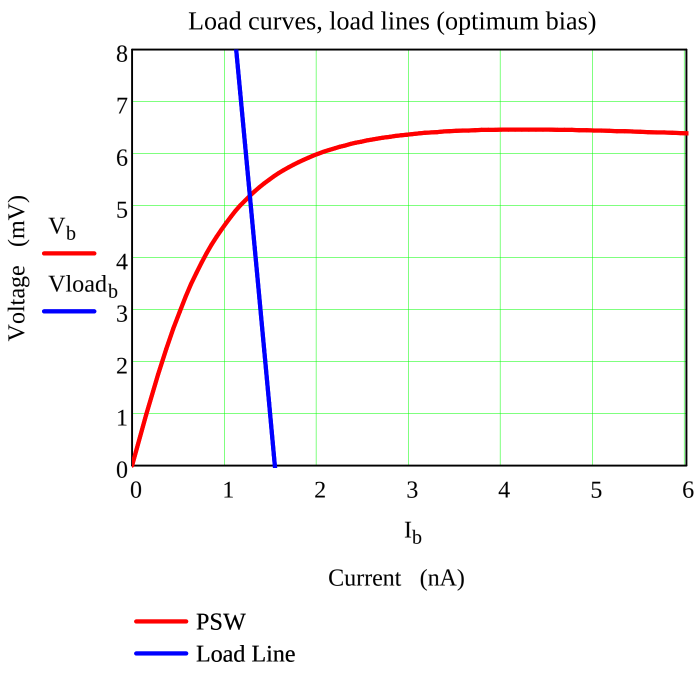

Dynamic impedance (MW)

$$Z_b := \frac{Gd_b + \alpha_b \cdot P_b}{Gd_b - \alpha_b \cdot P_b} \cdot R_b$$

Heat capacity (J K-1)

$$C_b := Co \cdot 10^{-12} \cdot \left(\frac{To \cdot \phi_b}{0.300} \right)^{\rho}$$

DC Responsivity (V W-1):

$$S_b := \mathrm{if}\left[I_b = 0, 1, \frac{(R_b - Z_b) \cdot 10^6}{2 \cdot V_b \cdot 10^{-3}} \cdot \frac{R_{L_{ch}}}{Z_b + R_{L_{ch}}} \right]$$

Normalised responsivity

$$Snorm := \frac{S}{\max(S)}$$

Operating point for maximum responsivity

$$Sopt_b := \mathrm{if}(Snorm_b = \max(Snorm), b, 0) \qquad \max(Sopt) = 29$$

Bolometer voltage (mV) and current (nA) at optimum operating point for peak responsivity

$$I_{\max(Sopt)} = 1.17 \qquad V_{\max(Sopt)} = 5.00$$

Optimum bias voltages (mV) - for peak responsivity

$$Vo\_opt := V_{\max(Sopt)} + I_{\max(Sopt)} \cdot R_{L_{ch}} \qquad Vo\_opt = 27.5$$

Note that this is slightly lower bias points than for optimum NEP

Phonon NEP:

$$NEPp_b := \text{if}\left[I_b = 0, 1, \left[4\cdot kb\cdot To^2\cdot GS0_{ch}\cdot\frac{\beta_{ch}+1}{2\cdot\beta_{ch}+3}\cdot\frac{(\phi_b)^{2\cdot\beta_{ch}+3}-1}{(\phi_b)^{\beta_{ch}+1}-1}\right]^{0.5}\right]\cdot 10^{17}$$

Johnson NEP:

$$NEPj_b := \left[4\cdot kb\cdot To^2\cdot GS0_{ch}\cdot\frac{(\phi_b)^{2\cdot\beta_{ch}+2\cdot n+3}}{n^2\cdot(\delta_{ch})^{2\cdot n}\cdot\left[\left[\frac{(\phi_b)^{\beta_{ch}+1}-1}{\beta_{ch}+1}-\gamma_{ch}\right]\right]}\right]^{0.5}\cdot 10^{17}$$

Load resistor NEP:

$$NEPload_b := \left(\frac{4\cdot kb\cdot To}{R_{L_{ch}}\cdot 10^6}\right)^{0.5}\cdot\left|\frac{Z_b\cdot R_{L_{ch}}\cdot 10^6}{Z_b+R_{L_{ch}}}\right|\cdot\frac{1}{S_b}\cdot 10^{17}$$

Amplifier NEP:

$$NEPamp_b := \frac{enA}{S_b}\cdot 10^{17}$$

Total DC detector NEP at LIA output (W Hz-1/2 E-17):

$$NEPlia_b := \left[\left(NEPp_b\right)^2+\left(NEPj_b\right)^2+\left(NEPamp_b\right)^2+\left(NEPload_b\right)^2\right]^{0.5}$$

Optimum NEP values

$NEPop := \min(NEPlia)$ $\qquad NEPop = 6.71$

Optimum bias points for best NEP

$index_b := \text{if}\left(NEPlia_b = \min(NEPlia), b, 0\right)$ $\qquad p := \max(index)$ $\qquad p = 31$

Optimum bias voltages for best NEP

Bolometer voltage (mV) and current (nA) $\qquad I_p = 1.28$ $\qquad V_p = 5.18$

Optimum bias voltages (mV) $\qquad Vo\_opt := V_p + I_p\cdot R_{L_{ch}}$ $\qquad Vo\_opt = 29.7$

Responsivity (V W-1), time constants (ms), and 3-dB freq. at optimum bias

DC responsivity	Effective time constant (ms)	Physical time constant (ms)	3-dB freq. (Hz)	DC detector NEPop (W Hz$^{-1/2}$ E-17)
$Sop := S_p$	$\tau e := \frac{C_p}{Ge_p}$	$\tau phys := \frac{Ge_p}{Gd_p} \cdot \tau e$	$fo := \frac{1}{2 \cdot \pi \cdot \tau e}$	$NEPop = 6.7$
$Sop = 2.09 \times 10^8$	$\tau e \cdot 1000 = 7.79$	$\tau phys \cdot 1000 = 9.9$	$fo = 20.4$	

Detector NEP degradation at max signal freq. as a function of 3-dB freq.

$$Deg := \left[\frac{1}{1 + \left(\frac{felec(\sigma max_{ch})}{fo}\right)^2}\right]^{-0.5}$$

$Deg = 1.12$

Overall DC NEP (det. + photon noise) (W Hz-1/PM E-17)

$$NEPtot_b := \left[{NEPph_{tot}}^2 + \left(f_{ch} \cdot NEPlia_b\right)^2\right]^{0.5}$$

Overall DC NEP (det. + photon noise) (W Hz$^{-1/2}$ E-17) and DQE at op. point (referred to the power absorbed by the detector

$$NEPtotop\_DC := \left[{NEPph_{tot}}^2 + \left(f_{ch} \cdot NEPop\right)^2\right]^{0.5}$$

$$DQEop\_DC := \left(\frac{NEPph_{tot}}{NEPtotop\_DC}\right)^2$$

$NEPtotop\_DC = 11.25$

$DQEop\_DC = 0.61$

Overall NEP at max signal freq,

$$NEPtotop := \left[{NEPph_{tot}}^2 + \left(f_{ch} \cdot NEPop \cdot Deg\right)^2\right]^{0.5}$$

$NEPtotop = 11.8$

Overall NEP degradation factor at max signal freq

$$Deg\_max := \frac{NEPtotop}{NEPtotop\_DC}$$

$Deg\_max = 1.05$

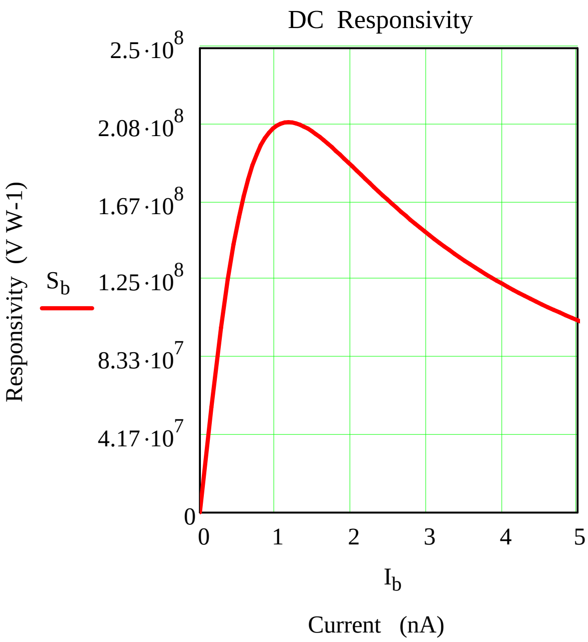

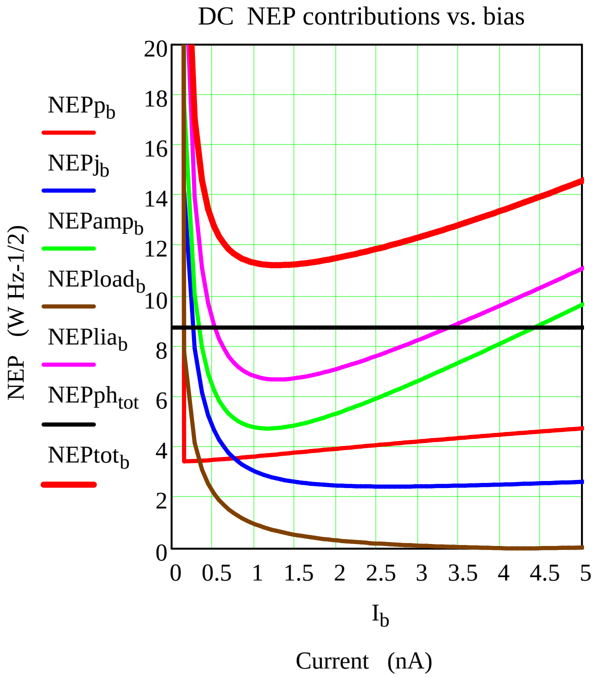

Total noise at LIA output (nV Hz$^{-1/2}$)

$$entot_b := NEPtot_b \cdot 10^{-17} \cdot S_b \cdot 10^9$$

DC DQE:

$$DQE_b := \left(\frac{NEPph_{tot}}{NEPtot_b} \right)^2$$

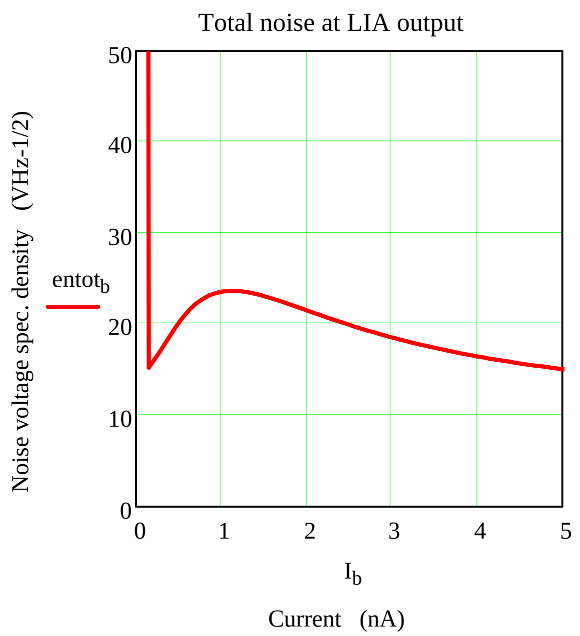

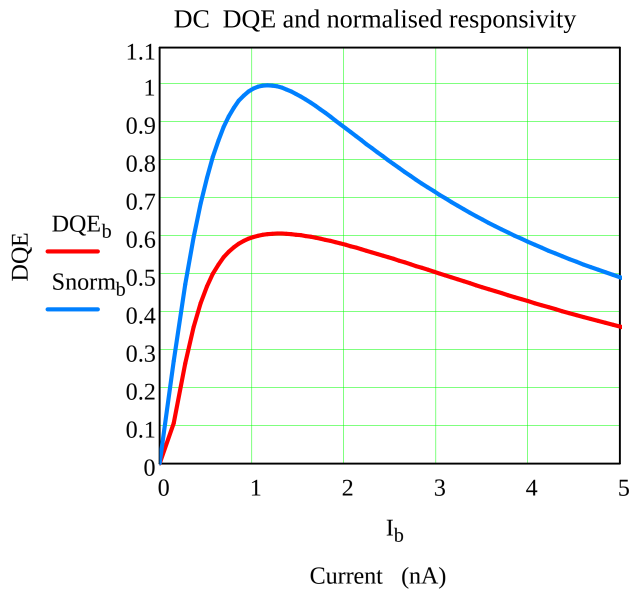

Total noise at LIA output at operating point(nV Hz$^{-1/2}$)

$$entot\_op := Sop \cdot NEPtotop \cdot 10^{-17}$$

$$entot\_op \cdot 10^9 = 24.7$$

Resolving power (unapodised) as a function of wavelength

Spectral resolution (cm-1 and GHz)

High-resolution mode (spectroscopy)

$\Delta\sigma\_H \equiv 0.04$ $\quad \Delta\nu\_H \equiv c\cdot\Delta\sigma\_H\cdot 100$ $\quad \Delta\nu\_H\cdot 10^{-9} = 1.20$

Medium-resolution mode (spectroscopy)

$\Delta\sigma\_M \equiv 0.25$ $\quad \Delta\nu\_M \equiv c\cdot\Delta\sigma\_M\cdot 100$ $\quad \Delta\nu\_M\cdot 10^{-9} = 7.50$

Low-resolution mode (spectrophotometry)

$\Delta\sigma\_L \equiv 1$ $\quad \Delta\nu\_L \equiv c\cdot\Delta\sigma\_L\cdot 100$ $\quad \Delta\nu\_L\cdot 10^{-9} = 30.0$

Resolving power in high and low-res modes

$$\mathrm{ResH}(i,\lambda) := \frac{\frac{10000}{\lambda}}{\Delta\sigma\_H} \qquad \mathrm{ResL}(i,\lambda) := \frac{\frac{10000}{\lambda}}{\Delta\sigma\_L} \qquad \mathrm{ResM}(i,\lambda) := \frac{\frac{10000}{\lambda}}{\Delta\sigma\_M}$$

$\lambda max_i =$	$\lambda min_i =$	$\mathrm{ResH}(i,\lambda max_i) =$	$\mathrm{ResH}(i,\lambda min_i) =$	$\mathrm{ResM}(i,\lambda max_i) =$	$\mathrm{ResM}(i,\lambda min_i)$	$\mathrm{ResL}(i,\lambda max_i)$	$\mathrm{ResL}(i,\lambda min_i)$
324	193	771	1293	123	207	31	52
672	316	372	792	59	127	15	32

Plot unapodised resolving power vs. wavelength

$lw := 300, 301 .. 670$ $\quad \mathrm{ResLWH}_{lw} := \mathrm{ResH}(1, lw)$ $\quad \mathrm{ResLWM}_{lw} := \mathrm{ResM}(1, lw)$ $\quad \mathrm{ResLWL}_{lw} := \mathrm{ResL}(1, lw)$

$sw := 190, 191 .. 325$ $\quad \mathrm{ResSWH}_{sw} := \mathrm{ResH}(2, sw)$ $\quad \mathrm{ResSWM}_{sw} := \mathrm{ResM}(2, sw)$ $\quad \mathrm{ResSWL}_{sw} := \mathrm{ResL}(2, sw)$

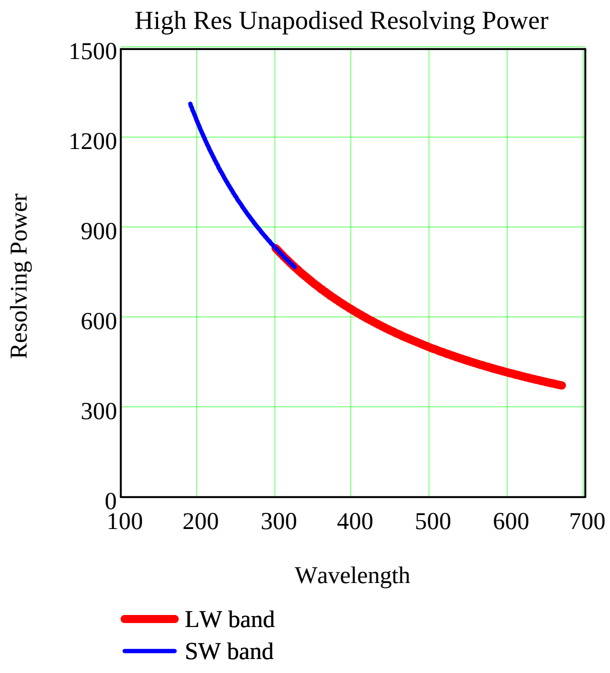
High Res Unapodised Resolving Power
Resolving Power
Wavelength
1500
1200
900
600
300
0
100
200
300
400
500
600
700
LW band
SW band

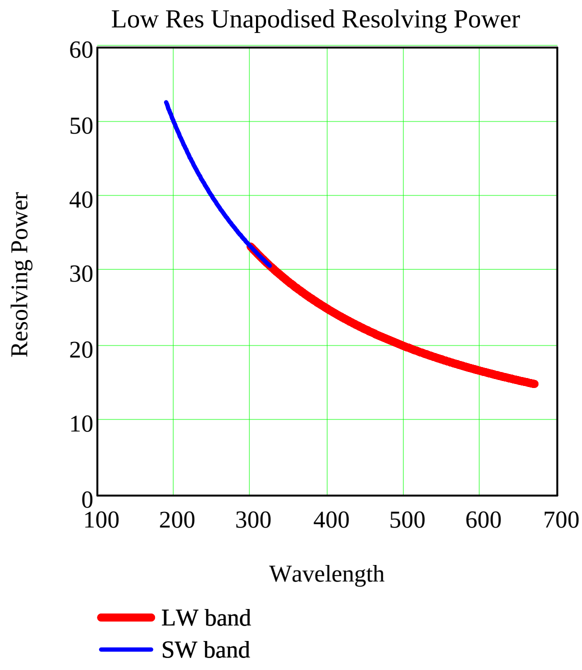
Low Res Unapodised Resolving Power
Resolving Power
Wavelength
60
50
40
30
20
10
0
100
200
300
400
500
600
700
LW band
SW band

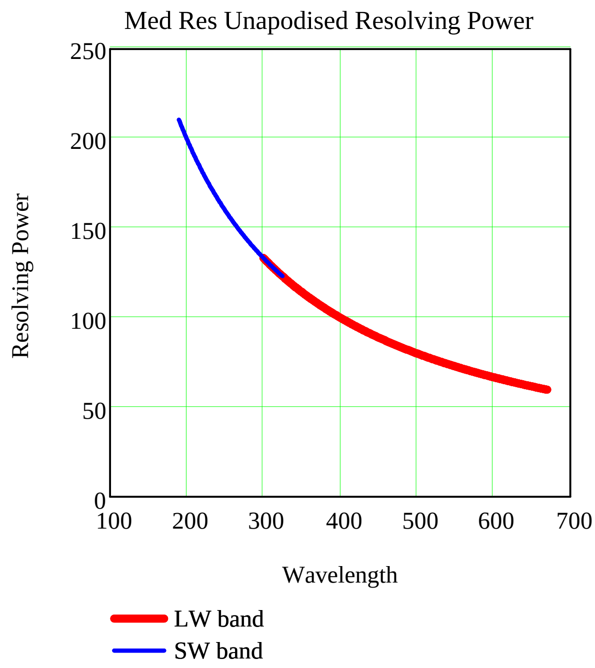
Med Res Unapodised Resolving Power
Resolving Power
Wavelength
250
200
150
100
50
0
100
200
300
400
500
600
700
LW band
SW band

Per-detector Noise Equivalent Flux Densities (NEFDs) and limiting sensitivities for the various observing modes

Basic NEFD (Jy Hz$^{-1/2}$)

$$\mathrm{NEFD\_basic}(\nu, \Delta\nu) := \frac{\mathrm{NEPtotop} \cdot 10^{-17} \cdot 10^{26} \cdot 2^{0.5}}{\eta_A(\nu) \cdot \eta_{\mathrm{feed}_{ch}} \cdot \eta\mathrm{cosq} \cdot \mathrm{Atel} \cdot t_{sky}(\nu) \cdot \Delta\nu}$$

$\mathrm{NEFD\_basic}(\nu o_{ch}, \Delta\nu\_L) = 0.84$

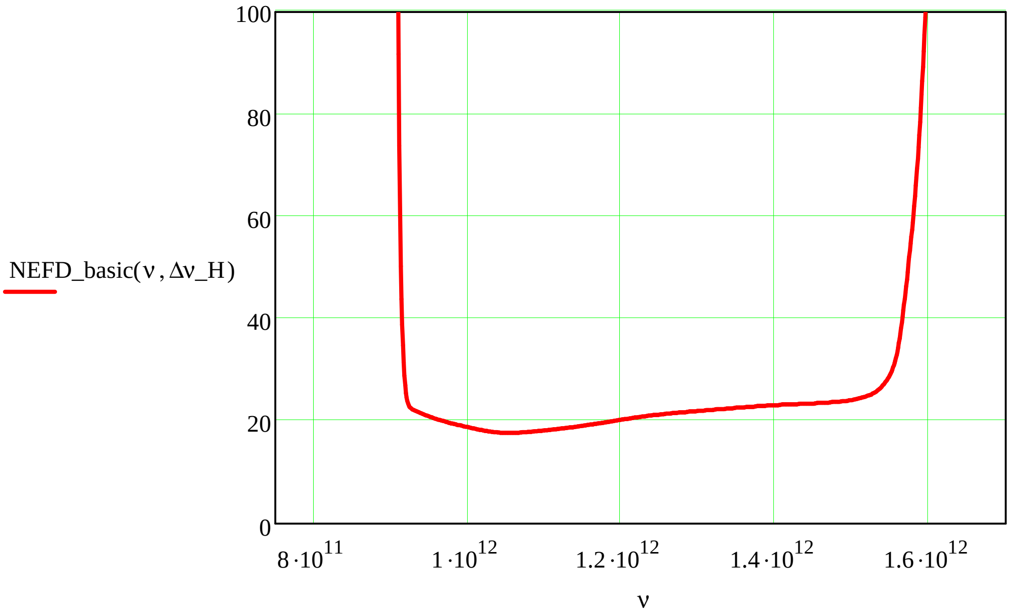

ch = 1.0

$Pess := 1$ $ch = 1$ $Q_{tot} = 4.1$ $NEPph_{tot} = 8.8$ $NEPtotop = 11.8$ $Vo = 0.0297$

1-s ; 1 sec. limiting sensitivities for point source detection:

Point source spectroscopy (SOF 1):

Limiting flux density (mJy)

High resolution

$$\Delta SH\_1\sigma\_1s\_pt(\nu) := \frac{NEFD\_basic(\nu, \Delta\nu\_H)}{2^{0.5}} \cdot 1000$$ $\Delta SH\_1\sigma\_1s\_pt(\nu o_{ch}) = 1.5 \times 10^4$

$$\Delta SH\_5\sigma\_1hr\_pt(\nu) := \frac{5 \cdot \Delta SH\_1\sigma\_1s\_pt(\nu)}{3600^{0.5}}$$ $\Delta SH\_5\sigma\_1hr\_pt(\nu o_{ch}) = 1241$

Medium Resolution

$$\Delta SM\_1\sigma\_1s\_pt(\nu) := \frac{NEFD\_basic(\nu, \Delta\nu\_M)}{2^{0.5}} \cdot 1000$$ $\Delta SM\_1\sigma\_1s\_pt(\nu o_{ch}) = 2383.3$

$$\Delta SM\_5\sigma\_1hr\_pt(\nu) := \frac{5 \cdot \Delta SM\_1\sigma\_1s\_pt(\nu)}{3600^{0.5}}$$ $\Delta SM\_5\sigma\_1hr\_pt(\nu o_{ch}) = 199$

Low resolution

$$\Delta SL\_1\sigma\_1s\_pt(\nu) := \frac{NEFD\_basic(\nu, \Delta\nu\_L)}{2^{0.5}} \cdot 1000$$ $\Delta SL\_1\sigma\_1s\_pt(\nu o_{ch}) = 595.8$

$$\Delta SL\_5\sigma\_1hr\_pt(\nu) := \frac{5 \cdot \Delta SL\_1\sigma\_1s\_pt(\nu)}{3600^{0.5}}$$ $\Delta SL\_5\sigma\_1hr\_pt(\nu o_{ch}) = 49.7$

Limiting line strength (W m-2 E-17)

High resolution

$$\Delta FH\_1\sigma\_1s\_pt(\nu) := \frac{\Delta SH\_1\sigma\_1s\_pt(\nu)}{1000} \cdot \Delta\nu\_H \cdot 10^{-26} \cdot 10^{17}$$ $\Delta FH\_1\sigma\_1s\_pt(\nu o_{ch}) = 17.9$

$$\Delta FH\_5\sigma\_1hr\_pt(\nu) := \frac{\Delta SH\_5\sigma\_1hr\_pt(\nu)}{1000} \cdot \Delta\nu\_H \cdot 10^{-26} \cdot 10^{17}$$ $\Delta FH\_5\sigma\_1hr\_pt(\nu o_{ch}) = 1.49$

Medium Resolution

$$\Delta FM\_1\sigma\_1s\_pt(\nu) := \frac{\Delta SM\_1\sigma\_1s\_pt(\nu)}{1000} \cdot \Delta\nu\_M \cdot 10^{-26} \cdot 10^{17}$$ $\Delta FM\_1\sigma\_1s\_pt(\nu o_{ch}) = 17.9$

$$\Delta FH\_5\sigma\_1hr\_pt(\nu) := \frac{\Delta SH\_5\sigma\_1hr\_pt(\nu)}{1000} \cdot \Delta\nu\_H \cdot 10^{-26} \cdot 10^{17}$$ $\Delta FH\_5\sigma\_1hr\_pt(\nu o_{ch}) = 1.49$

Low resolution

$$\Delta FL\_1\sigma\_1s\_pt(\nu) := \frac{\Delta SL\_1\sigma\_1s\_pt(\nu)}{1000} \cdot \Delta\nu\_L \cdot 10^{-26} \cdot 10^{17}$$ $\Delta FL\_1\sigma\_1s\_pt(\nu o_{ch}) = 17.9$

$$\Delta FL\_5\sigma\_1hr\_pt(\nu) := \frac{\Delta SL\_5\sigma\_1hr\_pt(\nu)}{1000} \cdot \Delta\nu\_L \cdot 10^{-26} \cdot 10^{17}$$ $\Delta FL\_5\sigma\_1hr\_pt(\nu o_{ch}) = 1.49$

Pess := 2 $p := 1 .. 200$ $\nu_p := 4\cdot 10^{11} + \frac{2\cdot 10^{12}}{200}\cdot p$ $\lambda_p := \frac{c\cdot 10^6}{\nu_p}$ ch = 1   **SSW**

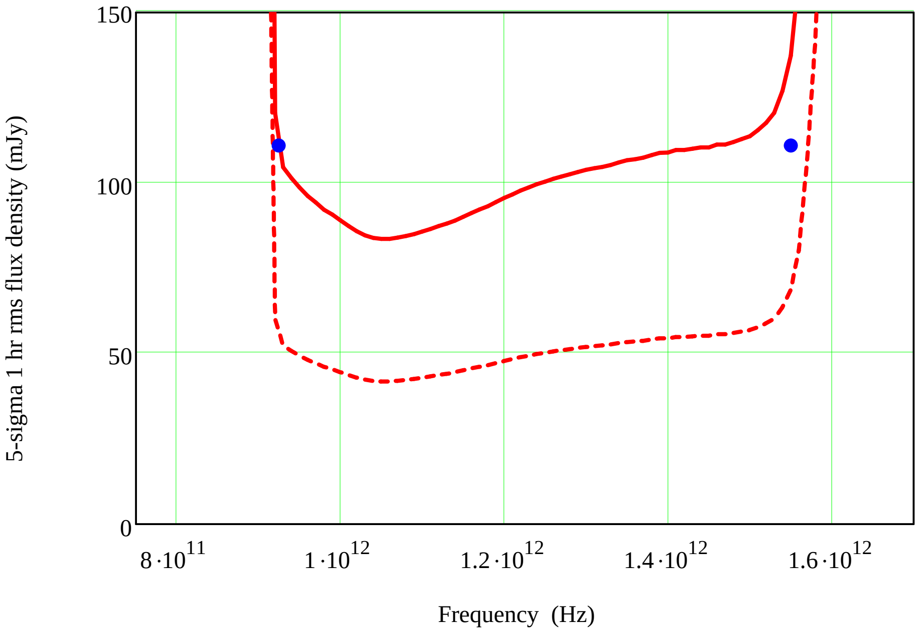

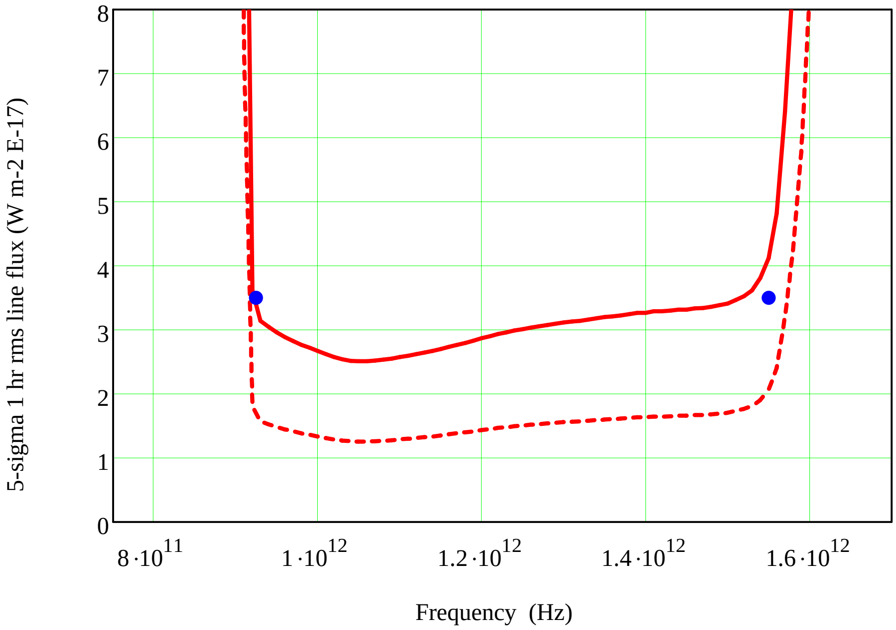

Plot limits

$cc := 1, 2 .. 2$

$\lambda plotL_{cc} := \begin{array}{|c|}\hline 170 \\ \hline 300 \\ \hline\end{array}$

$\lambda plotU_{cc} := \begin{array}{|c|}\hline 350 \\ \hline 700 \\ \hline\end{array}$

$LowX_{cc} := \begin{array}{|c|}\hline \frac{c \cdot 10^6}{\nu max_{ch}} \\ \hline \frac{c \cdot 10^6}{\nu max_{ch}} \\ \hline\end{array}$

$LowY_{cc} := \begin{array}{|c|}\hline 0 \\ \hline 200 \\ \hline\end{array}$

$HighX_{cc} := \begin{array}{|c|}\hline \frac{c \cdot 10^6}{\nu min_{ch}} \\ \hline \frac{c \cdot 10^6}{\nu min_{ch}} \\ \hline\end{array}$

$HighY_{cc} := \begin{array}{|c|}\hline 0 \\ \hline 200 \\ \hline\end{array}$

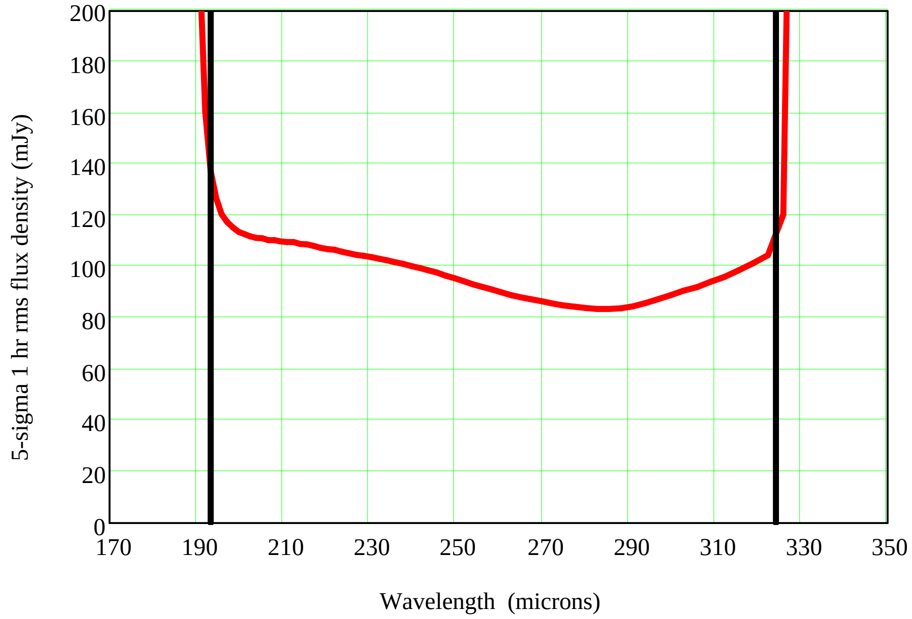

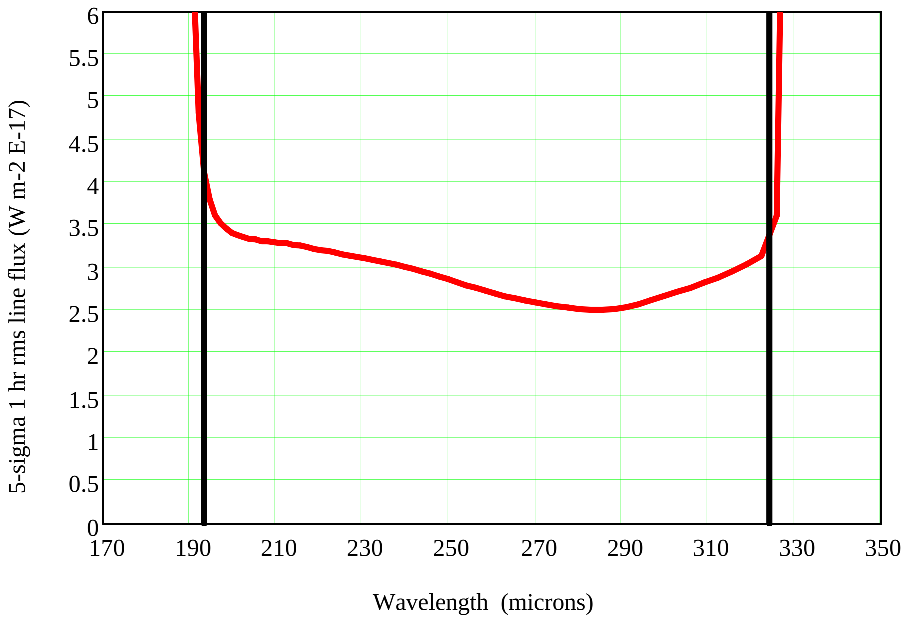

Annex 3 Telescope Obscuration Factor

Herschel_Obscuration.mcd 6 April 2004

Calculates the throughput loss factor resltting from the Herschel telescope obscuration (central hole + hexapod supports)

Read in image and generate corresponding array $Image := READBMP("shadowing.bmp")$ $M := 255 - Image$

Define edges of mirror $rows(M) = 557$ $cols(M) = 531$

$a := 0, 1 .. rows(M) - 1$ $b := 0, 1 .. cols(M) - 1$

Dummy array for display $M1 := M$

Four white lines define a square enclosing the primary aperture

Left $M1_{a,10} := 255$ **Right** $M1_{a,523} := 255$

Top $M1_{26,b} := 255$ **Bottom** $M1_{540,b} := 255$

Horizontal cut (black line) $M1_{283,b} := 0$

X-axis: Left edge = 10
Right edge = 523

Centre: $\frac{533}{2} = 267$

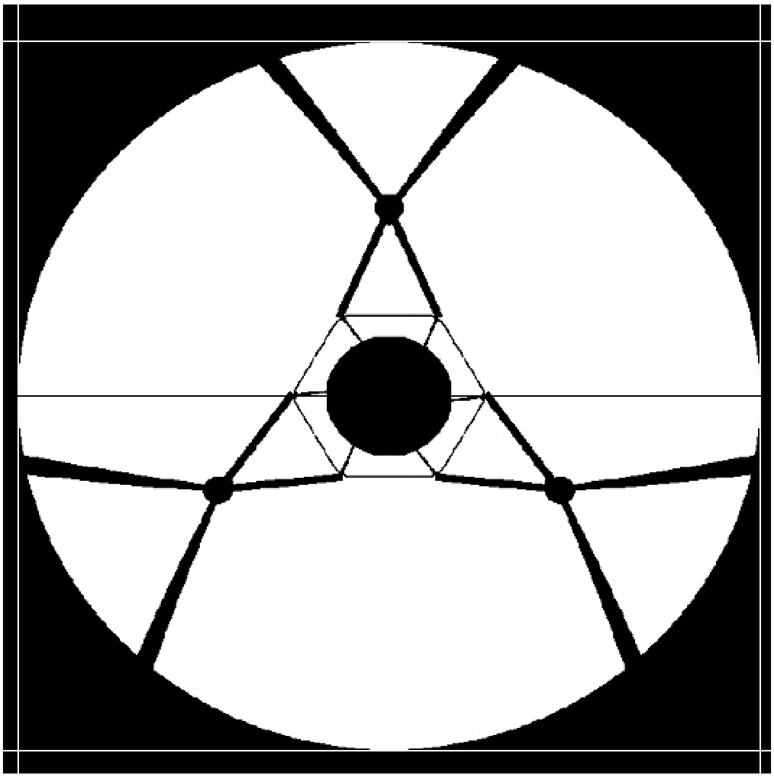

Y-axis: Top edge = 26
Bottom edge = 540

Centre: $\frac{566}{2} = 283$

Centre pixel is (283,267)

Radius of mirror (left-right) = 267-10 = 255 pixels

Radius of mirror (top-bottom) = 283-26 = 257 pixels

Take mean of these: 256. This corresponds to a radius of 1.75 m

Used diameter of the primary is 3.29-m, so the edge of the used portion corresponds to

$\frac{3.29}{3.5} \cdot 256 = 241$ **pixels from the centre.**

Define edge taper (db) wrt used diameter of 3.29 m $Taper := 8$ $R\_edge := 10^{\frac{-Taper}{10}}$ $R\_edge = 0.158$

So we want R = 0.158 at 241 pixels from the centre: a = 283-241 = 42 b = 267-241 = 25

Therefore the HWHM corresponds to $\theta o := \frac{241}{(-\ln(0.158))^{0.5}}$ $\theta o = 177$ **pixels from the centre**

Define 2-D Gaussian

$$R_{a,b} := \exp\left[-\left[\frac{\left[(a-283)^2+(b-267)^2\right]^{0.5}}{\theta o}\right]^2\right] \qquad \max(R) = 1$$

Check edge taper

$R_{42,267} = 0.158$ $\quad {}_{3,25} = 0.156$ **OK**

Create array for telescope illumination pattern (truncated at 3.29-m diameter)

$$\text{Untruncated\_Beam} := R\cdot 255$$

$$\text{Beam}_{a,b} := \text{if}\left[\left[(a-283)^2+(b-267)^2\right]^{0.5} > 241, 0, R_{a,b}\cdot 255\right]$$

Plot illumination profile and obscuration profile

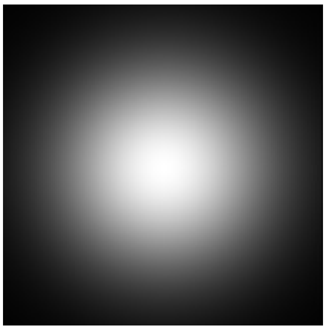

Untruncated

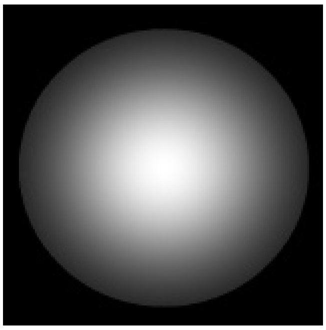

Truncated

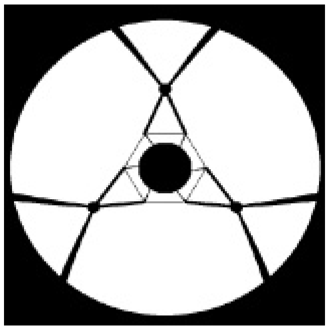

Plot horizontal and vertical cuts through the centre:

$$\text{ATel\_cut} := \frac{M^{\langle 267\rangle}}{255} \qquad \text{ABeam\_cut} := \frac{\text{Beam}^{\langle 267\rangle}}{255}$$

$$MT := M^T \qquad \text{BeamT} := \text{Beam}^T$$

$$\text{BTel\_cut} := \frac{MT^{\langle 283\rangle}}{255} \qquad \text{BBeam\_cut} := \frac{\text{BeamT}^{\langle 283\rangle}}{255}$$

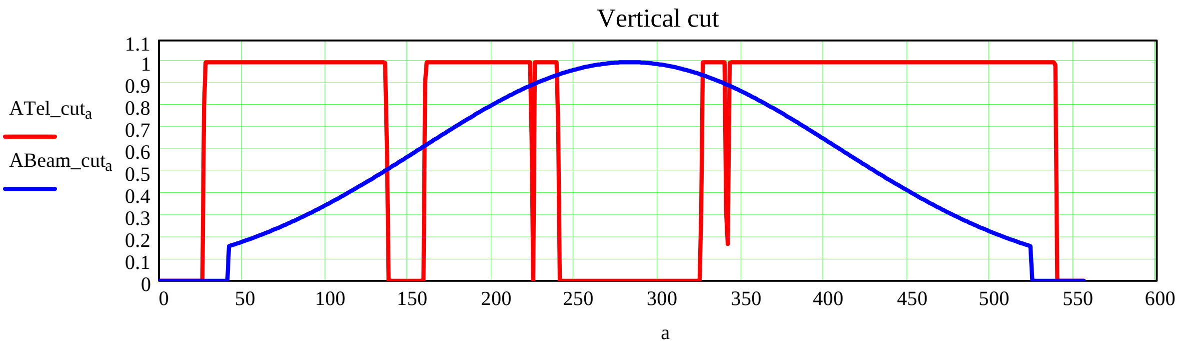

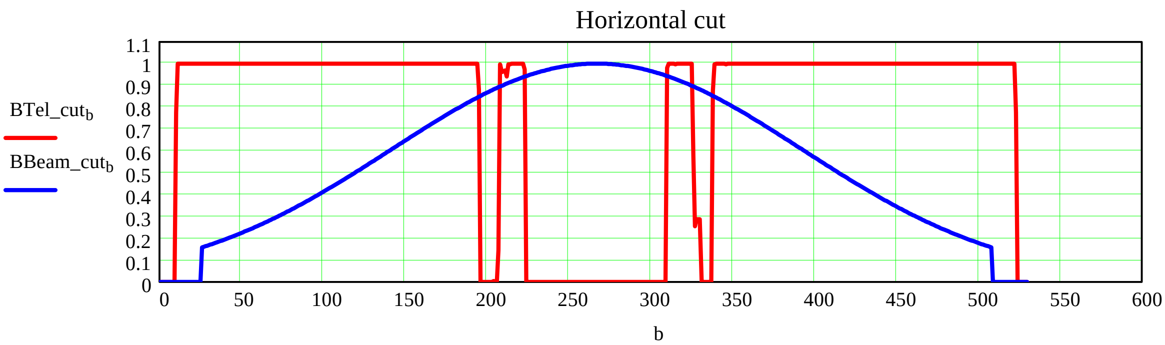

Calculate throughput loss:

With obscuration: multiply the two arrays with telescope array normalised to unity. Throughput is proportional to the sum of all the array elements

$$\mathrm{Product}_{a,b} := \frac{M_{a,b} \cdot \mathrm{Beam}_{a,b}}{255}$$

$$\mathrm{Throughput\_actual} := \sum_{a=0}^{\mathrm{rows}(M)-1} \sum_{b=0}^{\mathrm{cols}(M)-1} \mathrm{Product}_{a,b}$$

$$\mathrm{Throughput\_actual} = 1.852 \times 10^{7}$$

Without obscuration: throughput is proportional to area under the 2-D illumination profile

$$\mathrm{Ideal}_{a,b} := \mathrm{Beam}_{a,b}$$

$$\mathrm{Throughput\_ideal} := \sum_{a=0}^{\mathrm{rows}(M)-1} \sum_{b=0}^{\mathrm{cols}(M)-1} \mathrm{Ideal}_{a,b}$$

$$\mathrm{Throughput\_ideal} = 2.123 \times 10^{7}$$

$$\mathrm{Loss} := \frac{\mathrm{Throughput\_actual}}{\mathrm{Throughput\_ideal}} \qquad \mathrm{Loss} = 0.872$$

Conclusion: Througput loss due to telescope obscuration is approximately 13%

Effective illumination profile

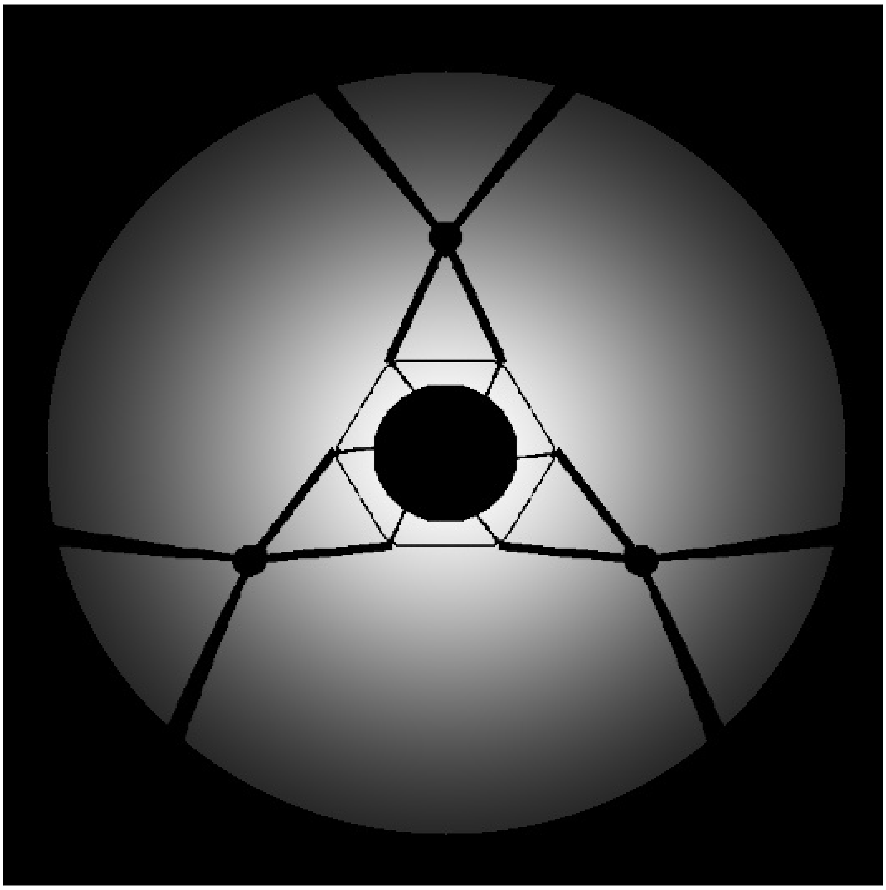

Annex 4: SPIRE beams and S/N enhancement from pixel coaddition

FWHM_vs_Edge_Taper.mcd April 6 2004

Calculates the beam profile on the sky as a function of the pupil edge taper

Normalised aperture and wavelength **Aperture** $d := 1$ **Wavelength** $\lambda := 1$

$$\lambda\_over\_D := \frac{\lambda}{d}\cdot\frac{360}{2\cdot\pi}\cdot 3600 \qquad \lambda\_over\_D = 2.06\times 10^{5}$$

Herschel primary used diameter (m) $Dtel := 3.285$

Herschel primary hole radius (m) $Dhole := 0.56$

Normalised radius of Herschel central hole

$$rhole := \frac{Dhole}{Dtel} \qquad rhole = 0.170$$

Defina a range of edge tapers $t \equiv 1, 2..15$ $T_t \equiv t$

Convert edge taper to 1/e width

$$\sigma(T) := \frac{\sqrt{20}}{2\cdot\sqrt{T\cdot\ln(10)}}$$

Define Gaussian illumination function:

$$f(r,T) := \exp\left[-\left(\frac{r}{\sigma(T)}\right)^2\right]$$

Hankel transform of f(r) with its conjugate variable, q. Start the integral at rhole, corresponding to the central hole obscuration. Truncate the integration at r = 0.5.

Without central obscuration **With central obscuration**

$$hu(q,T) := 2\cdot\pi\cdot\left(\int_0^{0.5} f(r,T)\cdot J0(2\cdot\pi\cdot q\cdot r)\cdot r\,dr\right) \qquad h(q,T) := 2\cdot\pi\cdot\left(\int_{rhole}^{0.5} f(r,T)\cdot J0(2\cdot\pi\cdot q\cdot r)\cdot r\,dr\right)$$

Normalised beam profile

$$Bu(q,T) := \frac{(|hu(q,T)|)^2}{(|hu(0,T)|)^2} \qquad B(q,T) := \frac{(|h(q,T)|)^2}{(|h(0,T)|)^2}$$

Range variable over which q will be calculated

$$j := 1..2000 \qquad q_j := \frac{j}{1000}$$

Convert q to arcseconds

$$arc_j := \frac{q_j\cdot\lambda}{d}\cdot 206265$$

q = 1.22 corresponds to 1.22l/D

Plot beam profiles

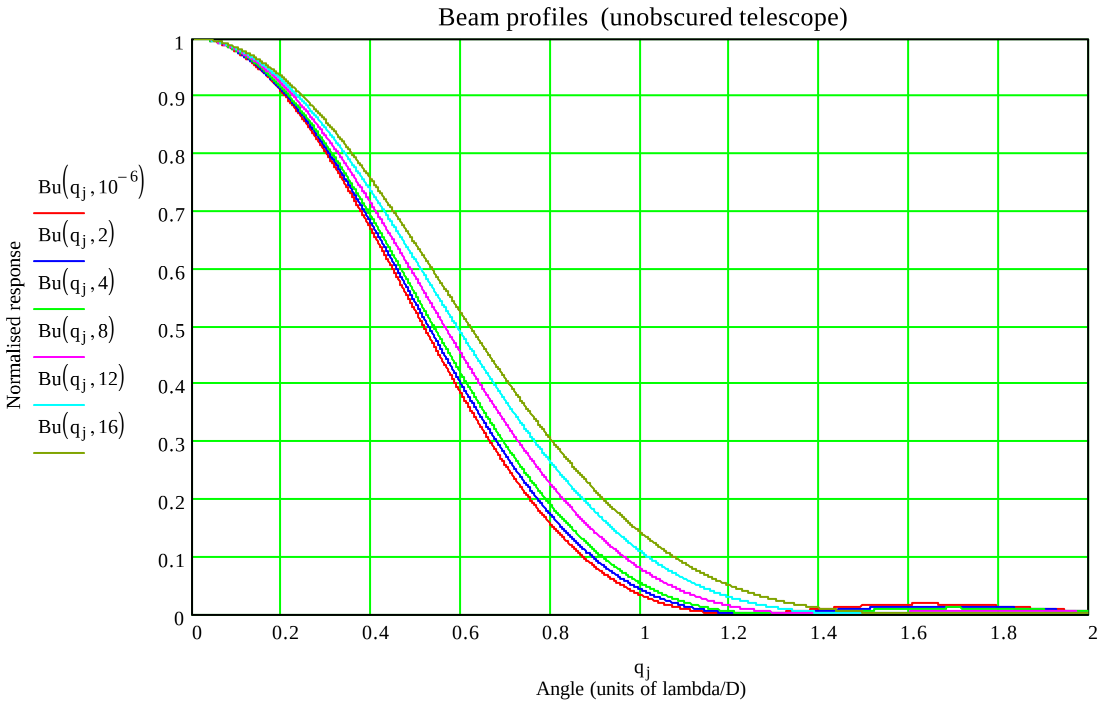

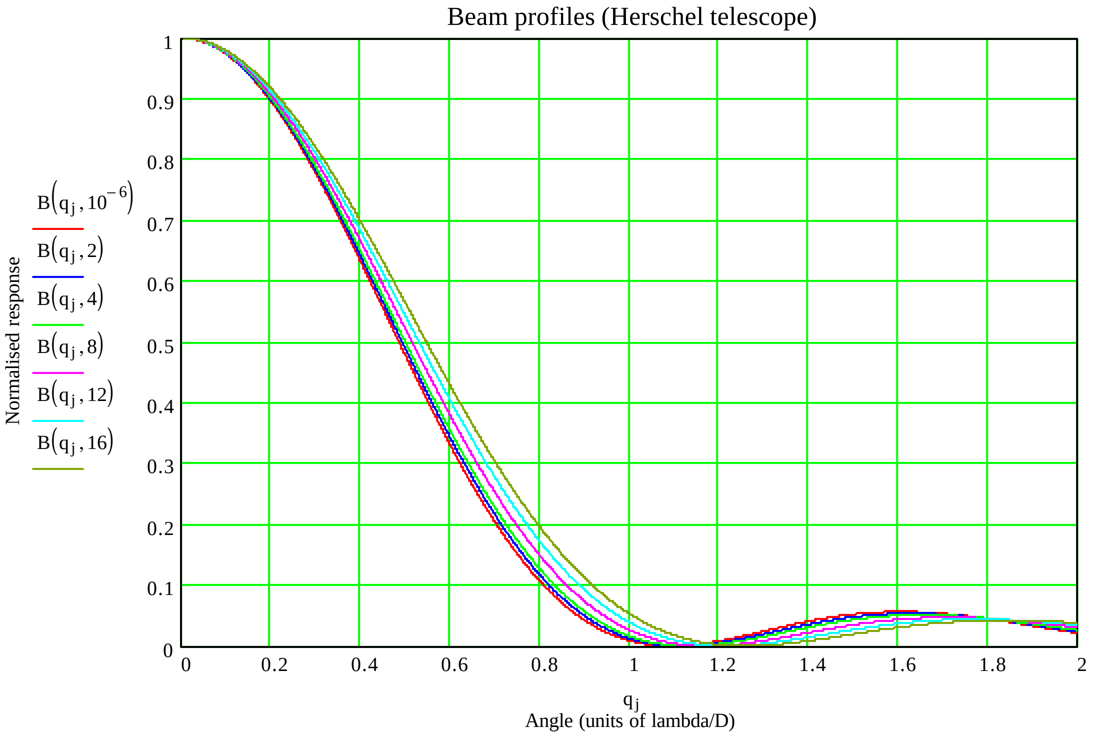

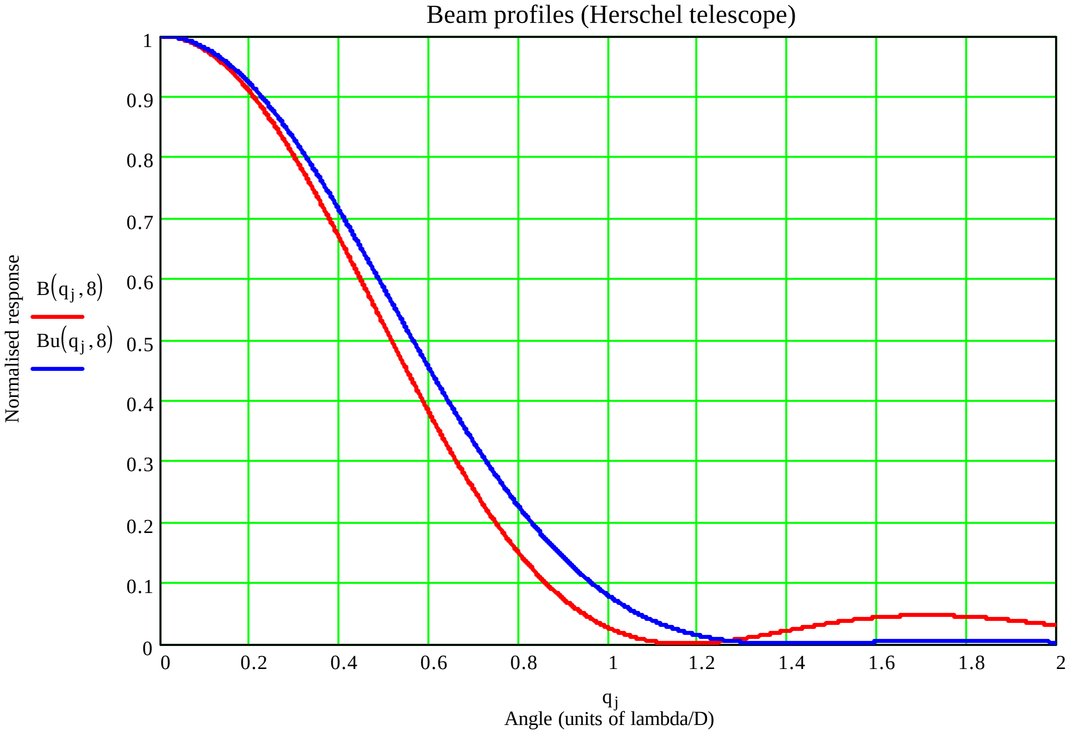

Beam profiles (Herschel telescope)
Normalised response
B(qj, 8)
Bu(qj, 8)
1
0.9
0.8
0.7
0.6
0.5
0.4
0.3
0.2
0.1
0
0
0.2
0.4
0.6
0.8
1
1.2
1.4
1.6
1.8
2
qj
Angle (units of lambda/D)

Determine FWHM as a function of edge taper

Parameter which equals zero at the HWHM point

$B0_j := \left|B\left(q_j, 10^{-6}\right) - 0.5\right| \qquad B1_j := \left|B\left(q_j, 1\right) - 0.5\right| \qquad B2_j := \left|B\left(q_j, 2\right) - 0.5\right|$

$B8_j := \left|B\left(q_j, 8\right) - 0.5\right| \qquad B4_j := \left|B\left(q_j, 4\right) - 0.5\right| \qquad B12_j := \left|B\left(q_j, 12\right) - 0.5\right|$

$B16_j := \left|B\left(q_j, 16\right) - 0.5\right|$

Find the value of j that correspond to the HWHM points

$ind_j := \mathrm{if}\left(B0_j = \min(B0), j, 0\right) \qquad j0 := \max(ind) \qquad j0 = 484 \qquad B\left(q_{j0}, 10^{-6}\right) = 0.500$

$ind_j := \mathrm{if}\left(B1_j = \min(B1), j, 0\right) \qquad j1 := \max(ind) \qquad j1 = 488 \qquad B\left(q_{j1}, 1\right) = 0.499$

$ind_j := \mathrm{if}\left(B2_j = \min(B2), j, 0\right) \qquad j2 := \max(ind) \qquad j2 = 491 \qquad B\left(q_{j2}, 2\right) = 0.500$

$ind_j := \mathrm{if}\left(B4_j = \min(B4), j, 0\right) \qquad j4 := \max(ind) \qquad j4 = 498 \qquad B\left(q_{j4}, 4\right) = 0.500$

$ind_j := \mathrm{if}\left(B8_j = \min(B8), j, 0\right) \qquad j8 := \max(ind) \qquad j8 = 513 \qquad B\left(q_{j8}, 8\right) = 0.5003$

$ind_j := \mathrm{if}\left(B12_j = \min(B12), j, 0\right) \qquad j12 := \max(ind) \qquad j12 = 529 \qquad B\left(q_{j12}, 12\right) = 0.5$

$ind_j := \mathrm{if}\left(B16_j = \min(B16), j, 0\right) \qquad j16 := \max(ind) \qquad j16 = 545 \qquad B\left(q_{j16}, 16\right) = 0.5005$

Plot FWHM vs. edge taper

$u := 1, 2 .. 7$

$$Taper_u := \begin{pmatrix} 0 \\ 1 \\ 2 \\ 4 \\ 8 \\ 12 \\ 16 \end{pmatrix} \qquad FWHM_u := \begin{pmatrix} q_{j0} \cdot 2 \\ q_{j1} \cdot 2 \\ q_{j2} \cdot 2 \\ q_{j4} \cdot 2 \\ q_{j8} \cdot 2 \\ q_{j12} \cdot 2 \\ q_{j16} \cdot 2 \end{pmatrix} \qquad FWHM_u = \begin{pmatrix} 0.968 \\ 0.976 \\ 0.982 \\ 0.996 \\ 1.026 \\ 1.058 \\ 1.09 \end{pmatrix}$$

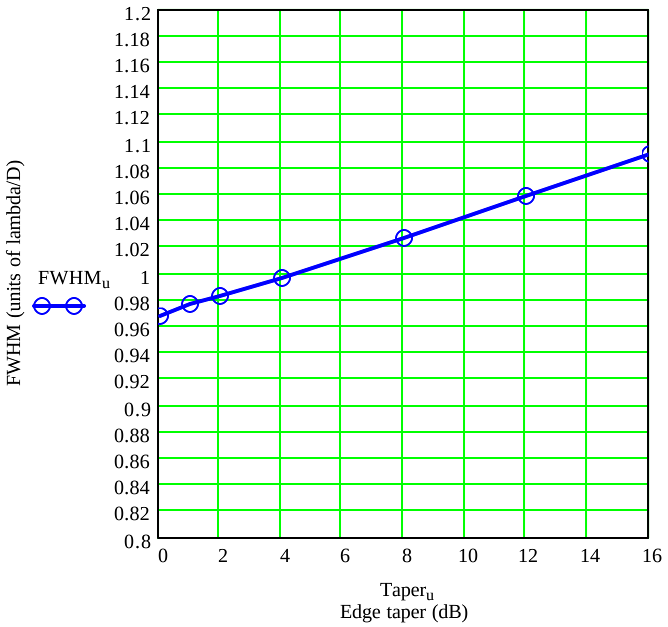

FWHM beam widths (") for PSW, PMW, PLW bands

$$\frac{1.03 \cdot 250 \cdot 10^{-6}}{3.285} \cdot \frac{360}{2 \cdot \pi} \cdot 3600 = 16.2$$

$$\frac{1.03 \cdot 360 \cdot 10^{-6}}{3.285} \cdot \frac{360}{2 \cdot \pi} \cdot 3600 = 23.3$$

$$\frac{1.03 \cdot 520 \cdot 10^{-6}}{3.285} \cdot \frac{360}{2 \cdot \pi} \cdot 3600 = 33.6$$

S/N improvement from pixel coaddition in extraction of a point source from a map

Assumptions:

1. **Beam profile corresponds to 8-dB edge taper**
2. **Map is sampled on a square grid with a spacing of 0.5l/D**
3. **Point source is centred on a pixel**
4. **Signals from the centre and eight neighbours are added together**

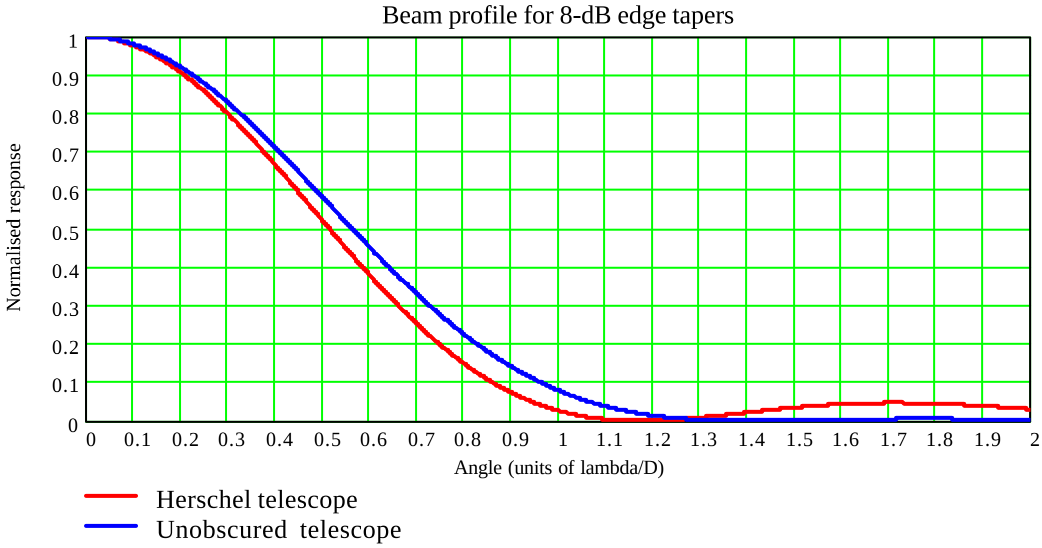

Signal for center pixel	$\text{Centre} := 1$	
Relative signal for top, bottom, left, right	$\text{Side} := B(0.5, 8)$	$\text{Side} = 0.519$
Relative signal for four corners	$\text{Corner} := B\left(0.5 \cdot 2^{0.5}, 8\right)$	$\text{Corner} = 0.242$
Total signal (adding up the nine pixels)	$\text{Sigtot} := 1 + 4 \cdot \text{Side} + 4 \cdot \text{Corner}$	$\text{Sigtot} = 4.05$
Increase in noise due coaddition of nine pixels	$\text{Ntot} := 9^{0.5}$	
Improvement in S/N from pixel coaddition	$\text{SNimp} := \dfrac{\text{Sigtot}}{\text{Ntot}}$	$\text{SNimp} = 1.35$

A better way to combine the signals is to give appropriate weighting to the different pixels.

We have nine estimates of the signal level in the centre pixel, which is directly proportional to the source strength:

One measurement of the centre pixel itself, with S/N = so - let this be normalised to 1

$$\sigma o := 1$$

Four measurements from the side pixels, each with S/N = ss = s(o)*(Ratio of signals, Side/Centre)

$$\sigma s := \frac{\text{Side}}{\text{Centre}} \qquad \sigma s = 0.519$$

Four measurements from the corner pixels, each with S/N = sc = s(o)*(Ratio of signals, Corner/Centre)

$$\sigma c := \frac{\text{Corner}}{\text{Centre}} \qquad \sigma c = 0.242$$

Factor by which the final S/N is improved when combining all the nine pixels is then

$$\text{SN\_factor} := \left[1 + 4 \cdot (\sigma s)^2 + 4 \cdot (\sigma c)^2\right]^{0.5}$$

This gives a slightly better value for the improvement in S/N than the simple coaddition above

$$\text{SN\_factor} = 1.52$$